TRACE METALS AND COPPER ISOTOPE DYNAMICS

IN THE ALA WAI WATERSHED, O‘AHU

A THESIS SUBMITTED TO THE GRADUATE DIVISION
OF THE UNIVERSITY OF HAWAI‘I AT MĀNOA IN PARTIAL FULFILLMENT OF
THE REQUIREMENTS FOR THE DEGREE OF

MASTER OF SCIENCE

IN

OCEANOGRAPHY

DECEMBER 2018

By

Lucie Anna Christa Maria Knor

Thesis Committee:

Olivier Rouxel, Chairperson
Eric H. De Carlo
Chris Measures

Content

Abstract…… 5
Rationale…… 6
Hypotheses…… 8
Introduction…… 9
1. Trace Metal Geochemistry of Streams and Estuaries
2. Isotope Geochemistry of Copper and Iron
3. Geology and Hydrology of the Study Area
4. Trace Metal Geochemistry of the Study Area

Methods…… 21
1. Site Selection
2. Sampling Sites
3. Sampling Technique, Filtration, and Collection of Ancillary Data
4. Major and Trace Element Concentrations
5. Purification for Isotope Measurements
6. Measurement of Isotope Ratios
7. Reproducibility

Results and Discussion…… 40
1. LFM (Low Flow Manoa) Results
2. UAW (Urban Ala Wai) Results
3. SFA (Storm Flow Archives) Results
4. Dissolved and Particulate Concentrations at Low Flow Manoa Stations
5. Isotopic Composition of Dissolved and Particulate Fractions at Low Flow Manoa Stations
6. Dissolved and Particulate Concentrations at the Urban Ala Wai Stations
7. Isotopic Composition of Copper in Dissolved and Particulate Fractions at Urban Ala Wai Stations
8. Dissolved Concentrations in SFA (Storm Flow Archive) Samples
9. Isotopic Composition of Copper and Iron in Dissolved Storm Flow Archive Samples

Synthesis…… 65
1. Redox Cycling and Soil Processes
2. Interactions Between Particulate and Dissolved Loads
3. Rock Weathering and Groundwater
4. Anthropogenic Copper
5. Storm Runoff
6. Estuarine Mixing

Conclusions…… 85
Future Research…… 86
Acknowledgements…… 86
References…… 87

Figures

1. *Schematic of sources and processes with potential influence on $\delta^{65}Cu$ of streams*..... 11
2.1 *Ala Wai watershed and the stream system sampled in this study*..... 16
2.2 *Bedrock types in Manoa valley, streams of Ala Wai watershed and sampling stations of this study*..... 16
3. *Schematic of dissolved and particulate transport by a river as a function of discharge*.....18
4.1 *Sampling stations*..... 21
4.2 *USGS stream gauges*..... 22
5. *Waiakeakua stream at station MWK (Waiakeakua)*..... 23
6. *Wa'ihi stream at station MWH (Wa'ihi)*..... 24
7. *Manoa stream at station MRC (Rec Center)*..... 25
8.1 *Manoa stream at station MKW (Kanewai)*..... 26
8.2 *Storm drain just upstream of station MKW (Kanewai)*..... 27
9. *Urban Ala Wai sampling stations*..... 28
10.1 *Manoa-Palolo drainage channel at station KHS (Kaimuki High School)*..... 29
10.2 *Pollution near station KHS (Kaimuki High School)*..... 29
11. *Ala Wai Canal at station AWFW (Fairway Villa)*..... 30
12. *Ala Wai Canal at station AWHB (harbor bridge)*..... 31
13. *Pre-concentration and purification workflow*..... 33
14. *Cu isotopic composition of all samples*..... 40
15. *Correlations between dissolved trace elements across LFM samples*..... 54
16. *Isotopic composition and inverse concentrations of Cu in LFM sample set*..... 55
17. *Isotopic composition and inverse concentrations of Fe in LFM sample set*..... 56
18. *Ti-normalized Cu concentrations and Cu isotopic composition of particulate UAW samples*..... 60
19. *Concentrations of dissolved Cu*..... 61
20. *Dissolved concentrations of major elements*..... 62
21. *Discharge, $\delta^{65}Cu_{DIS}$ and Cu concentrations at MWK during the 01/31/1999 storm*..... 64
22. *Schematic of Fe oxidation at the interface of reduced ground- and soil waters and oxic stream water*..... 66
23. *$\delta^{65}Cu$ and Cu concentrations along the Ala Wai watershed*..... 69
24. *Schematic of the reactions that control the dissolved Cu isotopic composition of upper watershed baseflow*....73
25. *Dissolved concentrations of Cu of major world rivers, and the current dataset*..... 75
26. *$\delta^{65}Cu$ and Ti-normalized particulate Cu concentrations along the Ala Wai watershed*..... 76
27. *Isotopic ratios of LFM and UAW samples, and composition of possible sources of particulate Cu*..... 77
28. *Schematic of water source contributions to stream flow*..... 78
29. *Concentrations of dissolved K against Cu*..... 81
30. *Cu isotopic composition vs. inverse Cu concentration of low flow and storm samples*..... 81
31. *Concentrations of dissolved P against K*..... 83

Tables

1. *Sampling times and locations of LFM stations*..... 22
2. *Sampling trips, times and locations of UAW stations*..... 27
3. *Storm events and number of samples at MWK and KHS stations*.....32
4.1 *First purification step: Batch metal elution*..... 35
4.2 *Second purification step: Fe/Cu/Zn separation*..... 35
5. *Cu yields of Spex standards*..... 37
6. *Precision of $\delta^{65}Cu$ measurements*..... 38
7. *Detection limits and reproducibility*..... 39
8. *Ancillary data for LFM stations*..... 41
9.1 *Dissolved concentrations and isotopic composition of LFM samples*..... 42
9.2 *Particulate concentrations and isotopic composition of LFM samples*..... 43
10. *Ancillary laboratory data for UAW stations*..... 44

11.1 *Dissolved concentrations and isotopic composition of UAW samples*..... 45
11.2 *Particulate concentrations and isotopic composition of UAW samples).* 46
12. *Discharge for all storm samples*..... 48
13.1 *Dissolved concentrations and Fe and Cu isotopic ratios of SFA samples at MWK.* 49
13.2 *Dissolved concentrations and Fe and Cu isotopic ratios of SFA samples at KHS*..... 51
14*. Fe/Al of particles and average values for Honolulu Volcanics and Ko'olau Series*..... 52
15. *Offset between Fe and Cu isotope ratios of dissolved and particulate fractions of LFM samples*..... 57
16. *Statistics of δ^{65}Cu for SFA samples*..... 63
17*. Ti-normalized Cu concentrations of particles at LFM and UAW stations*..... 68
18.1 *Ratios of dissolved major elements and Cu/Si in LFM samples*..... 71
18.2 *Dissolved major element ratios of LFM samples and groundwater and bedrock endmembers*..... 72
19. *Average dissolved major element concentrations*..... 78
20. *Average ratios of dissolved major element in LFM samples and in seawater and cement endmembers*..... 80

Abstract

Transfer of material from land to sea is important to our understanding of global geochemical cycles. High rates of weathering and erosion in Hawai'i create an ideal laboratory to study natural weathering processes. However, increasing urbanization has led to concerns about heavy metal contamination in both urban streams and coastal waters. Additionally, storm runoff is often enriched in contaminants compared to baseflow, and storms are expected to increase in intensity due to anthropogenic climate change. The transport of the transition metal copper (Cu), both a bio-essential nutrient and toxic pollutant, is investigated in the small, tropical Ala Wai watershed. Distinguishing the natural versus anthropogenic sources of Cu and determining the key processes that influence its distribution and transport are critical to developing a base for the evaluation of Cu contamination and toxicity in ecosystems.

Concentrations of various elements, as well as isotopic ratios of Cu (δ^{65}Cu) and Fe in suspended particles and the dissolved fraction are analyzed. Sampling sites extend from pristine mountain streams to an urban canal, and cover baseflow and storm conditions, providing a transition from natural to anthropogenic dominance in Cu supply and cycling.

Dissolved δ^{65}Cu during baseflow is heavier than both bedrock and particulate fractions, and relatively consistent throughout the watershed, indicating control by complexation with organic ligands, while particulate δ^{65}Cu is more variable. Urban stations and storm runoff are both enriched in Cu compared to upstream, baseflow sites. Heavier δ^{65}Cu of estuarine particles likely stems from road-derived materials, and δ^{65}Cu of storm runoff indicates both light, low concentration- and heavy, high concentration sources of Cu, potentially from soils, fungicides, and vehicle-related sources.

Rationale

River transport is an important source of reactive trace metals to the coastal ocean, and investigating the transfer of elements from land to the oceans is of utmost importance to our understanding of global biogeochemical cycles and anthropogenic pressure (Shiller, 1997; Little et al., 2014; Wiederhold, 2015). The behavior of the transition element copper (Cu) is of particular interest for several reasons.

Copper combines versatile chemical properties and molecular structures with multiple oxidation states, both in solution and solids (Pokrovsky et al., 2008). It is a bio-essential element, but also toxic at very low concentrations (Brand et al., 1986). The toxicity of Cu essentially depends on its chemical form, with the free Cu^{2+} ion causing the most harm to organisms. In the aquatic environment, dissolved Cu is largely complexed by organic ligands, which renders Cu toxicity considerably less severe than when it is present as free Cu ions (Mills et al., 1982). Understanding Cu speciation and transfers is therefore pivotal for the assessment of pollution problems and biological uptake. Environmental Cu contamination mostly stems from industrial activities like smelters and mining, from antifouling paints, pesticides, and automotive vehicle traffic, with about 30% of Cu entering the atmosphere derived directly from human activities (Rauch & Pacyna, 2007).

Distinguishing the natural from the different anthropogenic sources of Cu, and determining the key processes that influence its distribution and transport are critical challenges that need to be overcome to develop a base for the evaluation of threats Cu poses to terrestrial and coastal ecosystems.

Hawai'i constitutes an ideal laboratory to study natural weathering processes. A combination of steep topography, warm climate and frequent orographic rain due to prevailing trade winds leads to high weathering rates and erosion (Murphy et al., 2016). Hawai'i mountain streams in particular provide a pristine setting to investigate natural processes. Additionally, the islands are far removed from sources of atmospheric pollution.

However, increasing population, industrialization and urbanization, mostly on the island of O'ahu, have led to concerns about heavy metal contamination in both streams and coastal waters (De Carlo et al., 2004). High Cu burden was observed in fish from Manoa stream (Schmitt & Brumbaugh, 1990), and Ala Wai Harbor waters were found to exceed the Hawai'i State water quality criterion for Cu concentration in marine waters (De Carlo et al., 2004). Additionally, anthropogenic enrichment of soils and road deposited sediments was observed in the Ala Wai watershed, and neighboring watersheds (Sutherland & Tolosa, 2000; Andrews et al., 2003). The transition from natural to anthropogenic dominance in Cu supply and cycling can be studied along O'ahu watershed transects from unspoiled mountain streams, through varying urban and agricultural landscapes.

In tropical volcanic islands such as O'ahu, storm events dominate material transfer of terrestrial materials to the coastal ocean, while stream baseflow accounts for a much smaller portion of transport (Milliman and Syvitski 1992, De Carlo et al., 2004). While groundwater inputs

dominate stream baseflow, storm runoff is characterized by flushing of shallower soil regions in mountain streams and of paved roads and other impervious surfaces in urbanized catchment areas (Stumm & Morgan, 2012). Consequently, in developed areas, storm runoff is usually enriched in anthropogenic heavy metals, such as Cu, that are washed off of urban surfaces (Cole et al., 1984; Davis et al., 2001; De Carlo et al., 2004). Anthropogenic climate change is expected to lead to a decrease in overall rainfall in Hawai'i, but an increase in intensity of the strongest storm events (Fletcher, 2010). Therefore, storm events in O'ahu (1) access different Cu pools from baseflow conditions, likely with a significant anthropogenic component, and (2) their importance is expected to increase over time. Because greater runoff volume dilutes concentrations, this impedes making statements about changing inputs of elements (by measuring their concentrations only). Stable isotopes, however, provide a source tracer that is not influenced by dilution. Thus, when it comes to identifying sources of- and processes influencing Cu in aqueous environments, stable isotope ratios provide valuable insight.

Metal stable isotope geochemistry is a rapidly developing tool for resolving both basic scientific questions and environmental challenges (e.g. Anbar & Rouxel, 2007; Wiederhold, 2015). Methodological improvements and increasing precision allow us to measure extremely subtle variations in isotope ratios, even of heavier elements such as Cu, Zn and Cd, in a wide range of materials (Wiederhold, 2015). These variations, usually due to slight differences in mass that lead to systematic fractionation, can be used to track both sources and pathways of environmental samples.

Copper has two stable isotopes of mass 65 and 63, and their ratio is commonly expressed, in reference to a standard, as δ^{65}Cu (e.g. Maréchal et al., 1999). Copper also has the largest observed variation in isotope ratios of all transition metals investigated to date (Song et al., 2016). The dissolved Cu load of both rivers and the oceans is isotopically heavy compared to the continental crust, largely due to the preference of organic ligands for heavy Cu (e.g. Vance et al., 2008; Ilina et al., 2013b; Little et al., 2014, Fuji et al., 2014). Heavy dissolved Cu pools appear to be balanced by a preference for the lighter isotope during retention of Cu in soils, adsorption to suspended particles, and precipitation of authigenic minerals (e.g. Little et al., 2014; Pokrovsky et al., 2008; Babscányi et al., 2014). The relative importance of these light Cu reservoirs remains poorly known, which reveals a need to further develop our understanding of Cu isotope fractionation controls during riverine transport and between aqueous pools (Vance et al., 2016).

Copper isotopes have been used to track contamination from acid mine drainage (e.g. Song et al., 2016), and a tentative global mass balance of Cu isotopes ratios has been established (Little et al., 2014). However, the potential for tracking multiple anthropogenic sources, including metal production, anti-fouling boat paints, pesticides, wood preservatives, and motorized vehicles, largely remains unexplored. Measurement of Cu isotope ratios along a Hawai'i watershed to investigate biogeochemical processes, constrain the natural baseline, and develop source tracking of Cu in natural waters will contribute greatly to our understanding of the natural global cycle of Cu, and potential anthropogenic disturbances.

Hypotheses

Three hypotheses are addressed in this study. They are tested through the analysis of Cu in suspended particulate matter (SPM) and the dissolved load of streams using a combined approach of major- and trace element concentrations and Cu and iron (Fe) isotopic ratios, to investigate the transport of Cu from land towards the sea throughout a small, tropical watershed.

Hypothesis 1: **Basalt weathering controls δ^{65}Cu in Manoa stream**. Isotopic exchange between dissolved and particulate Cu species creates an offset from basaltic parent material.

Hypothesis 2: **Anthropogenic Cu input increases downstream.** Urban areas supply additional Cu that can be traced with Cu isotopic ratios. Increasing ionic strength and changes in the flow regime through the Ala Wai Canal estuary control the transfer of Cu into coastal waters, and δ^{65}Cu can reveal processes during estuarine mixing.

Hypothesis 3: **Storm events enhance runoff of heavy metals, and mobilize different Cu pools from baseflow conditions**. δ^{65}Cu allows tracing of temporal and spatial changes in inputs.

Introduction

1. Trace Metal Geochemistry of Streams and Estuaries

Trace elements are defined as having concentrations below 1mg/L (Gaillardet, 2014). In most natural waters, that encompasses all elements except for those present as major ions: sodium (as Na^+), potassium (as K^+), calcium (as Ca^{2+}), magnesium (Mg^{2+}), silica (Si; as silicates, e.g. SiO_4^{4-}), carbon (as HCO_3^- and CO_3^{2-}), sulfur (as SO_4^{2-}), chloride (as Cl^-), and, more rarely, nitrogen (e.g. as NO_3^-). Even elements that are major components of rocks, such as aluminum (Al), Fe, and titanium (Ti), are usually trace elements in aqueous systems, due to their low mobility and solubility in aqueous solution. Rock weathering, atmospheric deposition (wet and dry), and anthropogenic activities are the most significant sources of major and trace elements to rivers (Gaillardet, 2014). Atmospheric deposition includes sea salts, soil dust, and fine volcanic particles, as well as elements mobilized by industrial sources. In many river systems, anthropogenic inputs from industry, traffic, agriculture and waste water treatment exceed the natural levels of a number of trace metals (Förstner & Wittmann, 2012; Gaillardet, 2014). The abundance of trace elements in rivers is influenced by their distribution in the catchment bedrock and other sources, as well as their mobility. For example, Gaillardet (2014) classifies Cu as "moderately mobile", and Fe as "nonmobile", with mobilities ~10 times and 10-100 times less than Na, respectively.

Trace element concentrations in rivers are usually reported for operationally defined "dissolved" and "particulate" fractions. Rock weathering releases soluble elements into the dissolved phase, while insoluble elements become more concentrated in the weathered solid material, which is represented by soils, suspended sediments, and bed sediments. The composition of dissolved and particulate phases can therefore reflect the influence of chemical processes during weathering.

The characteristics of dissolved and particulate fractions are strongly dependent on filtration techniques. This arises because the operational distinction between "dissolved" and "particulate" is commonly made somewhat arbitrarily based on filter pore size (often 0.45µm or 0.22µm). Colloids, which are particles so fine that they do not settle (~1nm to 1µm in size, Lead & Wilkinson, 2006), are an important phase for trace element transport, especially due to their large surface area to volume ratios, which favor adsorption of a variety of other species. They pass through conventional filters and have historically often been considered as part of the dissolved fraction.

Chemical processes taking place during river transport can greatly complicate the rock weathering signature. Concentrations of most trace elements can vary to a large extent between different watersheds and over time, with Fe and Mn and associated elements typically exhibiting the greatest variability (Shiller, 1997). The prevailing chemical form and concentration of a given element in solution is dependent on various environmental factors, including mobility (during weathering and transport), amount of total suspended solids, pH, biological activity, ligand availability and, potentially, redox regime.

Both Cu and Fe are redox sensitive elements. These elements exist as Cu (I) and Cu (II) and Fe (II) and Fe (III) in solution, depending on the redox state of the system. Reduced Fe(II) is abundant in anoxic environments, and is highly soluble. Oxidized Fe(III), however, is particle-

reactive, therefore less mobile, and often precipitates at boundaries of oxic and anoxic water bodies, such as the interface between pore water or groundwater and a river water column. Some elements show similar transitions between mobilization and immobilization at redox boundaries (such as Mn), while others (e.g., V, Cr, Cu) exhibit the opposite behavior, i.e., an immobile reduced form (e.g. Barnhart, 1997; Bonatti et al., 1971). In low-temperature aqueous environments, Cu is mostly present as Cu(II), except in sulfide minerals (Moynier et al., 2017).

Copper displays a very interesting aqueous chemistry. The vast majority of dissolved Cu in most rivers and streams is found as Cu(II) complexed by various organic ligands (McBride et al., 1981; Mills et al., 1982; Skrabal et al.,1997; Wells et al.,1998; Muller et al., 2001, 2005; Tang et al., 2002; Shank et al., 2004a, b). On solid phases, Cu(II) is often found as an adsorbed species, bound to either Fe-oxyhydroxides (Peacock & Sherman, 2004; Tessier et al., 1996) or to organic particles (Davis, 1984).

In estuaries and river mouths, mixing of high and low- salinity and ionic strength waters causes non-conservative behavior of many trace elements. Additionally, estuaries are places with enhanced biological activity, which has a considerable effect on their geochemical makeup. Iron-rich colloids flocculate and coagulate into larger particles as salinity increases along estuaries, scavenging many other trace elements from the dissolved- to the particulate phase (Boyle et al., 1977; Sholkovitz et al., 1978). Although Cu is often associated with organic-rich colloids, both conservative (e.g. Hunter, 1983) and non-conservative (e.g. Hassani et al., 2017; Karbassi et al., 2010) behaviors of Cu have been observed during estuarine mixing. This indicates that the partitioning of Cu between dissolved and particulate phases in estuaries is complicated by biogeochemical processes and the specific nature and properties of the colloidal material (Dai & Martin, 1995).

2. <u>Isotope Geochemistry of Copper and Iron</u>

Reactions during weathering and riverine transport, as well as speciation in the aqueous environment, can lead to fractionation of isotopic ratios of trace elements.

Isotopic ratios are reported as per mill (‰) deviation from a standard. For Cu the most common standard is NIST SRM 976, whereas for Fe the most widely used standard is IRMM-014. The isotopic ratios expressed in this manner:

$$\delta^{65}Cu_{sample} = 1000 \times \left(\left({}^{65}Cu/{}^{63}Cu_{sample}\right)/\left({}^{65}Cu/{}_{63}Cu_{SRM}\right) - 1\right)$$

$$\delta^{56}Fe_{sample} = 1000 \times \left(\left({}^{56}Fe/{}^{54}Fe_{sample}\right)/\left({}^{56}Fe/{}_{54}Fe_{IRMM}\right) - 1\right)$$

The main processes that have been invoked to explain Cu isotopic composition of river dissolved and particulate fractions are depicted in **Figure 1**. The most important processes are exchange between Cu adsorbed to inorganic or organic particles and colloids, and the organically complexed dissolved phase (e.g. Vance et al., 2008; Guinoiseau et al., 2017), along with dissolution of primary and secondary minerals (e.g. Mathur et al., 2012), pedogenetic

processes associated with Cu release from soils (e.g. Bigalke et al., 2011; Vance et al., 2016), and biological uptake by plants and plankton (e.g. Guinoiseau et al., 2017, Petit et al., 2013).

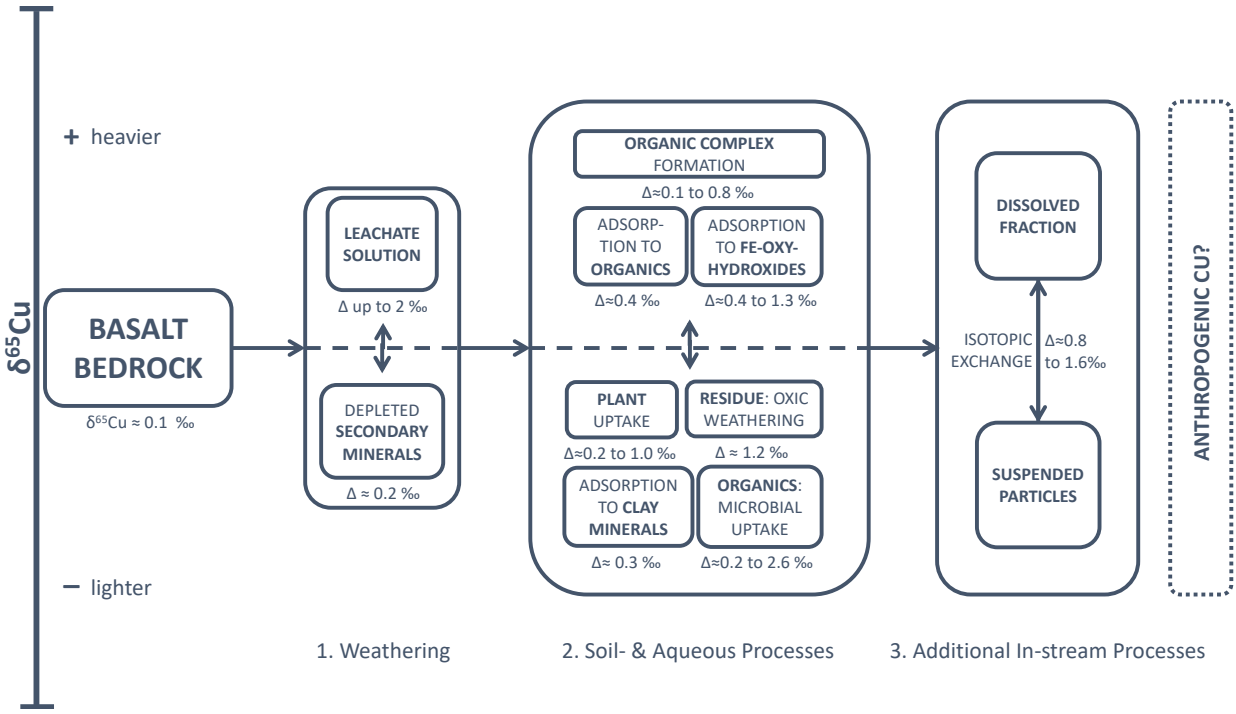

Figure 1. *Schematic of sources and processes with potential influence on δ^{65}Cu of streams. Data sources: Basalt bedrock: Liu et al., 2015; weathering: Fernandez & Borrock, 2009, Mathur et al., 2012; organic complex formation: Ryan et al., 2014; adsorption to organics: Navarrette et al., 2011; adsorption to Fe-oxyhydroxides: Clayton et al., 2005, Balistrieri et al., 2008, Pokrovsky et al, 2008; plant uptake: Weinstein et al., 2011; microbial uptake: Navarrette et al., 2011; adsorption to clay minerals: Li et al., 2015; oxic weathering residue: Vance et al., 2016; isotopic exchange: Vance et al., 2008).*

In most silicate rocks, Cu is a trace element mainly hosted by easily altered sulfide phases (Liu et al., 2014) and a range of igneous minerals (e.g. olivine). The δ^{65}Cu composition of igneous rocks has been estimated to cluster around 0‰ (Liu et al., 2015). Mid-ocean-ridge basalts (MORBs) and oceanic-island basalts (OIBs), like the bedrock of the Hawaiian Islands and Tahiti, have relatively homogenous isotopic compositions of δ^{65}Cu from 0.04 to 0.14‰ and -0.07 to 0.18‰, respectively, with an average of 0.09‰ (±0.13‰) (Liu et al., 2015).

Isotope fractionation of Cu in soils is controlled by adsorption onto mineral surfaces and organic matter, complexation by (in)organic ligands, variation in redox conditions, and biological processes (Weinstein et al., 2011). Fekiacova et al. (2015) found a range of -0.89 to 0.44‰ δ^{65}Cu in unpolluted and polluted soils. The observed variation overlaps with terrestrial rocks, and unpolluted soils are generally isotopically lighter (centered around 0‰) than polluted soils (centered around 0.2‰).

Fractionation of Cu isotopes occurs during weathering and soil biogeochemical cycling, but different studies have made diverging observations. Commonly, soils are depleted in isotopically heavy Cu compared to parent material as a result of oxidative weathering, during

which ^{65}Cu is enriched in solutions (e.g. Liu et al., 2014; Mathur et al., 2012). A depletion of Cu of 50% to 90% compared to parent material in oxic soils in Hawai'i was associated with preferential removal of ^{65}Cu from soils (Vance et al., 2016). The isotopic composition of the soil was therefore up to 1.2‰ lighter than its parent material (Vance et al., 2016). The authors attribute this to equilibrium fractionation between (lighter) Cu sorption onto residual Fe-oxy(hydr)oxides and (heavier) Cu complexation with aqueous organic species.

A contrasting observation, however, was made by Bigalke et al. (2011). Oxic weathering did not produce significant isotopic fractionation in the profiles they investigated, but there was an overall trend of lower (lighter) δ^{65}Cu values with depth, indicating mobilization and downward transport of light Cu (Bigalke et al., 2011). These authors concluded that, as primary minerals weather and release Cu, ^{65}Cu preferentially binds to cation-exchange sites and is incorporated in secondary (pedogenic) minerals, whereas ^{63}Cu is more mobile (Bigalke et al., 2011).

Climatic conditions and weathering intensity might also play an important part in the extent and direction of Cu isotope fractionation in soils, as dominant fractionating processes are impacted by factors such as rainfall and temperature. Differences in weathering regime are likely one of the reasons for the contrasting observations by Bigalke et al. (2011) and Vance et al. (2016). Liu et al. (2014) found systematic differences between saprolite profiles in tropical versus subtropical regions, which supports the notion that weathering intensity influences Cu isotopic fractionation during pedogenesis. In a tropical Chinese soil, high rainfall and weathering intensity seem to favor desorption and downward transport of heavy Cu, depleting Cu concentrations and the heavy isotope, ^{65}Cu, in upper soil horizons (Liu et al., 2014). Residual, organic-matter bound Cu is enriched in the lighter ^{63}Cu isotope (Liu et al., 2014), similar to observations of Vance et al. (2016). Hence, in this tropical soil, Cu isotopic composition is controlled by desorption and biologically derived materials. In a dryer, less weathering intensive North Carolina soil, however, Cu isotope ratios are likely controlled by re-precipitation and adsorption of heavier Cu to secondary minerals, which is reflected in ^{65}Cu enrichment in the upper soil horizons, similar to the observations of Bigalke et al. (2011). The climate on O'ahu is tropical, and Cu isotopic fractionation is expected to be consistent with the observations in other soils exposed to similar weathering regimes by Vance et al. (2016) and Liu et al. (2014).

In reducing soils, which are almost completely stripped of Cu, the small residual pool shows a large variation in δ^{65}Cu (Vance et al., 2016). Due to the reductive dissolution of Fe-oxy(hydr)oxides when conditions become anaerobic, the sorbed (lighter) Cu isotopes are lost from the soil, and Cu isotopic composition of the residue trends back towards that of parent material (Vance et al., 2016). Therefore, there is a transition from light- to heavy Cu isotope enrichment as the soil becomes anoxic (Vance et al., 2016; Bigalke et al., 2010a). This process where ^{63}Cu is preferentially retained under oxic conditions, and lost due to reductive dissolution of Fe-oxides under waterlogged conditions, creates a "rainfall gradient" in soil Cu isotopic composition. A shift in iron isotopes also occurs when light residual Cu is mobilized (Vance et al., 2016). In addition to the release of sorbed light Cu, waterlogging and associated changes in redox potential shift δ^{65}Cu towards heavier compositions in another way: ^{63}Cu is also preferentially lost during redox cycles (Bigalke et al., 2011). Reduction of aqueous Cu(II) to less soluble Cu(I) brings about an enrichment of up to 4‰ of the solid phase in the light isotope (Zhu et al., 2002; Pokrovsky et al., 2008). Overall, it seems that "in many soil settings it is the equilibrium

partitioning of (…) Cu (…) and [Cu-]isotopes between dissolved organic complexes in an aqueous phase versus sorption to residual secondary minerals in the soil that appears to dominate trace metal distributions" (Moynier et al., 2017).

Cu isotope fractionation induced by reactions in plants is on the same order of magnitude as fractionation observed in soils (Weinstein et al., 2011). Because organisms generally preferentially take up light isotopes, plants should deplete the soil of light isotopes in the short term, whereas subsequent degradation of plants should release isotopically light Cu (Weinstein et al., 2011).

Bacteria have a metabolically-driven preference for uptake of the light Cu isotope, and much of the intracellular "Cu-machinery" is universal among species (Navarrete et al., 2011). In one study, marine planktonic cells were enriched in heavy Cu isotopes by around 0.23‰ during adsorption, whereas adsorption onto freshwater species caused no significant fractionation (Pokrovsky et al., 2008).

Few comprehensive studies have been executed on the δ^{65}Cu of rivers and streams. Isotopic exchange between organic ligands and particulate bound Cu likely is a major control on riverine Cu isotopic composition (Vance et al., 2008). There is an overall tendency for rivers with the highest Cu concentrations to have a dissolved Cu pool with isotopic compositions close to 0‰. The estimated isotopic composition of Cu influx into the ocean, however, is 0.63‰ (Little et al., 2014). The dissolved Cu in rivers is generally isotopically heavier than the average continental crust, which is consistent with retention of light Cu by soils (Vance et al., 2008). However, in a study on Maui soils, Vance et al. (2016) concluded that preferential retention of light Cu in oxic soils during weathering and Cu mobilization could not be the only mechanism required to balance the heavy dissolved isotopic signature of rivers. They invoke adsorption of light isotopes to SPM during riverine transport as another mechanism (Vance et al., 2016). Enrichment of heavy isotopes on the solid surface of Fe and Al-oxy(hydr)oxides in solution produces an isotopic offset (solid-solution) of 0.6 to 1.3‰ (±0.1‰) (Pokrovsky et al., 2008). Precipitation of light Cu from solution is another mechanism that removes light Cu from the dissolved phase (Little et al., 2014).

In a study of boreal, organic-rich streams, the homogeneity of the Cu isotopic composition within colloidal and truly dissolved pools indicated either a high rate of isotopic exchange between colloidal and ionic metal species or could be associated to the strong similarity and stability of various Cu complexes with compounds of different molecular weight (Ilina et al., 2013b).

The average isotopic ratio of dissolved Cu in seawater is around 0.9‰ (Little et al., 2014), and universally heavier than the average riverine dissolved pool, and lithological sources. This has been explained with preferential scavenging and output of isotopically light Cu to Fe-Mn-oxides (Little et al., 2014, Takano et al., 2014).

The Fe isotopic system is the most well-studied of all the transition metals (see recent review by Dauphas et al., 2017). In low temperature systems, equilibrium and kinetic Fe isotopic fractionation can be caused by a variety of processes, such as redox reactions, adsorption, dissolution, precipitation and diffusion. Oxidation of aqueous Fe(II) to aqueous Fe(III) enriches the oxidized form in heavy isotopes, but subsequent precipitation of ferrihydrite causes a shift to a lighter isotopic composition in the precipitate (Dauphas & Rouxel, 2006). Dissolution of Fe-

bearing minerals often (e.g. Brantley et al., 2001), but not always (e.g. Skulan et al., 2002), preferentially releases light Fe isotopes into solution. When Fe(II) adsorbs to Fe(III)-rich particles (e.g. goethite, hematite), enrichment of the particles in heavy Fe takes place (e.g. Icopini et al., 2004; Crosby et al., 2005).

Ocean Island Basalts from Hawaii (the Makapu'u stage of the Ko'olau range, as well as Lo'ihi Seamount) were analyzed by Teng et al. (2013) and found to range in Fe isotopic composition between +0.05‰ to +0.14‰.

During weathering and pedogenesis of Maui soils, rainfall has a considerable influence on the processes governing Fe concentrations and isotope ratios (Thompson et al., 2007). Intense rainfall induces waterlogging and enhances reductive dissolution, which is the most efficient pathway to remove otherwise relatively immobile Fe from soils. Consequently, a spatial gradient in rainfall results in a gradient in redox conditions, with increasing rainfall leading to increasing loss of Fe from soils (Thompson et al., 2007). This leads to Rayleigh fractionation between isotopically light Fe that is preferentially lost, and heavy Fe that is preferentially retained by the soils (Thompson et al., 2007). As stated above, this process has the opposite effect on Cu isotopic composition, because light Cu is retained, and heavy Cu is lost with increasing reductive dissolution.

During river runoff, δ^{56}Fe values of suspended particles cluster around the igneous rock composition, and dissolved Fe tends to be isotopically lighter (Beard et al., 2003; Fantle & DePaolo, 2004; Escoube et al., 2015). Ingri et al. (2006) inferred from mass balance calculations that two different colloidal pools in boreal rivers have distinct isotopic compositions. Organic-rich Fe colloids show light (negative) δ^{56}Fe, while Fe-oxyhydroxide colloids resulting from oxidation of groundwater-derived Fe(II) are enriched in heavy Fe (Ingri et al., 2006). In large Arctic rivers, dissolved Fe is isotopically relatively homogeneous, and slightly lighter than bulk continental crust (Escoube et al., 2015). Iron in smaller, organic-rich Arctic river systems, on the other hand, showed a large spread in isotopic values, largely due to an enrichment in heavy Fe in small colloidal pools (Escoube et al., 2015). As stated previously, Fe is largely removed from the water column during estuarine mixing due to flocculation of colloids (Boyle et al., 1977; Sholkovitz et al., 1978). Thus, it appears that despite its near-complete removal of the dissolved Fe pool, this process causes no major shifts in δ^{56}Fe (Escoube et al., 2009). In the marine environment, the pervasive heavy δ^{56}Fe signatures of seawater presumably result from non-reductive dust Fe dissolution and/or binding by organic ligands (Conway and John, 2014; Fitzimons; Radic et al. 2011). Hence, similarly to Cu isotope systematics, if organic ligands bind and stabilize Fe(III) remaining in solution, equilibrium isotope effect would concentrate heavy Fe isotopes in the strongest Fe-ligand complexes (Morgan et al., 2010, with the unbound Fe(III) presumably lost to precipitation (i.e. in the particulate pool).

3. Geology and Hydrology of the Study Area

O'ahu is a tropical volcanic island that was formed by hotspot volcanism of the Hawaiian mantle plume. The major mountain ridges in the west and east of the island are remnants of two shield volcanoes: Waianae volcano, the older (2.2-3.8 Ma), western ridge, and the younger (1.8-2.6 Ma) Ko'olau stretching from the north eastern to the southeastern tip of the island

(MacDonald et al., 1983; Sherrod et al., 2007). All sampling sites discussed in this study are associated with the Ko'olau range in the east of the island.

Hawaiian volcanism is effusive, and features three distinct phases of activity (Roden et al., 1984). The onset of volcanic activity, commonly termed the pre-shield stage, is characterized by production of smaller amounts of melt at the edge of the hotspot that create basalts of predominantly alkali composition (Rowland and Garcia, 2005). Next, the volcano enters the shield stage, increasing melt production and forming of tholeiitic basalt lava flows (Rowland and Garcia, 2005). The final phase of volcanic activity for the Hawaiian hotspot is the post-shield stage where, again, mostly alkali basalts form (Rowland and Garcia, 2005). The Ko'olau range is missing evidence of a post-shield alkali basalt phase, either because it did not occur or because all traces have been eroded (Rowland and Garcia, 2005). It consists chiefly of subaerial shield lavaflows of tholeiitic composition that are between 1.8 and 2.6 million years old. A long phase of dormancy followed the formation of the tholeiitic shield-stage basalts of the Ko'olau Series, but a rejuvenation of volcanic activity occurred from less than one million until about 50,000 to 30,000 years ago (Clague and Frey, 1982). The lava flows and tuffs created by those later, more explosive events at vents scattered across the shield, are classified as the post-erosional Honolulu Volcanic Series (Clague and Frey, 1982). It is a distinct phase, making up less than 1% of the volume of the Ko'olau range. The Honolulu Volcanic Series consists largely of alkali, melilite, and nephelite basalts, whose compositions differ considerably from the tholeiitic Ko'olau Series (Clague et al., 2016). For instance, the Honolulu Volcanic Series is higher in Fe, Ca, Rb, Ba, Sr, Mg, Ni, and Cr than the Ko'olau Series, and is more heterogeneous in a suite of other elements (Clague et al., 2016). Some of the most famous landmarks of the island of O'ahu, including Diamond Head Crater and Hanauma Bay, were formed during eruptions in the Honolulu Volcanic Series (Rowland and Garcia, 2005). The north-western and southern parts of Manoa valley, the drainage area of some headwaters for the watershed studied here, are made up of two post-erosional lava flows, Tantalus and Sugarloaf, which are both nepheline melilite basalts (Clague et al., 2016). The extent of the two dominant basalt types, Honolulu Volcanic Series and Ko'olau Series, is depicted in **Figure 2.2**.

Figure 2.1 *Ala Wai watershed in Honolulu, Hawai'i, and the stream system sampled in this study.*

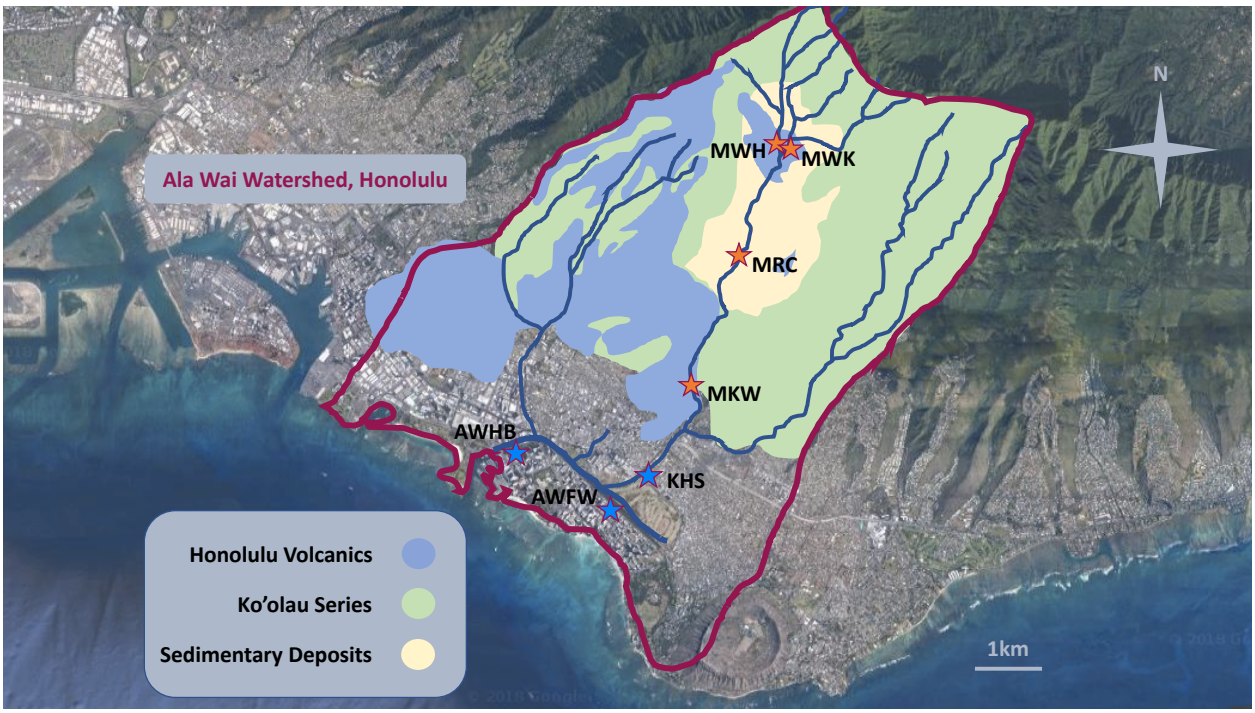

Figure 2.2 *Dominant bedrock types in Manoa valley, redrawn from Clague et al., (2016), and overlain with streams of Ala Wai watershed and sampling stations of this study.*

Manoa stream systems flow through a steep, basaltic environment in continuously humid, warm climate, which produces high weathering and erosion rates (e.g. Hoover, 2002).

Soils of the region are usually highly weathered and lateritic, i.e. rich in Al and Fe, which is typical for tropical soils (Tardy, 1997).

The Ala Wai watershed (**Figure 2.1**) extends over 48.7km^2, cutting through 9km of urban Honolulu landward of the tourist area of Waikiki, into Manoa valley and the surrounding steep mountains of the Ko'olau ridge (De Carlo et al., 2004). The elevation varies from 914 m at the top of the Ko'olau to sea level at the coast, with extremely variable amounts of rainfall from the mountains to the ocean, spanning a range of 50 cm annually at the coast up to 450 cm per year in the back of Manoa valley (Giambelluca et al. 2013). Accommodating more than 143,000 inhabitants, and 72,000 visitors per day (US Army Corps of Engineers, 2013), around 53% of the watershed are highly urbanized (City and County of Honolulu Department of Environmental Services, 2015). The remaining 46% of the area are used for conservation purposes, and are largely forested (City and County of Honolulu Department of Environmental Services, 2015).

The Ala Wai Canal is an artificial, tidally influenced estuary constructed in 1927 that separates Waikiki from Moili'ili and Ala Moana. It is 3.1km long, up to 51m wide, with an average depth of 2m (Gonzalez, 1971; Laws et al., 1993). Discharge varies strongly, but the average is 2.2x10^5 m^3/d. The sedimentation rate in the canal is highly variable but very high (1-4 cm yr^{-1}), and sediments consist chiefly of detrital silt and clay, containing high concentrations of mainly terrestrial organic carbon and authigenic calcium carbonate (Glenn et al., 1995; McMurtry et al., 1995).

There are conflicting classifications of the canal as a Type A (salt wedge; e.g. Glenn et al., 1995; De Carlo & Spencer, 1995) and Type B (partially mixed, moderately stratified; e.g. Gonzalez, 1971; Laws et al., 1993) estuary according to the classification by Biggs & Cronin (1981). These types are determined by the ratio of freshwater discharge to tidal flow, which makes it reasonable to assume that the Ala Wai Canal has characteristics of either depending on discharge volume. During baseflow, the estuary is likely closer to Type B, dominated by tides, whereas a Type A salt wedge forms during higher runoff volumes, when freshwater flow mostly reduces oceanic influence to deeper layers.

The canal is polluted by road runoff and sewage, and highly eutrophic, with some of the highest rates of primary production in the world. Laws et al., (1993) calculated an organic carbon influx of 2.84 tons per day (14 g m^{-2} d^1), which is four times greater than values for any area that was investigated in a study of estuarine organic carbon by Nixon (1981). Particulate nitrogen inputs were found to be 800 mg m^{-2} d^1, which is large even compared to the 26 mg m^{-2} d^{1}in the heavily fertilized Chesapeake Bay (Laws et al., 1993; Jaworski, 1981). Gross photosynthetic rates increase 3 to 5-fold inland from the mouth of the Ala Wai to the head, where surface conditions that are ideal for phytoplankton allow growth rates near the theoretical maximum (Laws et al., 1993; Glenn et al., 1995). Out of this massive primary production, 70% is respired in situ, 18% is sedimented, and 12% washes out to the coastal ocean (Laws et al., 1993).

The transfer of material across the terrestrial-marine boundary on mountainous tropical islands such as O'ahu is dominated by freshwater pulses due to storm events (Milliman and Syvitski 1992, DeCarlo et al., 2004). These episodes of increased water inputs to the coastal ocean are highly variable over very short time scales, with river flow readily increasing 60-fold within

15 minutes, and turbidity increasing 30-fold within 5 minutes (Tomlinson & DeCarlo, 2003). Due to anthropogenic climate change, the intensity of storm events in Hawai'i is increasing even further (Fletcher, 2010).

Overall, material transfer during Hawai'i river runoff is dominated by dissolved material during low flow conditions, and by suspended particles during high flow (Li, 1988). As runoff increases, the total load of dissolved material increases, because dissolution initially increases with increasing runoff (Li, 1988). However, concentrations of major ions and soluble trace elements decrease, due to dilution with rainwater. Particles, on the other hand, are suspended increasingly the more vigorous the discharge. This is illustrated schematically in **Figure 3**, assuming that with increasing river flow, the total amount of material in the dissolved fraction increases linearly (with basalt dissolution), while the particle transport increases exponentially (with suspension) (Li, 1988).

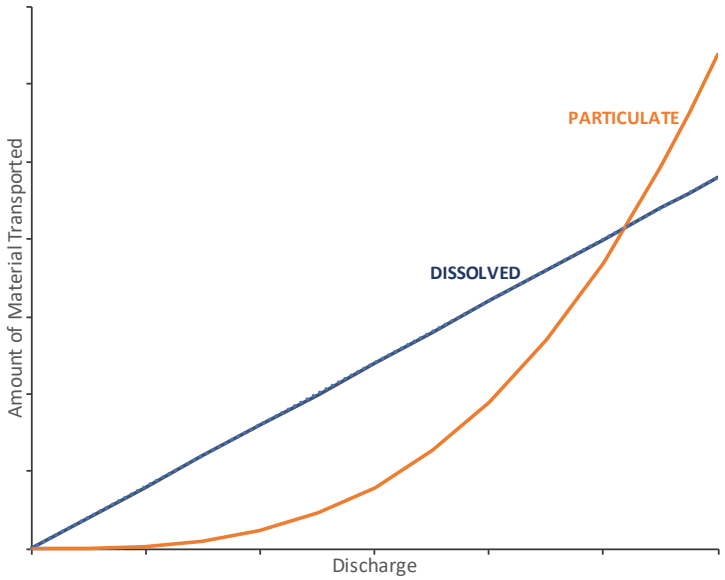

Figure 3. *Schematic of the amount of dissolved and particulate material transported by a river as a function of discharge.*

Groundwater contributes significantly to material transfer from the Hawaiian Islands into the coastal ocean, both directly as submarine groundwater discharge, and indirectly via contribution to streamflow (e.g. Schopka & Derry, 2012). Li (1988) estimates the groundwater denudation rate of O'ahu to be similar in magnitude to denudation by river runoff. Exact amounts of groundwater contribution to river flow depend on current conditions, prevailing patterns, as well as antecedent rainfall events and streamflow (Mair & Fares, 2010).

4. Trace Metal Geochemistry of the Study Area

The most extensive research on trace elements, specifically transition metals, in stream waters and suspended particles on O'ahu was done by DeCarlo et al. (2004). Their main

conclusion was that, during storm flow events, three sources of trace elements can be distinguished in the Ala Wai watershed (specifically the Manoa watershed). According to DeCarlo et al. (2004), elevated concentrations of Cu, Co, Ba, Zn, and Pb were largely due to anthropogenic inputs, whereas Cr, Ni, and V were mostly derived from mineralogical processes, namely the chemical and physical weathering of basalt. The third group of elements, composed of As, Cd, and U was said to be of predominantly agricultural origin (De Carlo et al., 2004). During low flow conditions, an increase in dissolved Cu, Ni, and Zn concentrations was observed downstream going from the high elevations towards the ocean within the Manoa watershed. Due to the high particle reactivity of most transition metals, and the high particle concentrations in the streams during high flow events, the majority of the metals examined were associated with the suspended matter rather than the dissolved fraction (De Carlo et al., 2004).

Other studies of trace elements in O'ahu watersheds predominantly examined the concentrations found in soils and riverbed sediments, as opposed to the river water itself (e.g. De Carlo et al., 2005; Anthony et al., 2004; Sutherland & Tolosa, 2000). In their NAWQA (National Water Quality Assessment) report for the USGS, Anthony et al. (2004) found that metal pollution was evident in multiple watersheds across O'ahu, stating that "trace elements were elevated above background levels in streambed sediments associated with urban and agricultural land use. (…) Chromium and Cu exceeded guidelines in all land uses but not due to pollution but rather as a result of high natural abundance in Hawaii rocks and soil." In their study, contrary to the findings of DeCarlo et al. (2004) for Cu in the Manoa watershed, concentrations of Cr, Ni, and Cu were found to vary little with different land use characteristics, which was taken as an indicator of natural abundances overshadowing any potential anthropogenic inputs of these elements (Anthony et al., 2004).

Cu is anthropogenically enriched in soils and road-deposited sediments in the Manoa watershed (Sutherland & Tolosa, 2000) and the neighboring Nuuanu watershed (Andrews & Sutherland, 2003). In addition to characterizing the total Cu concentrations in road-deposited sediments as elevated above background, Sutherland & Tolosa (2000) found that the leachable fraction of Cu in these sediments is enriched to a much larger extent, and is primarily derived from vehicle inputs. High leachable proportions of potentially toxic metals are environmentally relevant, because they are more mobile and bioavailable (Sutherland & Tolosa, 2000). The low cation-exchange-capacity of the road sediments indicates that metals in road runoff tend to remain in solution upon mobilization, from where they are typically most easily taken up by organisms (Sutherland & Tolosa, 2000). As vehicle contributed contamination increases the concentration of the leachable fraction, flushing of this more bioavailable pool could significantly enhance inputs of environmentally relevant Cu into the coastal ocean.

Sediments from the Ala Wai Canal exhibit elevated concentrations of heavy metals due to anthropogenic activity in the watershed, with continuously high inputs of Cu, Cd, Pb and Zn. The occurrence of a subsurface maximum of Pb is consistent with the now discontinued use of leaded gasoline, whereas other metals peaked in the most recently deposited sediments (De Carlo & Spencer, 1995). An additional putative input of anthropogenic metals is anti-fouling boat paint, which contains large amounts of Cu. Widespread use of these paints on boat hulls in the marinas are likely one of the reasons why Cu exceeded the Hawaii State acute and chronic exposure water quality criterion for marine waters of 2.9 µg/kg (De Carlo et al., 2004). Scavenging

of trace elements during flocculation of colloids along the salinity gradient was also hypothesized to significantly concentrate many anthropogenic heavy metals in Ala Wai sediments with occasional resuspension of diagenetically altered particles into the water column (De Carlo & Spencer, 1995).

Methods

1. <u>Site Selection</u>

Sites for this study were located in the Ala Wai Canal watershed (**Figure 4**) and were selected to represent a gradient in land use conditions ranging from nearly pristine mountain streams to highly urbanized channelized streams, as described previously by De Carlo et al. (2004).

Three sets of samples were collected for this study to capture both temporal and spatial variability of the aqueous geochemistry and copper isotopic composition in the Ala Wai watershed. The sampling program was designed to provide samples from a range of environmental conditions, with a comparison of baseflow and storm flow, as well as high and low tide in the lower reaches of the watershed.

Figure 4.1 *Sampling stations of low flow Manoa (LFM), Urban Ala Wai (UAW), and storm flow archive (SFA) sample sets in the Ala Wai watershed.*

Figure 4.2 *Locations and IDs of USGS stream gauges measuring discharge.*

2. <u>Sampling Sites</u>

The first set of samples collected for this study include the following:

LFM (*"low flow Manoa"*), refers to baseflow samples taken from four stream stations along the upper watershed in Manoa valley in February 2017 (**Table 1**). The stations mark a transition from undeveloped mountain streams to a moderately urbanized channel.

Station	Location	Date and Time
Waiakeakua (MWK)	21°19'41.1"N 157°47'58.5"W	2017-02-26 10:10
Waihi (MWH)	21°19'43.6"N 157°48'02.8"W	2017-02-26 11:00
Manoa Rec Center (MRC)	21°18'50.2"N 157°48'22.5"W	2017-02-26 11:25
Kanewai (MKW)	21°17'44.9"N 157°48'48.6"W	2017-02-26 12:05

Table 1. *Sampling times and locations of LFM stations.*

Station Waiakeakua (MWK) is a nearly pristine mountain stream (**Figure 5**) at Waaloa Way that drains the eastern portion of the Ko'olau range in the back Manoa valley. Except for some flower farms in the area, and some use by military in the past, there is no development upstream of this location.

Figure 5. *Waiakeakua stream at station MWK (Waiakeakua).*

Station Waihi (MWH, **Figure 6**) is also along Waaloa Way, about 100m to the north-west of MWK. Waihi stream is fed by the drainage of the north-western flank of the valley. Upstream of the site, there are a few houses, a modestly developed nature park, and a University of Hawai'i research facility (Lyon Arboretum), above which the watershed is undeveloped. Waihi and Waiakeakua streams join about 100m downstream from this station to form Manoa stream.

Figure 6. *Wa'ihi stream at station MWH (Wa'ihi).*

Manoa stream proper was sampled at station Manoa Recreation Center (MRC, **Figure 7**). The site is nearly in the middle of the valley, within a district park adjoining a housing development and an elementary school. The stream is not channelized with concrete at this site, but it is a modified channel, with some channelized sections of Manoa Stream located upstream of this location. Numerous small intermittent streams and storm drain outlets also deliver water to the stream above this station.

Figure 7. *Manoa stream at station MRC (Rec Center).*

Station Kanewai (MKW, **Figure 8.1**) is also along Manoa stream, below most of the University of Hawai'i Manoa campus, and the stream here has traversed all of Manoa valley, and has received additional storm drain runoff during periods of rain, specifically from a large storm drain outlet just above the site (see **Figure 8.2**). Some very small tributaries flow into Manoa stream upstream of this site, and several sections above Kanewai are concrete channels.

Figure 8.1 *Manoa stream at station MKW (Kanewai).*

Figure 8.2 *Storm drain just upstream of station MKW (Kanewai).*

The second set of samples, **UAW** *("urban Ala Wai")* was taken during three sampling trips in April and May 2018 at three channelized estuary stations (**Table 2**). These range from a drainage channel, through the Ala Wai Canal, to the mouth of the canal at the Ala Wai harbor (see **Figures 4, 9**).

	Location	Sampling	Date and Time
Kaimuki High School (KHS)	21°17'05.4"N 157°49'13.2"W	4	2018-04-02 09:50
		5-H	2018-05-14 15:30
Fairway Villa (AWFW)	21°16'47.9"N 157°49'25.0"W	4	2018-04-02 10:10
		5-L	2018-05-14 08:50
		5-H	2018-05-14 15:45
Harbor Bridge (AWHB)	21°17'15.5"N 157°50'22.9"W	4	2018-04-02 10:20
		5-L	2018-05-14 08:55
		5-H	2018-05-14 15:50

Table 2. *Sampling trips, times and locations of UAW stations.*

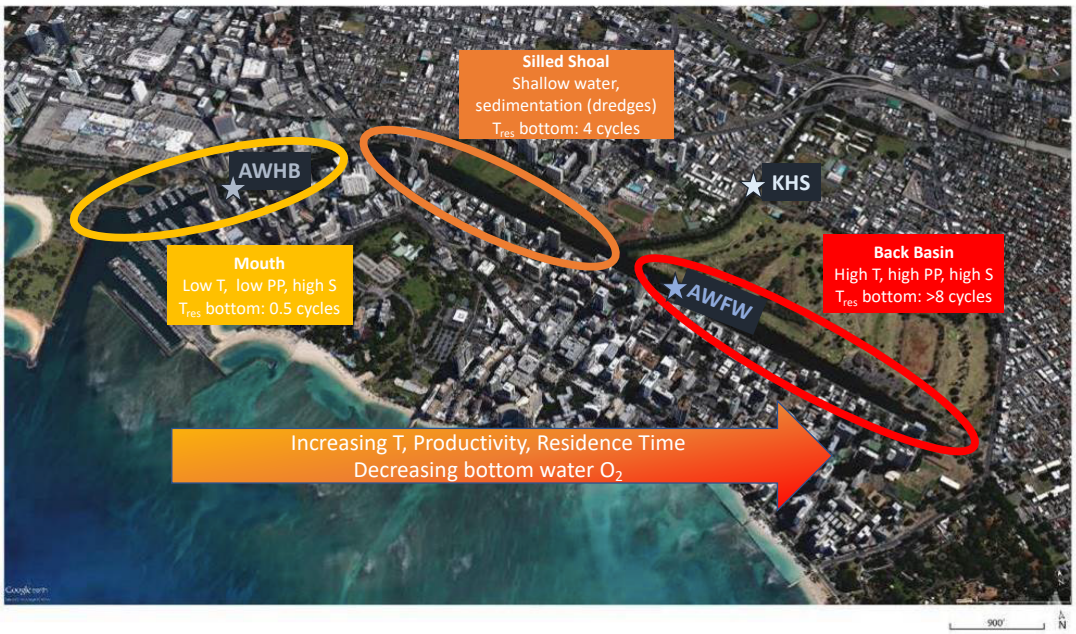

Figure 9. *Urban Ala Wai sampling stations and characteristic water quality parameters and residence times of Ala Wai Canal regions (Laws et al., 1993; Gonzalez, 1971).*

Station Kaimuki High School (KHS, **Figure 10.1**) is located in the Manoa-Palolo Drainage Channel, just upstream of its outlet into the Ala Wai Canal. The channel includes concrete lined sections upstream of the sampling location, and lies above a relict reef carbonate substrate. Flow at this site represents a mixture of water from both Manoa and Palolo streams, as well as urban runoff from a large number of urban storm drains. There is considerable pollution (**Figure 10.2**)

Figure 10.1 *Manoa-Palolo drainage channel at station KHS (Kaimuki High School).*

Figure 10.2 *Pollution near station KHS (Kaimuki High School).*

A reduction in flow velocity, as the drainage channel empties into the brackish Ala Wai Canal and makes a sharp right turn, leads to heavy sedimentation at the inlet, creating a sill that impedes tidal flow into the upper portion of the Ala Wai canal. The sill separates the eastern arm of the Ala Wai, which forms a dead end, from the lower sections, which host most of the active circulation (due to stream flow and tidal pumping).

Station Fairway Villa (AWFW, **Figure 11**) is on the left (southern and oceanward) bank of the Ala Wai Canal in the back basin behind the sill, east of the Manoa-Palolo drainage inlet. Because of the hindrance to flow associated with the sediment sill at the Manoa-Palolo drainage inlet, there is very little circulation at this location. Slow tidal flushing and occasional runoff during high rainfall within the lower portion of the Ala Wai watershed lead to a water column that is heavily stratified and bottom sediments are anoxic below a few centimeters from the sediment-water interface (see De Carlo and Spencer, 1995; Spencer et al., 1995).

Figure 11. *Ala Wai Canal at station AWFW (Fairway Villa).*

The harbor bridge station (AWHB, **Figure 12**) is located on the left (eastern) bank of the Ala Wai canal, immediately upstream from the bridge that separates the outflow of the canal and the saline Ala Wai Harbor. The Ala Wai Canal receives a large amount of road runoff at this location, delivered both by storm drains and overland sheet flow, and includes all the flow from the Manoa-Palolo drainage channel and Makiki stream, which together drain almost 1/3 of Honolulu (49/177 km^2).

Figure 12. *Ala Wai Canal at station AWHB (harbor bridge).*

All UAW stations are estuarine, and influenced to a varying degree by seawater. After an initial trip covering all stations in April 2018 during an approaching low tide (sampling 4, see **Table 2**), a second and third sampling trip were executed at low- and high tides, respectively in May 2018 (sampling 5-L, and 5-H), to investigate tidal influences on the trace element and isotopic composition of the water.

Finally, a third sample set, **SFA** (*"storm flow archives"*) was added to investigate long-term temporal variability. These archived samples were collected at stations MWK (covered in LFM) and KHS (covered in UAW) between 1999 and 2001 (see **Table 3**), by Eric De Carlo's research group at the University of Hawai'i at Manoa, using ISCO sequential samplers set up to sample automatically at 30-min intervals when water rose above a preset level during rain storms (see De Carlo et al., 2004). Samples passed through acid pre-cleaned Teflon® or silicone tubing into 500mL HDPE bottles, and were then filtered through 0.22µm Millipore membranes in the clean laboratory. Filtrates were acidified with ultra-pure quartz distilled nitric acid (HNO_3) or hydrochloric acid (HCl), and stored in plastic bags and boxes in a cabinet after aliquots were analyzed by De Carlo's group. Samples were stored until further preparation in 2017. To make sure that no precipitate formed during storage, all SFA bottles were re-acidified with concentrated HNO_3 (1mL nitric/100mL), and heated gently on a hot plate at 60°C. Samples analyzed for this study are from both KHS and MWK and were collected on November 7, 1999,

and February 11-13, 2001, with additional samples from MWK obtained during three other storm events. The total number of samples from MWK is 39, and 16 were from KHS. Additional data collected during quarterly sampling under baseflow conditions in the late 1990s to early 2000s, were examined to tease apart both changes between low flow and storm flow and changes over the approximately twenty years between the two studies. Because the corresponding filters were not available for SFA samples, only the <0.22µm fraction is discussed in this study.

Location	Storm Event	Number of Samples
Waiakeakua (MWK)	1999-01-30 to 1999-01-31	22
	1999-11-07	6
	1999-12-01	3
	2000-08-27	4
	2001-02-11 to 2001-02-12	4
Kaimuki High School (KHS)	1999-11-07	6
	2001-02-11 to 2001-02-12	10

Table 3. *Storm events and number of samples at MWK and KHS stations covered by storm flow archives (SFA).*

3. Sampling Technique, Filtration, and Collection of Ancillary Data

All LFM and UAW samples were collected using a PVC pole sampler and trace metal clean sampling techniques. The pole sampler housed a 500mL acid-cleaned PE bottle and sampling equipment and bottles were handled with nitrile gloves.

At LFM locations, individual 500-mL samples from each station were transferred into a 4L carboy. Approximately 1L of each sample was filtered through 0.22µm Millipore filters into two 500mL HDPE bottles, and these samples were treated as duplicates (A&B). Filtration was carried out in the laboratory within a few hours of sampling using a hand-held pump. A split sample from each station was filtered in the field using a 0.22µm syringe filter in order to examine the influence of different filtration techniques on the measurement results.

Ancillary measurements of pH, dissolved oxygen, chlorophyll fluorescence, and turbidity were made for the LFM samples using a YSI 6600 V2 probe.

UAW samples were taken into 1L HDPE bottles with a duplicate at one station per sampling trip, and were filtered in the laboratory within a few hours of sampling through 0.22µm Millipore filters under N_2 positive pressure. The salinity and pH of UAW samples were determined in the laboratory the day of sampling using a hand-held refractometer, and a Thermo pH electrode that was calibrated with a three-point calibration using NBS buffers.

LFM and UAW filtrates were acidified immediately after filtration using ≈1mL per 100mL sample of double-distilled trace metal grade 6M HCl or trace metal grade concentrated HNO_3.

Discharge and gauge height data for all sampling times (LFM, UAW and SFA) were obtained from USGS stream gauges at sampling stations MWK, MWH, KHS, and close to station MRC (**Figure 4.2**). There are no stream gauges available near MKW, or downstream from KHS.

4. Major and Trace Element Concentrations

Subsamples of filter residues were dissolved in concentrated HNO_3, and acidified filtrates were analyzed for concentrations of various major and trace elements using a High-Resolution ICP-MS (Thermo Element XR inductively coupled plasma mass spectrometer) at Ifremer in Brest, France. Most LFM samples were run in duplicate. Accuracy was evaluated using in-house water reference materials and the SLRS-5 river water standard, which was measured every five samples during analysis of the dissolved fractions of stream samples. Multi-elemental standards were used to verify accuracy of the analysis for digested particle measurements. Procedural blanks were measured every five samples for both filters and filtrates.

5. Purification for Isotope Measurements

A multi-step preconcentration and purification procedure was employed to prepare samples for the high-quality measurement of isotopic ratios necessary to detect small fractionation in low metal concentrations in the study system. The workflow is listed in **Figure 13.** Methods were adapted from previous studies (Baconnais et al., in press; Chever et al., 2015; Escoube et al., 2009; Rouxel & Auro, 2010).

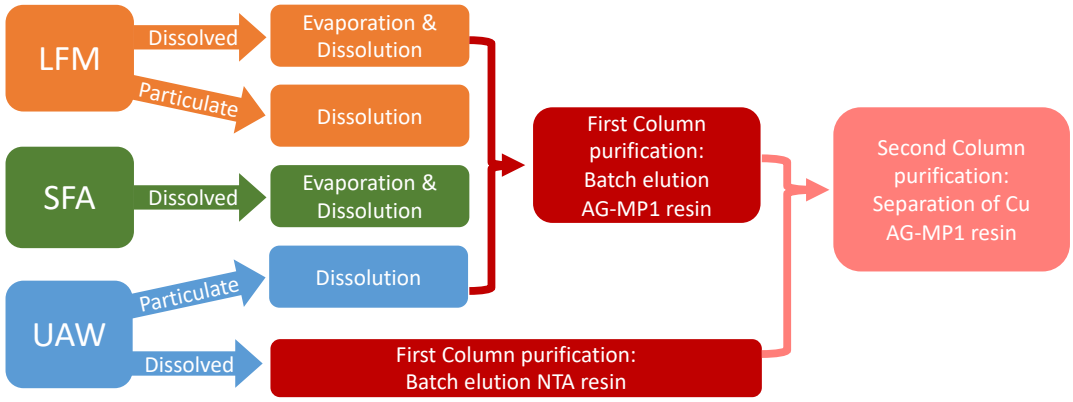

Figure 13. *Pre-concentration and purification workflow.*

All preconcentration- and purification steps were executed in a trace metal clean laboratory with positive air pressure. All acids used were analytical grade, and HCl and HNO_3 were distilled in the laboratory. PFA vials were acid-cleaned in 50% HNO_3, and all plasticware was acid-cleaned in 10% HCl.

Preconcentration:

To gather a sufficient mass of Cu and Fe for isotopic analysis from freshwater samples (LFM and SFA), accurately weighed aliquots of water samples were evaporated in a PFA vial on a hotplate to preconcentrate the material present. After evaporation, residues were dissolved in concentrated nitric- and hydrofluoric (HF) acid, heated on hotplates and evaporated again. For more material-rich samples, an additional dissolution step with concentrated HNO_3 and Optima-grade hydrogen peroxide (H_2O_2) was used to break down remaining refractory compounds. Finally, the residues were taken up in 2mL 6M HCl and 20µL of 30% H_2O_2. No preconcentration was necessary for filter residues. They were dissolved in PFA vials on hotplates using a sequence of concentrated HNO_3 (5mL) and HF (0.25mL), as well as H_2O_2 (1mL), to break down organic and inorganic particles.
Sample solutions were subsequently evaporated and re-dissolved in 2mL 6M HCl and trace H_2O_2.

Purification:

Trace metals were separated from the sample matrix and from each other using a two-step anion exchange resin column chromatography method (see **Table 4.1 & 4.2**, adapted from Borrok et al. (2007), Boyle et al. (2012), and Takano et al. (2013)). For freshwater samples (LFM and SFA) as well as for all filter residues (LFM and UAW), the first purification was a Fe/Cu/Zn batch elution using AG-MP1 (Bio-Rad®) resin. The samples were loaded onto the column, and the matrix fraction was removed with 6M HCl. Fe, Cu and Zn were then eluted using 3M HNO_3. The metal batch eluate was evaporated to near dryness and taken up in 2mL HCl and H_2O_2 for the second purification step.
Higher salinity samples (UAW) could not be evaporated directly for preconcentration. Hence, a different chelating resin, NTA (nitrilotriacetic acid) resin, was used for the first chromatography step of UAW samples. A sample volume of up to 500mL was loaded onto columns containing 1.8 mL NTA resin (wet volume). Matrix materials were removed with Milli-Q® water acidified to pH 2 with HNO_3^-. The batch elution of Fe and Cu from NTA was also carried out with 3M HNO_3.

The second purification step was applied uniformly to all samples and involved using AG-MP1 resin. After sample loading, the Cu fraction was eluted using 6M HCl, followed by the Fe fraction in 0.6M HCl, and finally the Zn fraction in 3M HNO_3. All final eluates were evaporated to near dryness and taken up in 1.8mL of 0.28M HNO_3 for isotopic analyses.

Every "run" of column chromatography included 12 columns for AG-MP1 resin, and 6 columns for NTA resin. For every 12 samples, one column blank (2mL HCl with H_2O_2), as well as a SPEX Cu/Fe standard (in 2mL HCl/H_2O_2) were processed in each purification step.

Metal batch elution: AG-MP1 resin (2.0mL)	
Volume (mL)	*Reagent*
1. Column washing	
10	HNO_3 3M
10	H_2O mmQ
4	HCl 6M
Sample load & matrix elution	
2	Sample HCl 6M
1	HCl 6M
2	HCl 6M
Fe+Cu+Zn fraction	
3	HNO_3 3M
3	HNO_3 3M
Column washing	
10	H_2O mmQ

Metal batch elution: NTA resin (2.0mL)	
Volume (mL)	*Reagent*
1. Column washing	
10	HNO_3^- 3M
10	H_2O mmQ, pH 2
Sample load & matrix elution	
500	Sample, pH 1.8
10	H_2O mmQ, pH 2
10	H_2O mmQ, pH 2
Fe+Cu+Zn fraction	
10	HNO_3^- 3M
	HNO_3^- 3M
Column washing	
10	H_2O mmQ

Table 4.1 *First purification step: Batch metal elution for pre-concentrated samples (left) and complete sample volume (right).*

Fe/Cu/Zn separation: AG-MP1 resin (2.0mL)	
Volume (mL)	*Reagent*
1. Column washing	
10	HNO_3 3M
10	H_2O mmQ
4	HCl 6M
Sample load & matrix elution	
2	Sample HCl 6M
1	HCl 6M
2	HCl 6M
Cu fraction	
3	HCl 6M
5	HCl 6M
5	HCl 6M
5	HCl 6M
Fe fraction	
2.5	HCl 0.6M
5	HCl 0.6M
5	HCl 0.6M
Zn fraction	
2.5	HNO_3 3M
5	HNO_3 3M
5	HNO_3 3M
Column washing	
10	H_2O mmQ

Table 4.2 *Second purification step: Fe/Cu/Zn separation for all samples.*

6. Measurement of Isotope Ratios

Measurement of Cu and Fe isotopic ratios was carried out at Ifremer using a Thermo-Scientific Neptune multi-collector inductively coupled plasma mass spectrometer (MC-ICP-MS). As stated above, isotopic ratios are reported as per mil deviation from a standard. The Cu standard used was NIST SRM 3114, which has a value similar to SRM 976, and the Fe standard was IRMM-014. The equations for δ^{65}Cu and δ^{56}Fe are:

$$\delta^{65}Cu_{sample} = 1000 \times \left(\left({}^{65}Cu/{}^{63}Cu_{sample}\right)/\left({}^{65}Cu/{}_{63}Cu_{SRM}\right) - 1\right)$$

$$\delta^{56}Fe_{sample} = 1000 \times \left(\left({}^{56}Fe/{}^{54}Fe_{sample}\right)/\left({}^{56}Fe/{}_{54}Fe_{IRMM}\right) - 1\right)$$

A combination of standard-sample bracketing technique and internal normalization was used to correct for instrument drift and mass bias for both Fe and Cu isotopic measurements, as described below.

All measurements of isotope ratios are affected by the mass bias of any given instrument, which mostly derives from processes occurring in the plasma- and interface region (Johnson et al., 2004; Maréchal et al., 1999). The relationship between the "measured" and "true" isotope ratio is given by:

$$R_M = R_T \times \left(\frac{m_i}{m_j}\right)^f$$

Where R_M is the measured isotope ratio; R_T is the true isotope ratio; $m_{i,j}$ is the masses of isotope i,j, and f is the exponential mass fractionation coefficient. To correct for the instrument mass bias, all Cu isotopic samples were doped with a Zn standard of known isotopic composition after measuring the sample's Cu concentration, to yield the same Cu/Zn concentration ratio in each sample. The ^{66}Zn/^{64}Zn ratios were then measured along with δ^{65}Cu, and used to calculate f_{Zn} for each sample solution as described in the following equation:

$$f_{Zn} = \ln\left(\left({}^{66}Zn/{}_{64}Zn\right)_{measured}/\left({}^{66}Zn/{}_{64}Zn\right)_{true}\right)/\ln\left({}^{m66}Zn/{}_{m64}Zn\right)$$

Subsequently, the calculated f_{Zn} was applied to measured Cu isotopic ratios through the equation below:

$$\left({}^{65}Cu/{}_{63}Cu\right)_{corrected} = \left({}^{65}Cu/{}_{63}Cu\right)_{measured} \times \left({}^{m65}Cu/{}_{m63}Cu\right)^{f_{Zn}}$$

The complete correction of δ^{65}Cu using both standard-sample bracketing and Zn doping method is described by:

$$\delta^{65}\mathrm{Cu}_{\mathrm{final}} = 1000 \times \left(\left({}^{65}\mathrm{Cu}/_{63}\mathrm{Cu}_{\mathrm{corrected\ (i)}} \right) / \left(\left({}^{65}\mathrm{Cu}/_{63}\mathrm{Cu}_{\mathrm{corrected\ standard(i-1)}} \right) \times 0.5 + \left({}^{65}\mathrm{Cu}/_{63}\mathrm{Cu}_{\mathrm{corrected\ standard(i+1)}} \right) \times 0.5 \right) - 1 \right)$$

The same approach was applied for Fe isotope measurements, using Ni isotope standard as internal standard (Poitrasson & Freydier, 2005; Rouxel et al., 2005).

7. Reproducibility

It is crucial to verify the yield of chromatography steps, as the column chemistry can cause very large isotopic fractionation that subsequently introduces inaccuracies into the δ^{65}Cu results, if the majority of the Cu is not recovered (Maréchal & Albarède, 2002). The yield was calculated for each column standard (see **Table 5**), and the recovery of samples was evaluated using concentrations determined by the Element XR ICP-MS. The uncertainty in yield determination was about 10%, considering sample preparation (e.g. dilution) and analytical uncertainties. Isotopic measurements with yield <50% (17 samples, 1 standard) or >150% (2 samples), reflecting either sample loss or contamination were excluded from subsequent interpretation. Appearance of high concentrations of Zn in the Cu fraction also indicate significant contamination during column chromatography, so samples with high measured Zn/Cu during isotopic analysis were also excluded.

Standard	Cu yield (%)	δ^{65}Cu	2SD
Spex-2x	92	0.08	0.14
Spex-2x	92	-0.16	0.04
Spex-2x	79	0.09	0.04
Spex-2x	104	0.04	0.04
Spex-2x	90	0.00	0.11
Spex-2x	86	-0.11	0.04
Spex-1x	140	0.12	0.12
Spex-1x	103	-0.02	0.04
Spex-1x	97	0.00	0.09
Spex-1x	89	-0.07	0.07
Spex-1x	103	0.02	0.08
Spex-1x	95	0.04	0.08
Spex-nta	80	0.07	0.04
Spex-nta	52	0.19	0.12

Table 5. *Cu yields (>50%) of Spex standards processed through AG-MP1 columns for step 2 only (Spex-1x), for steps 1&2 (Spex-2x), and through NTA and AG-MP1 columns (Spex-nta).*

Instrument precision (calculated as 2 standard deviations, 2SD) for the isotopic analysis was on average 0.07‰ for δ^{65}Cu, and 0.05‰ for δ^{56}Fe. External precision was determined from the duplicate column purification of the Spex standard (**Table 6**). Several standards were outside

the ±0.15‰ uncertainty of duplicate bottles, presumably due to analytical bias, and were excluded. The average value for Cu-Spex standards was 0.02‰ (reported value: 0‰), with a 2SD of 0.18‰, which is three times larger than the uncertainty of 0.06‰ reported by Baconnais et al. (in press). Precision of instrument measurements, as well as of duplicate bottles of samples was within the uncertainty of Spex standards. Consequently, the largest error in isotopic measurements is introduced by column chemistry. The detection limit for Cu isotopic measurements is given as 3SD of procedural blanks, which was 4.0 ng/g (i.e. 7.2ng of Cu in the purified and concentrated solution).

δ^{65}Cu Precision	Average 2SD of δ^{65}Cu in ‰
Instrument (n=69)	**0.07**
Duplicate bottles (n=13)	**0.15**
Spex standards (n=14)	**0.18**

***Table 6**. Precision of δ^{65}Cu measurements of individual samples, duplicate bottles, and Spex standards.*

Detection limits for concentration measurements were also calculated as 3SD of blank measurements (**Table 7**). Accuracy of Element XR concentration measurements was evaluated using the SLRS-5 river water standard (**Table 7**).

	Detection Limit	SLRS-5 average value	SLRS-5 Certified value	Accuracy of SLRS-5	Precision (from SLRS-5)
	µg/kg	*µg/kg*	*µg/kg*	*% deviation*	*µg/kg 2SD*
Cu	**0.02**	18.16	17.4	4.4	2.57
Li	0.02	0.37	0.45	-17.0	0.05
B	0.11	21.80	6.56	232.3	75.46
Rb	0.001	1.038	1.24	-16.3	0.04
Sr	0.02	50.78	53.6	-5.3	2.03
Y	0.0002	0.0799	0.112	-28.6	0.01
Mo	0.17	<LOD	0.27	-43.4	
Cd	0.003	<LOD	0.006	-74.5	
Ba	0.01	11.03	14	-21.2	0.83
Pb	0.03	0.57	0.081	609.9	1.39
U	0.001	0.072	0.093	-22.7	0.00
Mg	1.7	1996.41	2540	-21.4	94.02
Al	0.13	49.25	49.5	-0.5	4.44
Si	0.49	1511.97	1922	-21.3	57.16
P	0.73	41.04			56.49
S	1.6	1916.9	2368	-19.1	116.64
K	18	811	839	-3.3	262.90
Ca	24	9136	10500	-13.0	481.80
Ti	0.01	1.56	1.86	-15.9	0.14
V	0.001	0.263	0.317	-17.2	0.03
Cr	0.002	0.240	0.208	15.5	0.05
Mn	0.01	4.48	4.33	3.5	0.48
Fe	0.10	89.55	91.2	-1.8	13.75
Co	0.0003	0.053	0.05	5.7	0.01
Ni	0.02	0.73	0.476	54.0	0.49
Sb	0.001				
Sn	0.003				

Table 7. *Detection limits (3SD of blank measurements), and reproducibility as determined by measurements of SLRS-5 standard for Element XR ICP-MS concentration measurements.*

Results and Discussion

Concentrations of major and trace elements, isotopic measurements, and ancillary measurements are presented in this section. All concentrations are reported in µg/kg, where both dissolved and SPM fractions are given in µg per kg of water sample. Therefore, concentrations of Cu_{SPM}, expressed as µg per kg of water are a function of the amount of SPM present. Because SPM concentrations are variable, Cu_{SPM} concentrations were additionally normalized to the most immobile element measured, Ti (Hough et al., 1941), as a proxy for SPM concentrations. All Cu isotopic measurements are summarized in **Figure 14**.

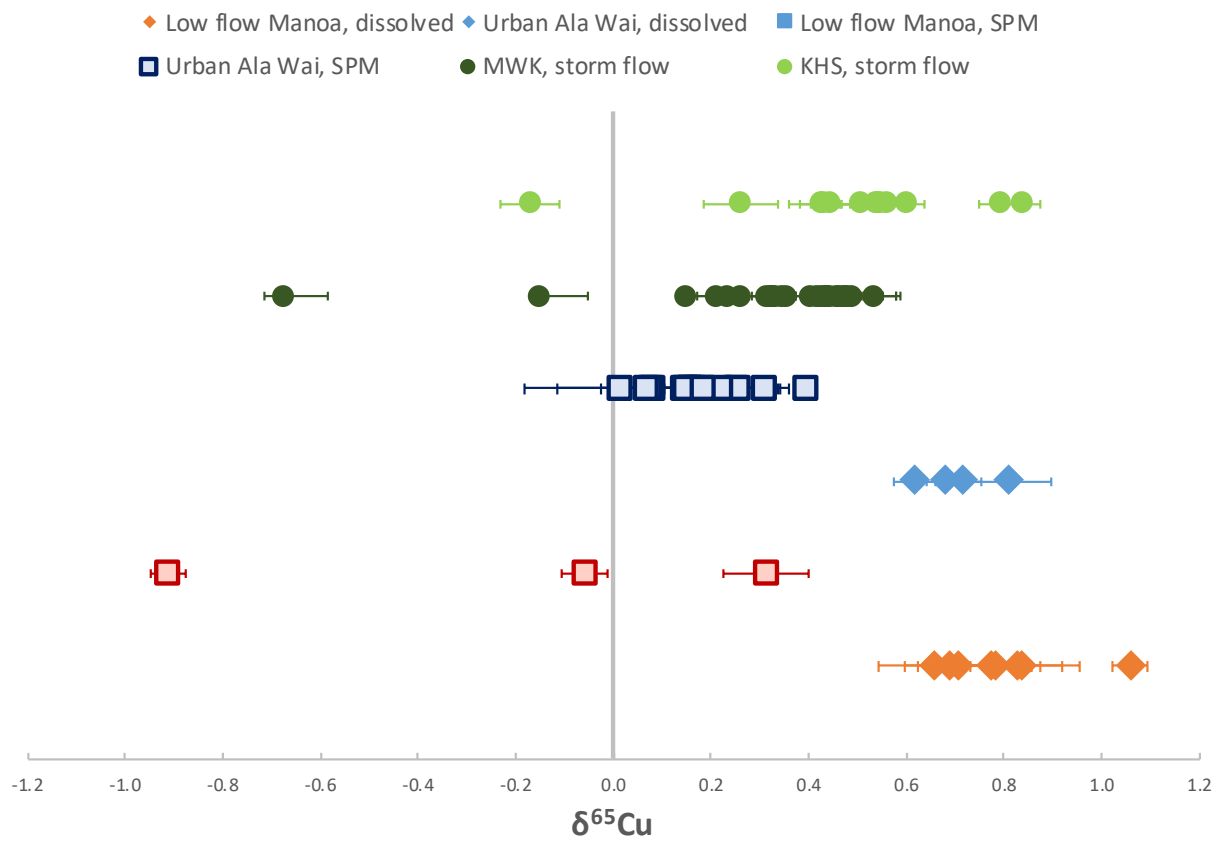

Figure 14. *Cu isotopic composition of all samples.*

1. LFM (Low Flow Manoa) Results

Table 8 below provides *in-situ* water quality data obtained concurrently with the collection of samples for trace element and isotope ratio analysis. **Table 9** contains concentrations and Fe and Cu isotopic ratios of SPM and the dissolved fraction.

	pH	**T** °C	**DO** mg/L	**Chlorophyll** µg/L	**Turbidity** NTU	**Conductivity** µS/cm	**Discharge** cubic ft/cm
Waiakeakua (MWK)	7.7	19.9	8.7	12.0[1]	3.2	149	3.37
Waihi (MWH)	7.5	19.9	8.5	1.8	3.3	170	1.04
Manoa Rec Center (MRC)	7.8	20.7	8.8	0.2	0.8	171	5.34
Kanewai (MKW)	7.9	20.5	8.9	0.8	3.3	ND	ND

Table 8. *Ancillary data for LFM stations.*
[1]This measurement is suspect, because it is unexpectedly high and the sensor behavior was erratic.

Loc.	F.	B.	δ^{56}Fe	δ^{65}Cu	Mg	Si	S	K	Ca	Al	Ti	Mn	P	Fe	Cu	V	Cr	Co	Ni	Li	B	Rb	Sr	Y	Ba	Mo	Sb	Sn	Cd	Pb
MWK																														
	P	A	-0.08 +/- 0.05	1.06 +/- 0.04	6104	8703	800	576	7557	5.2	0.26	4.78	15.56	16.47	0.30	2.22	0.66	0.04	0.09	0.06	15.97	0.51	42.78	0.01	1.07	0.02	0.01	0.21	<LOD	<LOD
	P	B	-0.09 +/- 0.05	0.83 +/- 0.09	6142	8827	783	578	7534	7.3	0.33	4.71	18.22	13.87	0.74	2.30	0.64	0.05	0.11	0.05	17.01	0.52	43.80	0.01	1.08	0.02	ND	ND	<LOD	0.02
	S				6896	9227	1160	566	7876	6.8	0.19	4.72	2.54	25.50	0.20	2.40	0.59	0.04	0.14	0.07	16.18	0.55	41.14	0.01	1.18	<LOD	0.01	0.01	<LOD	<LOD
MWH																														
	P	A	-0.14 +/- 0.05	0.71 +/- 0.08	7008	7137	1020	699	8348	4.4	0.13	33.65	54.54	62.83	0.22	0.42	0.11	0.18	0.41	0.08	15.54	0.72	66.13	0.01	3.04	0.03	ND	ND	<LOD	<LOD
	P	B	-0.12 +/- 0.05	0.84 +/- 0.12	7036	7191	1047	651	8315	5.6	0.07	33.25	25.28	72.21	0.30	0.42	0.12	0.19	0.32	0.08	15.02	0.71	67.04	0.01	3.27	0.04	0.02	0.17	<LOD	0.02
	S				8581	8116	1201	735	8698	5.1	0.27	32.31	26.58	204.28	0.30	0.55	0.11	0.19	0.34	0.07	15.23	0.73	61.36	0.01	3.34	<LOD	0.02	0.00	<LOD	<LOD
MRC																														
	P	A	-0.66 +/- 0.05	0.69 +/- 0.14	7253	8571	1339	685	8815	6.5	0.77	30.87	9.91	122.13	0.67	1.31	0.34	0.12	0.43	0.06	18.54	0.58	54.59	0.01	1.77	0.02	0.01	0.16	<LOD	<LOD
	P	B	-0.76 +/- 0.05	0.78 +/- 0.09	7208	8548	1307	630	8813	4.2	0.10	31.53	7.87	117.79	0.43	1.34	0.30	0.12	0.22	0.06	19.48	0.59	55.35	0.01	1.99	0.03	ND	ND	<LOD	0.02
	S				8342	9352	1511	677	9282	5.3	0.19	31.55	13.70	160.31	0.40	1.42	0.30	0.12	0.20	0.08	18.35	0.64	52.87	0.01	1.95	<LOD	0.02	0.01	<LOD	<LOD
MKW																														
	P	A	-0.60 +/- 0.05	0.66 +/- 0.06	8227	8815	1727	966	10306	6.4	0.28	8.75	13.91	103.22	0.63	1.49	0.32	0.05	0.29	0.06	22.24	0.80	66.36	0.01	2.17	0.07	0.03	0.13	<LOD	0.03
	P	B	-0.66 +/- 0.05	0.78 +/- 0.08	8145	8505	1708	945	10094	6.0	0.07	8.50	14.20	89.30	0.72	1.48	0.24	0.06	0.33	0.05	21.89	0.81	65.72	0.01	2.27	0.07	0.02	0.17	<LOD	0.07
	S				8036	8798	1689	967	10397	7.9	0.28	9.73	18.23	138.70	0.56	1.52	0.24	0.05	0.21	0.07	21.99	0.80	66.74	0.01	2.16	0.06	0.02	0.00	<LOD	<LOD
RSD (%)					24.20	14.91	19.58	6.13	6.12	45.41	34.01	2.21	51.99	9.73	25.02	5.49	19.39	4.26	36.92	16.72		10.92	6.43	16.78	10.18					

Table 9.1 *Dissolved concentrations (in µg/kg) and isotopic composition (in ‰) of LFM samples, and RSD of duplicate runs (F.: Filtration – P=pump, S=syringe; B.: Bottle).*

Loc.	B.	δ^{56}Fe	δ^{65}Cu	Mg	Al	P	S	K	Ca	Fe	Li	Rb	Sr	Y	Ba	Ti	Mn	Mo	Sb	Sn	V	Cr	Co	Ni	Cu	Cd	Pb
MWK		0.07 +/- 0.16		15	145.3	3.50	7.00	<LOD	<LOD	201.32	<LOD	0.009	0.16	0.0394	0.21	19.45	2.17	<LOD	0.0019	0.007	0.421	1.593	0.0637	0.4430	0.1861	<LOD	<LOD
MWH	A	-0.04 +/- 0.11		13	67.7	13.26	7.39	<LOD	<LOD	304.33	<LOD	0.008	0.21	0.0194	0.28	9.17	1.67	<LOD	0.0013	0.011	0.265	1.270	0.0310	0.2432	0.1420	<LOD	<LOD
	B		-0.06 +/- 0.05																								
MRC	A	-0.36 +/- 0.16		9	52.7	3.63	5.88	<LOD	<LOD	144.40	<LOD	0.005	0.11	0.0126	0.13	5.84	1.60	<LOD	<LOD	0.006	0.214	1.555	0.0230	0.1674	0.1006	<LOD	<LOD
	B		-0.91 +/- 0.04																								
MKW	A		0.31 +/- 0.09																								
	B	-0.21 +/- 0.11		14	66.7	3.81	4.20	<LOD	<LOD	154.66	<LOD	0.007	0.16	0.0179	0.20	7.36	3.63	<LOD	0.0017	0.010	0.210	1.299	0.0328	0.2067	0.1603	<LOD	<LOD
RSD (%)				5.25	6.46	3.47	4.79	7.99	6.30	2.29	5.06	3.22	2.92	2.28	4.78	4.18	3.90	9.50	3.59	3.13	4.13	4.23	1.77	2.23	2.05		

Table 9.2 *Particulate concentrations (in µg/kg) and isotopic composition (in ‰) of LFM samples, and RSD of duplicate runs (B.: Bottle).*

2. UAW (Urban Ala Wai) Results

Table 10 below shows pH and salinity of UAW samples, where salinity was only measured during sampling trip 5. **Table 11** contains concentrations and Cu isotopic ratios of SPM and the dissolved fraction.

		pH	Salinity
Kaimuki High School (KHS)	4	7.39	
	5-H	8.05	0
Fairway Inn (AWFW)	4	7.79	
	5-L	7.78	15
	5-H	7.92	35
Harbor Bridge (AWHB)	4	8.16	
	5-L	7.81	18
	5-H	8.05	20

Table 10. *Ancillary laboratory data for UAW stations.*

Loc.	T.	B.	δ^{65}Cu	Mg	Al	Si	P	S	K	Ca	Fe	Li	B	Rb	Sr	Y	Ba	Ti	Mn	Mo	V	Cr	Co	Ni	Cu	Cd	Pb
KHS	4	A	0.68+ /- 0.04	5159	7.8	3004	133.5	3013	2531	6268	23.77	0.35	<LOD	1.01	60	0.01	2.73	0.15	11.47	0.14	1.32	0.65	0.078	0.48	3.76	<LOD	0.04
	5-H	A	ND	17086	83.8	4870	58.6	12082	7787	11483	47.56	2.69	132	2.03	152	0.11	2.97	1.73	12.42	0.21	1.38	0.53	0.148	0.55	2.49	<LOD	0.08
AWFW	4	A	0.71 +/- 0.04	382609	15.4	3876	98.3	245629	161780	134900	5.59	48.65	1493	32.51	2843	0.03	10.51	0.16	29.73	2.70	3.05	0.98	0.311	0.73	2.64	<LOD	0.05
	5-L	A	ND	486329	305.9	5032	222.3	313768	206784	161213	25.30	66.48	1610	41.29	3404	0.25	9.16	4.38	34.12	3.23	2.25	0.91	0.475	0.78	2.35	0.03	0.09
	5-H	A	ND	928405	30.5	4954	18.6	598796	395170	306085	4.49	122.75	3059	80.21	6492	0.07	11.83	0.31	12.03	6.13	3.75	0.98	0.238	0.59	0.56	<LOD	0.07
AWHB	4	A	0.62 +/- 0.04	275418	11.8	3979	167.4	178309	117929	99300	8.10	35.57	1066	24.29	2040	0.02	10.80	0.30	16.44	2.19	3.47	1.25	0.165	0.57	3.57	<LOD	0.05
	4	B	0.81 +/- 0.09	261737	10.2	3655	82.5	171752	113135	96035	6.26	34.63	993	23.31	1938	0.02	10.47	0.09	15.42	2.10	3.29	1.23	0.155	0.59	3.63	<LOD	0.09
	5-L	A	ND	641870	13.1	5195	102.7	419977	276627	209688	5.55	82.59	2249	55.06	4408	0.04	10.87	0.25	26.54	4.31	2.61	0.67	0.240	0.47	0.88	<LOD	0.01
	5-H	A	ND	698000	28.3	3042	230.4	460900	302652	224434	8.04	93.76	2458	61.56	4897	0.06	7.64	0.77	23.77	4.77	2.02	0.68	0.209	0.48	1.80	<LOD	0.01
	5-H	B	ND	695535	25.8	2968	110.3	457207	304819	224684	6.33	92.64	2436	60.49	4815	0.07	7.68	0.32	22.93	4.76	2.00	0.62	0.203	0.62	1.60	<LOD	ND

Table 11.1 *Dissolved concentrations (in µg/kg) and isotopic composition (in ‰) of UAW samples (T.: Sampling trip; B.: Bottle).*

Loc.	T.	B.	F.	δ^{65}Cu	Mg	Al	P	S	K	Ca	Fe	Li	Rb	Sr	Y	Ba	Ti	Mn	Mo	V	Cr	Co	Ni	Cu	Cd	Pb	U
KHS	4	A	1	ND	188	1848	48.91	150	<LOD	329	2428	0.27	0.21	4.6	0.41	4.4	225.2	61.15	<LOD	3.80	7.58	0.954	5.07	6.26	0.02	2.27	0.02
	4	A	2	ND	283	2708	68.19	346	<LOD	511	3121	0.28	0.22	6.3	0.58	5.8	338.4	86.19	0.05	5.53	13.69	1.414	7.23	9.63	0.03	3.03	0.02
	4	A	3	ND	216	2083	54.14	183	<LOD	361	2681	0.29	0.23	5.1	0.47	4.8	253.4	70.55	0.04	4.27	8.75	1.103	5.70	6.63	0.02	2.47	0.03
	5-L	A	1	0.25 +/- 0.11	195	3000	58.96	96	<LOD	337	3869	0.40	0.20	4.9	0.75	4.7	317.0	81.12	0.04	5.93	12.57	1.201	8.07	4.69	0.02	1.48	0.04
	5-L	A	2	0.31 +/- 0.07	190	2979	59.57	100	<LOD	346	3958	0.40	0.19	5.2	0.64	4.7	381.2	80.63	0.04	6.48	12.67	1.322	8.36	4.99	<LOD	1.62	0.04
	5-H	A	1	0.15 +/- 0.05	93	1120	24.07	66	<LOD	170	1225	0.18	0.09	<LOD	0.27	1.2	106.9	14.89	<LOD	1.99	5.76	0.327	3.08	1.45	<LOD	0.62	0.01
	5-H	A	2	0.39 +/- 0.08	107	1339	29.04	66	<LOD	146	1497	0.19	0.11	<LOD	0.33	1.3	124.6	18.05	<LOD	2.38	6.60	0.383	3.57	1.70	<LOD	0.74	0.02
AWFW	4	A	1	ND	220	533	27.39	184	<LOD	216	649	0.16	0.16	<LOD	0.14	1.4	59.4	9.19	<LOD	1.09	2.41	0.265	1.71	2.08	<LOD	1.94	<LOD
	4	A	2	0.08 +/- 0.14	153	386	12.51	86	<LOD	153	487	0.11	0.11	<LOD	0.10	1.0	27.8	6.15	<LOD	0.83	1.90	0.183	1.19	1.57	<LOD	1.44	<LOD
	5-L	A	1	0.16 +/- 0.26	409	1038	34.97	284	244	250	1218	0.29	0.13	5.0	0.25	0.6	105.8	31.49	<LOD	2.25	5.38	0.317	2.60	1.52	<LOD	0.50	0.02
	5-L	A	2	0.17 +/-0.18	310	950	15.13	221	<LOD	179	1105	0.28	0.12	4.3	0.23	0.6	67.9	31.90	<LOD	1.92	4.93	0.320	2.57	1.46	<LOD	0.48	0.02
	5-H	A	1	0.17 +/- 0.04	320	148	26.01	242	<LOD	164	181	0.12	<LOD	3.5	0.04	<LOD	9.4	37.98	<LOD	0.47	1.48	0.086	0.40	0.30	<LOD	0.23	<LOD
	5-H	A	2	0.25 +/- 0.04	374	210	32.50	261	<LOD	217	259	0.16	<LOD	4.4	0.05	1.3	21.2	43.38	<LOD	0.60	2.09	0.114	0.59	0.42	<LOD	0.45	<LOD
AWHB	4	A	1	0.01 +/- 0.02	126	414	23.14	104	<LOD	173	464	0.11	0.11	<LOD	0.11	1.5	46.5	11.74	<LOD	0.80	2.93	0.223	1.17	2.45	<LOD	1.76	<LOD
	4	A	2	0.08 +/- 0.13	120	465	24.55	71	<LOD	192	528	0.12	0.11	<LOD	0.13	1.7	51.5	12.99	<LOD	0.93	2.36	0.245	1.32	2.60	<LOD	1.92	0.01
	4	A	3	0.07 +/- 0.08	437	609	33.27	413	228	425	646	0.20	0.19	7.5	0.17	2.2	67.5	15.73	0.03	1.20	5.38	0.312	1.99	3.10	<LOD	2.33	0.01
	4	B	1	ND	141	506	27.38	107	<LOD	201	554	0.13	0.13	<LOD	0.14	1.9	55.6	13.17	<LOD	0.98	2.91	0.258	1.42	2.93	<LOD	2.09	0.01
	4	B	2	0.14 +/- 0.04	252	634	32.61	232	<LOD	325	676	0.17	0.16	5.4	0.17	2.2	72.0	17.67	0.05	1.24	4.63	0.335	1.93	3.44	<LOD	2.28	0.01
	5-L	A	1	ND	137	160	18.54	97	<LOD	88	236	0.08	<LOD	<LOD	0.05	0.2	16.0	26.16	<LOD	0.49	1.11	0.110	0.41	0.40	<LOD	0.26	<LOD
	5-H	A	1	0.15 +/- 0.13	295	503	22.82	220	<LOD	170	639	0.18	0.08	<LOD	0.14	0.3	54.3	14.42	<LOD	1.15	2.91	0.152	1.39	0.93	<LOD	0.31	<LOD
	5-H	B	1	0.22 +/- 0.07	291	497	22.39	208	<LOD	165	572	0.16	<LOD	<LOD	0.13	0.3	48.1	12.68	<LOD	1.05	2.57	0.134	1.30	0.88	<LOD	0.27	<LOD
	5-H	B	2	0.18 +/- 0.10	297	503	21.88	212	<LOD	171	606	0.18	0.08	<LOD	0.14	0.3	53.0	14.87	<LOD	1.11	2.82	0.145	1.31	0.90	<LOD	0.29	<LOD

Table 11.2 *Particulate concentrations (in µg/kg) and isotopic composition (in ‰) of UAW samples (T.: Sampling trip; B.: Bottle, F.: Filter).*

3. SFA (Storm Flow Archives) Results

Discharge data from USGS stream gauges for each sample are reported in **Table 12**. Major- and trace element concentrations, as well as Cu and Fe isotopic ratios of dissolved storm flow samples can be found in **Table 13**.

Sample Site	Date	Time	Discharge (USGS) ft^3/s
MWK	1999-01-30	17:45	13
MWK	1999-01-30	18:12	12
MWK	1999-01-30	19:36	24
MWK	1999-01-30	20:06	18
MWK	1999-01-30	20:36	14
MWK	1999-01-30	22:43	17
MWK	1999-01-30	23:13	13
MWK	1999-01-31	3:11	49
MWK	1999-01-31	3:41	35
MWK	1999-01-31	4:11	25
MWK	1999-01-31	4:41	21
MWK	1999-01-31	5:11	18
MWK	1999-01-31	5:41	25
MWK	1999-01-31	6:11	28
MWK	1999-01-31	6:41	29
MWK	1999-01-31	7:11	45
MWK	1999-01-31	7:41	28
MWK	1999-01-31	8:11	25
MWK	1999-01-31	8:41	23
MWK	1999-01-31	9:11	20
MWK	1999-01-31	9:41	19
MWK	1999-01-31	10:11	17
MWK	1999-11-07	11:21	16
MWK	1999-11-07	11:51	19
MWK	1999-11-07	12:21	20
MWK	1999-11-07	12:51	23
MWK	1999-11-07	13:21	47
MWK	1999-11-07	13:51	30
MWK	1999-12-01	8:47	31
MWK	1999-12-01	9:17	57
MWK	1999-12-01	9:47	31
MWK	2001-02-11	16:59	ND
MWK	2001-02-11	17:29	ND
MWK	2001-02-12	18:27	ND
MWK	2001-02-12	18:57	ND
MWK	2000-08-27	0:47	22

Sample Site	Date	Time	Discharge (USGS) ft^3/s
MWK	2000-08-27	2:16	26
KHS	1999-11-07	13:49	81
KHS	1999-11-07	14:18	132
KHS	1999-11-07	14:48	132
KHS	1999-11-07	15:18	112
KHS	1999-11-07	16:12	88
KHS	2001-02-11	18:22	175
KHS	2001-02-12	15:32	206
KHS	2001-02-11	17:52	214
KHS	2001-02-12	19:20	543
KHS	2001-02-12	19:50	320
KHS	2001-02-12	20:20	219
KHS	2001-02-12	20:50	242
KHS	2001-02-12	21:20	317
KHS	2001-02-12	21:50	152
KHS	2001-02-13	3:35	136

Table 12. *Discharge in cubic feet per second for all storm samples from USGS discharge gauges at locations Waiakeakua (MWK) and Kaimuki High School (KHS).*

Date	Time	$\delta^{56}Fe$	$\delta^{65}Cu$	Mg	Al	Si	P	S	K	Ca	Fe	Li	B	Rb	Sr	Y	Ba	Ti	Mn	Mo	V	Cr	Co	Ni	Cu	Cd	Pb
1999																											
01/30	**17:45**		ND	3431	53.9	5137	50.4	936	1011	5379	46.94	<LOD	<LOD	0.70	33.71	0.05	1.66	2.70	0.38	0.03	1.13	0.69	0.021	0.99	1.45	<LOD	0.59
	18:12		ND	2963	41.2	4350	30.8	1084	1060	4392	40.16	<LOD	<LOD	0.75	29.73	0.06	0.99	2.80	0.41	0.03	0.75	0.50	0.017	0.63	2.98	<LOD	0.20
	19:36		ND	2189	51.5	3118	23.8	899	1081	3098	42.26	<LOD	<LOD	0.76	21.95	0.11	1.10	1.79	0.35	0.14	0.49	0.50	0.023	0.78	1.68	<LOD	0.11
	20:06		ND	2474	73.3	3578	30.4	810	1040	3437	66.03	<LOD	<LOD	0.72	24.26	0.10	1.14	3.45	0.58	0.08	0.62	0.59	0.023	0.77	1.50	<LOD	0.08
	20:36		ND	2674	137.3	3972	29.7	798	1121	4170	112.45	0.04	102	0.68	29.42	0.14	1.03	6.32	1.09	0.03	0.70	0.74	0.037	1.14	1.39	<LOD	0.40
	22:43		ND	2323	104.2	3311	49.2	783	1257	3013	90.02	0.03	<LOD	0.69	20.56	0.11	0.85	4.36	0.70	0.03	0.58	0.68	0.027	0.91	1.72	<LOD	0.42
	23:13		ND	2425	104.9	3515	38.1	752	1145	3407	88.26	<LOD	<LOD	0.64	22.50	0.09	1.05	4.91	0.72	<LOD	0.66	0.61	0.026	0.79	1.37	<LOD	1.33
01/31	**3:11**		ND	1998	101.5	2464	41.3	956	1868	3071	93.05	0.07	105	0.89	20.83	0.13	1.32	4.52	0.99	<LOD	0.59	0.78	0.036	1.64	2.04	<LOD	0.41
	3:41		ND	2095	146.6	2910	33.2	774	1573	3152	130.64	0.04	<LOD	0.74	22.06	0.15	1.42	6.93	0.95	<LOD	0.71	0.80	0.034	1.04	1.74	<LOD	0.25
	4:11		ND	2246	175.4	3120	25.0	741	1220	3146	123.24	<LOD	<LOD	0.56	21.69	0.18	0.78	7.29	1.02	<LOD	0.76	0.71	0.032	0.89	1.22	<LOD	0.10
	4:41		0.23 +/- 0.08	2331	140.3	2958	29.8	862	1444	3136	109.04	0.06	98.44	0.64	24.00	0.18	0.69	6.27	0.78	0.42	0.66	0.70	0.028	0.87	1.30	<LOD	1.15
	5:11		0.26 +/- 0.04	2593	143.1	3465	27.6	820	1361	3779	105.14	0.04	<LOD	0.61	26.36	0.18	1.27	6.09	0.82	<LOD	0.76	0.68	0.031	1.06	1.39	<LOD	0.13
	5:41		-0.15 +/- 0.10	2351	173.5	3315	44.0	776	1324	4769	136.23	<LOD	<LOD	0.59	23.25	0.13	1.20	7.94	1.07	<LOD	0.96	0.77	0.037	1.14	1.28	<LOD	0.20
	6:11		ND	2154	145.2	2940	36.4	776	1477	3037	116.16	0.04	<LOD	0.68	20.73	0.10	1.00	6.52	0.82	<LOD	0.68	0.72	0.033	1.14	1.34	<LOD	0.21
	6:41		0.31 +/- 0.04	2056	127.0	2788	23.3	796	1498	2863	94.28	<LOD	<LOD	0.70	20.53	0.09	1.09	5.28	0.71	<LOD	0.57	0.56	0.031	0.83	1.21	<LOD	0.30
	7:11		0.35 +/- 0.06	1565	80.0	2270	51.7	694	1560	3011	66.02	0.05	<LOD	0.74	21.92	0.10	5.86	2.97	1.05	0.07	0.65	0.73	<LOD	1.05	1.91	<LOD	0.51
	7:41		0.21 +/- 0.04	1770	106.0	2763	34.7	659	1299	2845	82.65	0.04	<LOD	0.62	20.79	0.12	1.23	4.34	0.93	<LOD	0.62	0.63	<LOD	1.11	1.23	<LOD	0.68
	8:11		0.34 +/- 0.01	1930	190.7	3179	28.1	656	1150	2709	130.72	<LOD	<LOD	0.55	21.19	0.13	0.77	7.50	1.02	<LOD	0.69	0.69	<LOD	0.83	1.13	<LOD	0.06
	8:41		-0.67 +/- 0.09	2017	112.8	3231	29.2	669	1243	2957	84.13	0.04	<LOD	0.59	22.33	0.13	0.99	4.59	0.68	0.09	1.74	0.66	<LOD	0.70	1.20	<LOD	0.15
	9:11		ND	2157	114.2	3550	26.5	644	1117	3093	84.04	0.04	<LOD	0.54	23.15	0.10	1.36	5.03	0.77	0.06	0.72	0.61	<LOD	0.88	1.03	<LOD	0.25
	9:41		0.32 +/- 0.04	2248	104.5	3856	35.4	677	1117	3250	73.23	<LOD	<LOD	0.55	23.13	0.07	0.93	4.50	0.73	0.03	0.80	0.58	<LOD	0.88	0.98	<LOD	0.19
	10:11		0.33 +/- 0.05	2456	98.4	3941	80.4	706	1226	3618	77.65	0.04	<LOD	0.56	23.03	0.06	0.68	4.31	0.63	<LOD	0.70	0.58	<LOD	0.76	0.80	<LOD	0.33

Table 13.1 *Dissolved concentrations (in µg/kg) and Fe and Cu isotopic ratios (in ‰) of SFA samples at MWK.*

Date	Time	δ^{56}Fe	δ^{65}Cu	Mg	Al	Si	P	S	K	Ca	Fe	Li	B	Rb	Sr	Y	Ba	Ti	Mn	Mo	V	Cr	Co	Ni	Cu	Cd	Pb
1999																											
11/07	**11:21**		0.46 +/- 0.12	2580	37.7	4545	53.2	680	1809	3507	32.79	0.04	<LOD	0.98	27.35	0.16	1.66	1.03	0.28	<LOD	0.98	0.56	<LOD	0.67	2.49	<LOD	0.16
	11:51		0.42 +/- 0.04	2207	43.9	3681	71.9	692	1652	2986	38.45	<LOD	<LOD	0.90	23.09	0.18	0.86	1.29	0.66	<LOD	0.87	0.53	<LOD	0.83	2.23	<LOD	0.26
	12:21		0.44 +/- 0.14	2612	91.6	4296	38.5	687	1642	4043	72.33	0.07	98	0.95	29.48	0.17	1.42	2.52	0.69	<LOD	0.95	0.68	<LOD	1.33	2.15	<LOD	0.51
	12:51		0.44 +/- 0.06	1950	73.2	3050	31.1	628	1697	2767	56.14	<LOD	<LOD	0.83	21.61	0.26	0.81	1.69	0.36	<LOD	0.71	0.64	<LOD	0.89	2.05	<LOD	0.07
	13:21		0.47 +/- 0.08	2111	69.1	2391	26.3	664	1785	2759	50.58	0.05	<LOD	0.88	21.21	0.23	1.71	1.22	1.58	<LOD	0.69	0.59	<LOD	1.47	2.16	<LOD	0.58
	13:51		0.33 +/- 0.04	1704	86.4	2438	32.0	646	1676	2614	64.66	0.04	<LOD	0.78	20.96	0.25	0.90	2.62	0.55	<LOD	0.74	0.61	<LOD	0.89	1.97	<LOD	0.52
12/01	**8:47**	0.30 +/- 0.05	0.48 +/- 0.04	2637	41.6	3559	39.4	895	2136	3829	44.35	0.04	<LOD	1.01	25.49	0.12	1.60	1.62	0.39	0.04	1.37	0.65	0.032	1.13	2.25	<LOD	0.04
	9:17	0.31 +/- 0.05	0.43 +/- 0.06	2058	46.7	2770	22.9	868	1920	3292	42.79	<LOD	<LOD	1.02	23.51	0.12	1.14	1.50	0.68	<LOD	0.80	0.52	0.031	1.01	1.89	<LOD	0.19
	9:47	0.31 +/- 0.05	0.46 +/- 0.04	2016	51.8	2483	59.1	691	1477	3024	40.85	<LOD	<LOD	0.74	21.35	0.22	0.57	1.38	0.44	<LOD	0.69	0.50	0.022	0.72	1.76	<LOD	0.13
2000																											
08/27	**0:47**	0.36 +/- 0.05	0.40 +/. 0.08	2511	59.6	3612	21.9	764	1254	3700	41.62	0.04	114	0.79	24.87	0.12	0.67	1.61	0.36	<LOD	1.06	0.47	0.034	2.28	1.67	<LOD	0.37
	1:16	0.32 +/- 0.05	0.47 +/- 0.04	2179	59.3	3334	50.4	722	1258	3263	52.50	0.03	<LOD	0.74	22.65	0.16	0.75	2.04	0.42	<LOD	0.94	0.44	0.032	1.22	2.51	<LOD	0.45
	1:46	0.33 +/- 0.05	0.32 +/- 0.18	2040	79.9	3032	18.4	719	948	3174	71.46	0.03	108	0.65	22.05	0.23	1.17	2.79	0.40	<LOD	0.94	0.51	0.034	0.83	1.66	<LOD	0.43
	2:16	0.27 +/- 0.05	0.44 +/- 0.04	1767	74.8	2642	23.8	674	840	2814	60.77	<LOD	<LOD	0.53	18.68	0.28	0.40	2.33	0.34	<LOD	0.81	0.46	0.030	0.62	1.48	<LOD	0.13
2001																											
02/11	**16:59**	0.25 +/- 0.05	0.53 +/- 0.06	3007	41.8	4565	29.1	789	2025	4715	43.04	0.05	<LOD	1.09	32.06	0.06	2.20	1.87	0.37	<LOD	1.17	0.62	0.036	1.14	2.03	<LOD	0.34
	17:29	0.11 +/- 0.05	0.15 +/- 0.08	2222	131.3	3108	27.8	795	1476	3322	96.00	0.04	<LOD	0.74	25.23	0.16	0.44	4.79	0.60	<LOD	1.13	0.60	0.038	0.78	1.55	<LOD	0.05
02/12	**18:27**	0.25 +/- 0.05	0.41 +/- 0.04	1748	88.5	2728	35.2	810	1482	3204	71.42	0.05	<LOD	0.81	19.33	0.14	1.55	3.21	0.76	<LOD	0.95	0.62	0.041	1.48	2.76	<LOD	1.30
	18:57	0.19 +/- 0.05	0.49 +/- 0.04	1761	100.8	2628	27.7	840	1403	2817	79.55	<LOD	<LOD	0.73	18.62	0.16	0.70	3.87	0.58	<LOD	1.02	0.58	0.037	1.04	1.80	<LOD	0.21

Table 13.1 ct'd.

Date	Time	δ^{65}Cu	Mg	Al	Si	P	S	K	Ca	Fe	Li	B	Rb	Sr	Y	Ba	Ti	Mn	Mo	V	Cr	Co	Ni	Cu	Cd	Pb
1999																										
11/07	**13:49**	ND	3477	20.5	3721	86.6	1326	2236	10291	18.70	<LOD	<LOD	1.23	68.33	0.02	2.86	0.59	<LOD	0.24	1.30	0.47	0.197	0.83	4.09	<LOD	0.08
	14:18	ND	2925	13.1	3595	130.3	1155	1719	5062	11.05	0.05	<LOD	1.11	43.37	0.04	2.03	0.28	<LOD	0.16	1.08	0.45	<LOD	0.65	3.14	<LOD	0.17
	14:48	0.42 +/- 0.04	2626	15.3	3209	37.1	1084	2190	4749	14.94	0.04	<LOD	1.12	37.74	0.05	1.82	0.39	<LOD	0.11	1.09	0.41	<LOD	1.20	3.18	<LOD	0.08
	15:18	0.44 +/- 0.04	2639	25.2	3186	96.3	1282	1804	4523	22.72	<LOD	<LOD	1.17	38.63	0.08	1.80	0.78	<LOD	0.13	1.05	0.49	<LOD	0.80	2.95	<LOD	0.08
	16:12	0.43 +/- 0.07	2560	35.9	2581	22.7	1249	1767	4246	31.76	0.05	104.86	1.15	36.91	0.09	1.73	1.34	0.43	0.11	0.85	0.47	<LOD	0.75	2.47	<LOD	2.13
2001																										
02/11	**17:52**	ND	12538	13.4	3380	123.2	8995	8101	14904	35.59	1.00	<LOD	2.81	163.45	<LOD	15.44	0.51	13.13	0.25	1.84	0.32	0.280	1.56	2.46	<LOD	0.08
	18:22	0.79 +/- 0.05	3263	70.3	3104	146.1	1831	2495	6471	75.51	0.05	115	1.32	57.06	0.05	3.70	2.05	0.50	0.20	2.05	0.58	0.056	1.24	3.40	0.11	0.17
02/12	**15:32**	0.84 +/- 0.04	2757	85.3	2504	134.2	1895	2984	8056	64.97	0.13	<LOD	1.40	77.68	0.06	9.61	2.17	0.51	0.55	2.97	0.83	0.073	2.12	7.64	<LOD	0.23
	19:20	-0.17 +/- 0.06	2886	63.1	2246	31.5	1720	2203	5089	58.66	0.05	<LOD	1.06	46.54	0.08	2.24	2.35	0.68	0.12	1.37	0.43	0.064	1.12	2.63	<LOD	0.08
	19:50	0.55 +/- 0.04	2223	70.8	2287	145.3	1373	2130	4850	54.52	0.05	<LOD	1.07	39.98	0.06	1.97	2.38	0.40	0.16	1.26	0.62	0.049	1.09	2.87	<LOD	0.05
	20:20	0.56 +/- 0.04	1862	91.7	1846	98.6	1213	1924	4197	63.69	<LOD	99	0.93	33.08	0.07	1.46	3.62	0.49	0.14	1.46	0.60	0.050	1.14	2.92	<LOD	0.22
	20:50	0.60 +/- 0.04	2533	104.5	2280	125.6	1586	2343	5376	78.62	0.06	90	1.13	45.29	0.06	2.50	3.74	0.58	0.17	1.30	0.77	0.053	1.09	3.06	<LOD	0.09
	21:20	0.54 +/- 0.07	2463	92.6	2210	96.5	1577	2540	6721	68.74	0.13	<LOD	1.19	61.42	0.06	5.58	3.20	0.67	0.27	1.53	1.01	0.058	1.51	5.00	<LOD	0.17
	21:50	0.54 +/- 0.04	2312	94.2	2091	157.8	1536	2242	5918	67.45	0.09	<LOD	1.06	50.30	0.05	4.13	3.21	0.42	0.22	1.61	0.83	0.056	1.28	3.97	<LOD	0.13
02/13	**3:35**	0.51 +/- 0.04	4115	92.3	4321	97.2	2295	2013	8417	88.87	<LOD	<LOD	1.05	66.33	0.06	3.04	4.27	0.66	0.10	1.54	0.71	0.052	1.14	2.58	<LOD	0.28

Table 13.2 *Dissolved concentrations (in µg/kg) and Fe and Cu isotopic ratios (in ‰) of SFA samples at KHS.*

4. Dissolved and Particulate Concentrations at Low Flow Manoa stations

The most pristine stream sampled in this study is located at MWK. Waiakeakua stream drains the eastern part of Manoa valley, and has the lowest concentrations of all major ions, except Si, as well as the lowest dissolved Fe concentrations compared to other LFM stations (see **Table 9**). The dissolved phase at MWK also shows higher Cr and V (2-3 fold), and lower Ni (about 50%) compared to the other LFM stations. The composition of suspended particles at MWK is consistent with bedrock lithology. Particulate V, Al, Cr, Ni, and Co are all 2-3 times higher here than observed at other LFM stations, and because these elements naturally occur at high concentrations in basalt, this indicates the presence of a large fraction of basalt (derived) particles in the suspended load.

The watershed surrounding the MWH station remains relatively undeveloped, with the exception of a botanical garden and a recreational facility/park. Waters from Wa'ihi have high dissolved Mn concentrations, and only about 50% as much dissolved V as the other LFM stations. Additionally, suspended particles here are rich in Fe, and have particularly high Fe/Al relative to the other stations. In combination, these features strongly suggest an enhanced source of Fe, probably related to redox processes (i.e input of reduced Fe(II)) at this station, which is explored further in the discussion. Rock particles from the post-erosional Honolulu Volcanic Series Tantalus and Sugarloaf lava flows are another potential source of excess particulate Fe at MWH that is absent at MWK. These very recent (76 ka, Clague et al., 2016) lava flows extend exclusively through western Manoa valley (see **Figure 2.2**). That should render their signatures more prominent at MWH, which drains western Manoa, than at MWK, whose drainage area is largely composed of the older tholeiitic Ko'olau Series shield stage basalts in the East. In fact, the Fe/Al ratio of particles at MWH (see **Table 14**) is close to the average composition of the post-erosional Honolulu Volcanic Series lavas, while that of MWK particles resembles Ko'olau Series composition.

	Honolulu Volcanic Series	MWH particles	Koolau Series	MWK particles
Fe/Al	4.9	4.5	1.7	1.4

***Table 14**. Fe/Al (g/g) ratios of particles at MWH and MWK stations (LFM), and average values for Honolulu Volcanics and Ko'olau Series from the literature (Clague & Frey, 1982; Frey et al., 1994; Norman et al., 2004; Patino, 2003; Roden et al., 1984; Sutherland, 1999; Sutherland & Tolosa, 1999).*

Suspended particles at MWH also contain about 13µg/kg P (see **Table 9**), while samples from all other LFM stations cluster around 3µg/kg. Dissolved P is similarly enriched. Partly, this can be explained by the lava flows of the Honolulu Volcanics containing around four times more P than the Ko'olau shield. Phosphorous is also weathered more easily from younger rocks (Honolulu Volcanics), while older rocks (Ko'olau Shield) are usually already depleted (Vitousek et al., 1997). Additionally, it is well-known that reduced Fe can scavenge phosphate from the water

column during oxidation and precipitation, which explains the coupled high particulate concentration of Fe and P (e.g. Van der Grift et al., 2014; Baken et al., 2015). It is also likely that fertilizer runoff from Lyon Arboretum, a botanical facility of the university of Hawai'i that is located directly upstream, contributes substantial amounts of P to MWH. Dissolved Cu at MWH is the lowest of all the LFM stations.

There is considerable residential development around Manoa stream at station MRC but little other land use. The dissolved fraction of water samples exhibits the highest concentrations of Fe in MRC samples, while particulate Fe is the lowest. Dissolved Mn concentrations are also high, which indicates a redox-related source of Mn and Fe, similar to MWH. Because the Fe is in the <0.2µm fraction, it is likely present as oxidized colloidal material, with some potentially in the truly dissolved reduced form. A surprising feature is that MRC samples show the lowest dissolved P concentrations along with the highest dissolved Fe, because Fe(III) generally scavenges very efficiently any phosphate from the water column (e.g. Sholkovitz & Copland, 1982) and, consequently, these two elements are often associated. Because MRC is the first station where water is expected to be affected by concrete channelizing, it is possible that some P is removed from the water due to adsorption to calcium in the channel bed (An & Li, 2008), or that there is biological removal.

The most urbanized station in the LFM set is MKW. It is the most downstream location, and significant portions of the channel upstream include concrete channelization. Additionally, a very large storm drain culvert empties into Manoa stream directly upstream of this station (**Figure 8.2**). Waters from MKW show the highest concentrations of K, S, Ca and Mg, which is consistent with increasing contributions downstream from surface runoff which likely incorporates surface deposited sea spray. Dissolved trace element concentrations, however, do not show a steady increase downstream, although dissolved Cu concentrations are the highest at station MKW. Dissolved tin (Sn) and particulate Mn are both about two times greater than in the remaining LFM samples. Elevated Sn could indicate anthropogenic signatures from wastewater or alloys.

De Carlo et al. (2004) characterized a pool of trace elements with lithological control in Manoa watershed, consisting of V, Cr, Co, and Ni. Interesting patterns, which can provide insight into weathering and transport behaviors and controls, emerge upon investigation of correlations between these elements and others in dissolved and particulate phases of LFM samples (**Figure 15**). Dissolved Cr concentrations show a strong positive correlation with V_{DIS} concentrations (R=0.95), indicating a common source, and they have been observed to behave similarly during basalt weathering (Aiuppa, 2000). Consequently, this study supports lithological control for dissolved V and Cr. Higher Co in the dissolved fraction corresponds to higher Mn_{DIS} and the lower Co values correspond to the lower Mn_{DIS} in LFM samples (R=0.95). The two high Mn samples, MWH and MRC, are the ones with a postulated reducing groundwater source, and Co_{DIS} is also much higher in these samples. Cobalt, which is high in local bedrock, preferentially adsorbs to Mn colloids, which leads to this strong positive correlation (McKenzie, 1989). Nickel also correlates positively with Co_{DIS} (R=0.68), but more strongly with Ba_{DIS} (R=0.87), which was characterized as an anthropogenically dominated element by De Carlo et al. (2004). Interestingly, the extreme points of all of these regressions are the two most untouched sampling stations,

MWK and MWH, with MWK low in dissolved Co, Ni, Ba, and Mn, and MWH high in these elements. This relationship is reversed for V_{DIS} and Cr_{DIS}, which are comparatively enriched at MWK, and depleted at MWH. Both MRC and MKW plot in the middle, roughly on a theoretical mixing line between MWK and MWH endmembers for all of these relationships.
Particles at MWK are the highest among LFM samples in all four predominantly lithogenic trace metals (Co, Cr, V, Ni), while all three other sites have relatively similar concentrations.

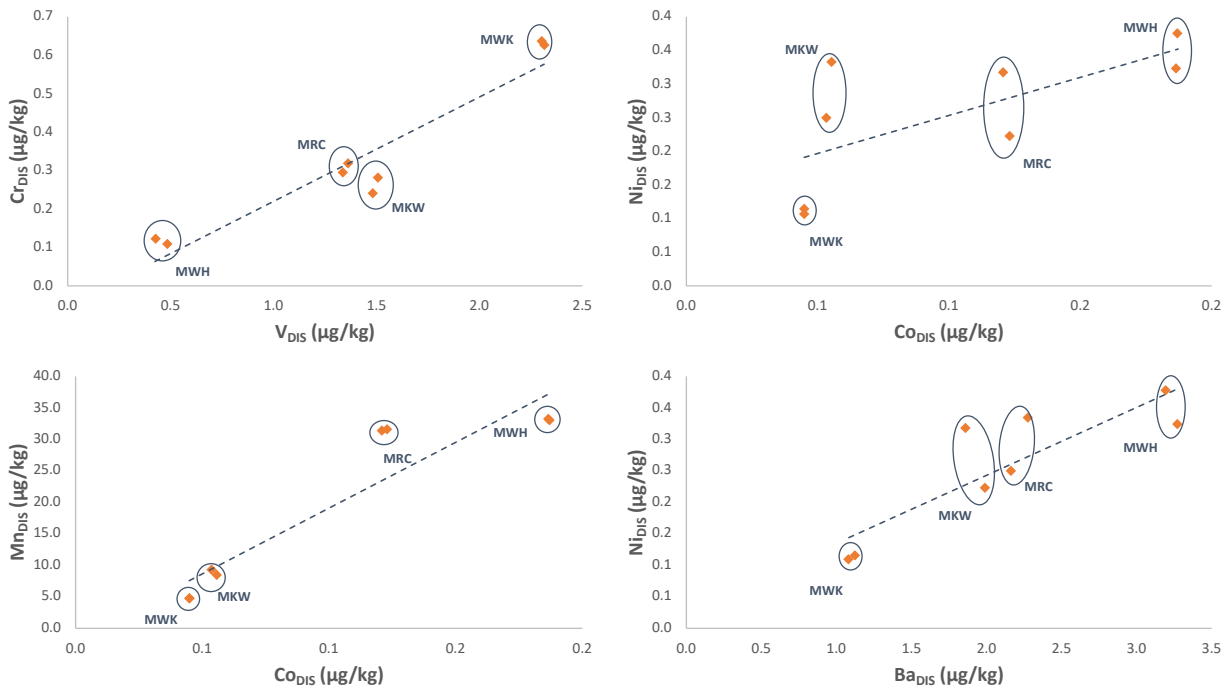

Figure 15. *Correlations between dissolved trace elements across LFM samples.*

5. <u>Isotopic Composition of Dissolved and Particulate Fractions at Low Flow Manoa stations</u>

Dissolved $\delta^{65}Cu$ ($\delta^{65}Cu_{DIS}$) values in water samples (**Table 9**, **Figure 16**) are positive, i.e. heavier than bedrock ratios (0.04-0.14‰, Liu et al. (2015)), at all stations. Values range from 0.66‰ at MKW to 1.06‰ at MWK. The $\delta^{65}Cu$ of particles ($\delta^{65}Cu_{SPM}$) is much more variable, and lighter (-0.91 to +0.31‰) than the dissolved load. Surprisingly, the particulate Cu concentrations (per kg of water) are similar, despite the large shifts in $\delta^{65}Cu_{SPM}$. Additionally, the Cu/Ti ratio, which can be used to normalize to the amount of SPM present, is virtually the same in all LFM samples, indicating a similar concentration of Cu per kg of particles, except for a ratio at station MWK that has much lower Cu/Ti. Here, particulate concentrations of Cu were too low to measure isotopic ratios.

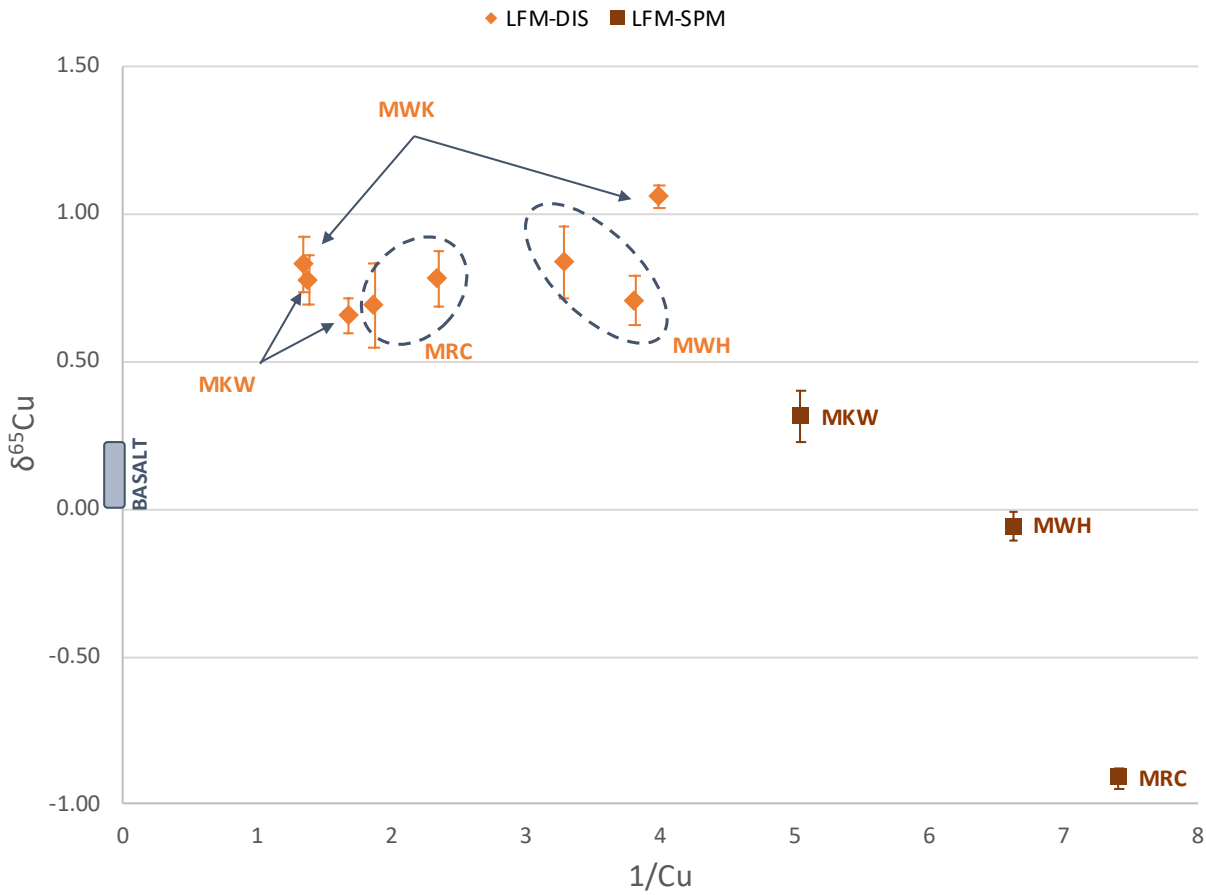

Figure 16. *Isotopic composition and inverse concentrations of Cu in dissolved (DIS) and particulate (SPM) samples of LFM sample set. Basalt δ^{65}Cu from Liu et al., 2015.*

Dissolved δ^{56}Fe ($\delta^{56}Fe_{DIS}$) values cluster in two groups (**Table 9**, **Figure 17**): One contains samples that have variable Fe concentrations and an isotopic signature close to 0‰ at MWK and MWH, the upstream stations, and another that includes samples with elevated Fe concentrations and much more negative in $\delta^{56}Fe_{DIS}$, observed at MRC and MKW, the more downstream stations. Particulate Fe isotopic compositions are less variable, with MWK and MWH also close to 0‰ (+0.07 and -0.04‰), and MRC and MKW, again, lighter than that (-0.36‰ and -0.21‰).

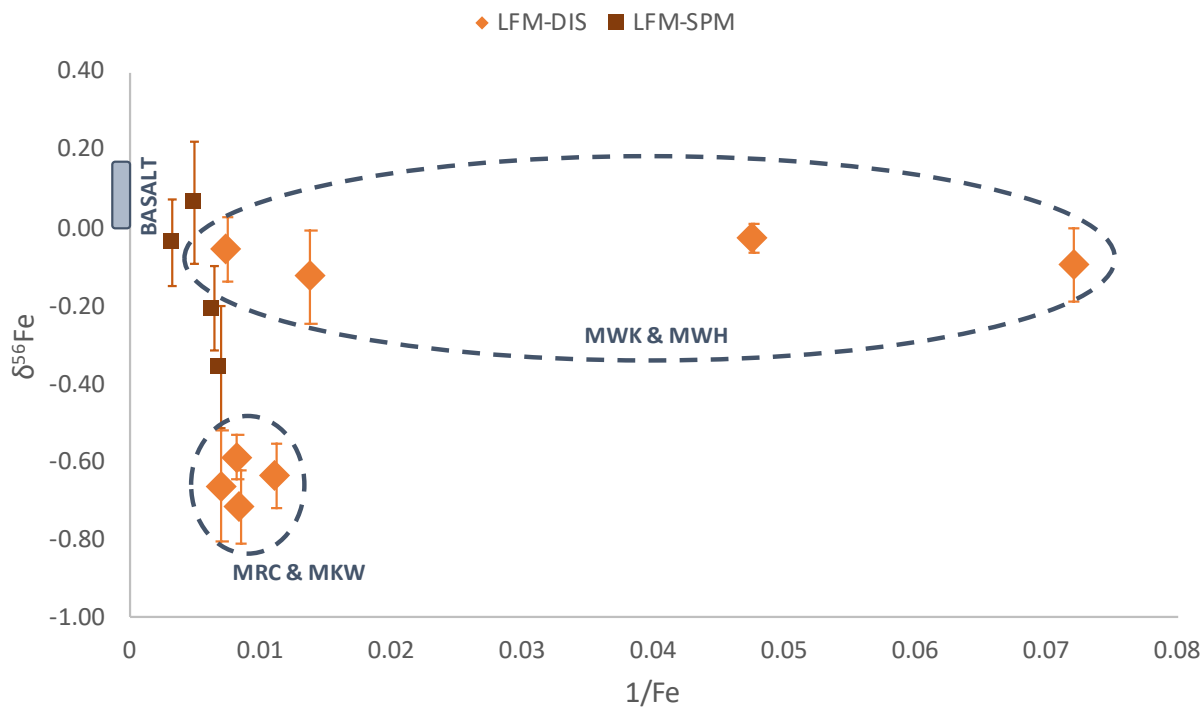

Figure 17. *Isotopic composition and inverse concentrations of Fe in dissolved and particulate samples of LFM sample set. Basalt δ^{56}Fe from Teng et al., 2013.*

The offset between the isotopic ratio of the dissolved and particulate fractions (**Table 15**) is described as:

$$\Delta^{56}Fe_{DIS\text{-}SPM} = \delta^{56}Fe_{DIS} - \delta^{56}Fe_{SPM}$$

$$\Delta^{65}Cu_{DIS\text{-}SPM} = \delta^{65}Cu_{DIS} - \delta^{65}Cu_{SPM}$$

Negative Δ^{56}Fe values are observed at all stations (albeit smaller than the uncertainty at two locations). This indicates lighter dissolved- than particulate δ^{56}Fe. This is a feature that has been observed in other river systems, but is not nearly as common as the characteristic heavy dissolved Cu pool. When dissolved δ^{56}Fe is light, it is often associated with inputs from soil solutions that have a redox influence (Schuth & Mansfeldt, 2016; Garnier et al., 2017). Additionally, an anthropogenic input of Fe was associated with light dissolved δ^{56}Fe (Chen et al., 2014) In multiple studies, river δ^{56}Fe was found to be isotopically homogeneous between dissolved and particulate phases (Bergquist & Boyle, 2006), or the dissolved fraction was isotopically heavier, often due to colloids enriched in heavy Fe (Bergquist & Boyle, 2006; Escoube et al., 2009; Ilina et al., 2013a; Mulholland et al., 2015).

The offset of Δ^{65}Cu of up to 1.69‰ between light Cu in particles and heavy Cu in the dissolved fraction is consistent with observations in other river systems, such as the data by Vance et al. (2008), who reported Δ^{65}Cu of +0.8 to +1.6‰.

Station	$\Delta^{56}Fe_{DIS-SPM}$	$\Delta^{65}Cu_{DIS-SPM}$
MWK	-0.09	ND[1]
MWH	-0.02	0.90
MRC	-0.31	1.69
MKW	-0.43	0.34

Table 15. *Offset between Fe and Cu isotope ratios of dissolved and particulate fractions of LFM samples. [1]Cu concentrations too low to measure isotopic ratios.*

6. Dissolved and Particulate Concentrations at the Urban Ala Wai Stations

Dissolved and particulate samples taken in the channel leading up to the Ala Wai Canal (KHS), as well as in the Canal itself (AWFW, AWHB), show vastly different composition from LFM samples (**Table 11**). Concentrations of Fe_{DIS}, Al_{DIS} and Ti_{DIS} are not much higher in UAW than in the samples collected during baseflow (LFM) in the upper watershed, but many elements with potentially large anthropogenic sources, such as Cu, Pb, Ba, are enriched considerably in the dissolved fraction of most UAW samples. Additionally, there is a much larger amount of SPM in UAW samples than in the LFM samples, as indicated by about ten-fold higher concentrations of Al_{SPM} and Ti_{SPM}.

The geochemical composition of the UAW samples is influenced by mixing of freshwater and seawater throughout the estuary, as evidenced by differences in salinity and major ion concentrations between samples collected at high- and low tides. The first sampling trip to KHS, AWFW and AWHB took place close to low tide (trip 4), and was supplemented with two more trips during low and high tides (5-L and 5-H, respectively). Consequently, differences in geochemical composition observed between the UAW stations can reflect tidal effects as well as differences between sampling days 4 and 5.

Stream discharge is expected to have an influence on the geochemistry of waters at UAW stations. To investigate differences between sampling days, data from a USGS station (16241600) in lower Manoa valley at Woodlawn Drive (see **Figure 4.2**) were evaluated for the 24 hours prior to each sampling trip. The discharge over 24h was similar for all three trips, with cumulative discharge of 1,391,544 ft^3 (4), 1,517,870 ft^3 (5-L) and 1,824,138 ft^3 (5-H). However, trip 4 had more discharge recorded in the three hours immediately before sampling (666,270 ft^3) compared to trips 5L and 5H (391,140 and 217,800 ft^3). The immediately antecedent conditions for each trip therefore represent: higher streamflow conditions and near low tide during trip 4; lower streamflow and low tide during 5L; and lower streamflow and high tide during 4L. These differences allow a clear distinction to be made between tidally- and discharge related influences on the geochemical properties of the water samples.

Station KHS in the Manoa-Palolo Drainage canal is located within the highly urbanized lower portion of the watershed. This part of the stream system receives the combined flows of Manoa and Palolo streams, and the input from numerous storm drains that flow into these streams, and into the combined stream channel. Concentrations of major constituents in these samples are quite variable, which is not surprising given the anticipated tidally influenced nature of the station. The 5H sample had higher concentrations of Mg, Ca, S, K, Rb and Sr (about 2-4 times), which is consistent with increased seawater influence both during high tide and during lower streamflow (**Table 11**). The seawater signature is pronounced despite a measured surface salinity of zero (the zero value is likely the result of the low sensitivity of the refractometer employed). The only element whose concentration was significantly lower in the dissolved fraction of KHS-5H compared to the low tides (by about 50%) is P, whereas most dissolved trace metals (Cu, V, Co, Ni, Cr) were present at similar concentrations in both samples. Particulate concentrations of Cu, V, Co, Ni, Cr, Fe, P and Mn, however, were all significantly lower in the 5-H sample than in either the 5-L or 4 samples. Because Ti and Al concentrations were also lower by about the same amount, it appears that that there was less SPM in the high tide sample. Normalization to the Ti content removes the effect of high vs. low SPM concentrations, revealing excess Cu independent of SPM concentrations. Cu/Ti of KHS-4 is higher (≈0.03) than KHS-5L and 5H (≈0.01), indicating excess Cu at KHS-4 (**Table 11**). Concentrations of Fe were greater (≈2x), and those of Al and Ti were both about ten times higher in the <0.22µm fraction of KHS-5H than in KHS-5L and 5H. This likely reflects contamination of the dissolved sample with particulate matter that passed by the filter or, less likely, the presence of very high colloid concentrations.

Station AWFW is located in the back basin of the Ala Wai Canal. It is behind the sediment sill at the mouth of the Manoa-Palolo Channel, and the bottom sediments at this location are often anoxic (Laws et al., 1993). This site is also characterized by very little circulation, except for slow tidal flushing (Laws et al., 1993). The dissolved fraction of water samples at AWFW shows a composition that indicates increased seawater influence during high tide (5-H) as opposed to the two lower tide sampling trips (4, 5-L): The elements that are typically abundant in seawater relative to stream water, i.e., Mg, S, K, Ca, Li, B, Rb, Sr, and Mo, all approximately double their concentrations at high tide (**Table 11**). Similar to what was observed at KHS, the concentration of P_{DIS} is dramatically lower, by about 90%, in AWFW-5-H compared to samples collected during low tide. The concentrations of Mn_{DIS} and Cu_{DIS} are also lower by 50% and 75%, respectively, in 5-H. The dissolved fraction of AWFW-5-L is very different from both samples 5-H and 4. Concentrations of Al_{DIS} and Ti_{DIS} are enriched 10- and 40-fold in 5-L, respectively, and the concentration of P_{DIS} is twice as high as in AWFW-4 (and 10x higher than in 5-H). Additionally, both the concentrations of Fe_{DIS} and Y_{DIS} are 5x higher in 5-L than in the other two. This could potentially reflect the resuspension of diagenetically altered nanoparticles from the anoxic bed sediment during low flow under the influence of tidal currents. However, there is no visible effect on the concentrations of Cu_{DIS} or other trace metals (Ni, Cr, Co, V) associated with this change in composition. Because there is no dissolved trace metal signature that is characteristic/diagnostic of diagenetic processes, contamination of the dissolved sample with particles is more likely than a diagenetic signature. Particulate concentrations (per kg of water) differ between all three samples at AWFW, with Fe_{SPM}, Al_{SPM} and Ti_{SPM} increasing about two-fold from 5-H < 4 < 5-L (**Table**

11). The concentrations of all transition metals in the particulate phase are also lower in the 5-H sample, except for Mn_{SPM}. The latter actually exhibits the highest Mn concentration of all AWFW samples: Mn/Fe and Mn/Al ratios in this sample are an order of magnitude larger than in 5-L and 4. Particulate Pb is enriched about 4-fold in the AWFW-4 samples (1.44-1.94 µg/kg) compared to both 5-L (0.48-0.50 µg/kg) and 5-H (0.23-0.45 µg/kg), with Pb/Ti at AWFW-4 (≈0.04) twice as high as in 5-H (≈0.02), and an order of magnitude higher than in 5-L (≈0.006).

Station AWHB is located immediately upstream of the Ala Moana Boulevard bridge before the Ala Wai Boat Harbor, and is very close to the coastal ocean. Because AWHB is well downstream into the higher salinity region of the Ala Wai Canal compared to the other canal stations, the difference in geochemistry between high and low tides (5-L vs. 5-H) here should not be as pronounced as the difference between streamflow regimes (4 vs. 5). This is confirmed by examining major ions as well as the trace elements in the three samples: Mg, S, K, Ca, Li, B, Rb, Sr, Mo are all present at about 50% lower concentrations in AWHB-4, which was collected when streamflow was higher, compared to AWHB-5, with little variation evident between 5-L and 5-H. Additionally, AWHB-4 exhibits about two-fold higher concentrations of Cu_{DIS} and Cr_{DIS} than the 5-L or 5-H samples. Concentrations of SPM (as indicated by Al_{SPM} and Ti_{SPM}) are of similar magnitude in 5-H and 4, with about 1/3 the amount present in 5-L (**Table 11**). Similar to what was observed at AWFW, this high-tide sample with the lower SPM concentration is enriched in Mn_{SPM} relative to both 5-L and 4, with Mn/Fe and Mn/Ti an order of magnitude greater than in the other samples from this station.

7. <u>Isotopic Composition of Copper in Dissolved and Particulate Fractions at Urban Ala Wai Stations</u>

Due to a low Cu yield (<50%) in the sample purification process, some $\delta^{65}Cu$ measurements of UAW samples had to be discarded, and are marked as "ND" (**Table 11**). The low yield could potentially reflect the presence of strong Cu-ligands in the water that prevented the complete adsorption onto NTA resin. The $\delta^{65}Cu_{DIS}$ could only be measured for the UAW-4 samples, while the $\delta^{65}Cu_{SPM}$ was not measured for samples KHS-4 and AWHB-5L. Therefore, $\Delta^{65}Cu_{DIS\text{-}SPM}$ could only be evaluated for the AWFW-4A and AWHB-4A and -B sample sets, where the offset was very constant at 0.63‰, 0.61‰, and 0.67‰, respectively (see **Table 11**). All $\delta^{65}Cu_{DIS}$ ratios of samples collected during trip 4 were very similar, between 0.68 and 0.81‰. The minimum and maximum values were both found in duplicate bottles at AWHB, so all UAW-4 samples have the same $\delta^{65}Cu_{DIS}$ within the uncertainty of duplicate bottles. The $\delta^{65}Cu_{SPM}$ of AWFW-4 and AWHB-4A and -B were 0.08‰ at AWFW, and 0.01 to 0.14‰ at AWHB. All particles recovered during the 5-L and 5-H sampling trips at KHS, AWFW and AWHB stations were more positive (heavier) in $\delta^{65}Cu_{SPM}$ (ranging from 0.15‰ at AWHB-5H and KHS-5H to 0.39‰ at KHS-5-H) than particles from AWFW-4 (0.08‰) and AWHB-4 (0.01 to 0.15‰). The large difference between duplicate filters in $\delta^{65}Cu$ values could point to an analytical or filtration issue, or indicate a pool of particulate Cu that is variable in isotopic ratios (i.e. having different settling velocity and therefore heterogeneously distributed).

Ti-normalized Cu values are extremely variable for both 5-L and 5-H, in contrast to sample set 4, which exhibits an overall lower Ti/Cu (i.e. more concentrated in Cu) and less variability (**Figure 18**). There is also a tendency for 5-H and 5-L samples to exhibit higher (i.e. heavier) $\delta^{65}Cu_{SPM}$, but the scatter is quite large. Surprisingly, samples with higher Ti/Cu, which are closer to Ti/Cu of bedrock, which is 117 (Clague & Frey, 1982; Frey et al., 1994; Norman et al., 2004; Patino, 2003; Roden et al., 1984; Sutherland, 1999; Sutherland & Tolosa, 1999) exhibit the $\delta^{65}Cu$ that are furthest from basalt Cu isotopic composition (average 0.09‰, Liu et al., 2015). Potential anthropogenic Cu enrichment and its sources in UAW samples is discussed further in the Synthesis section.

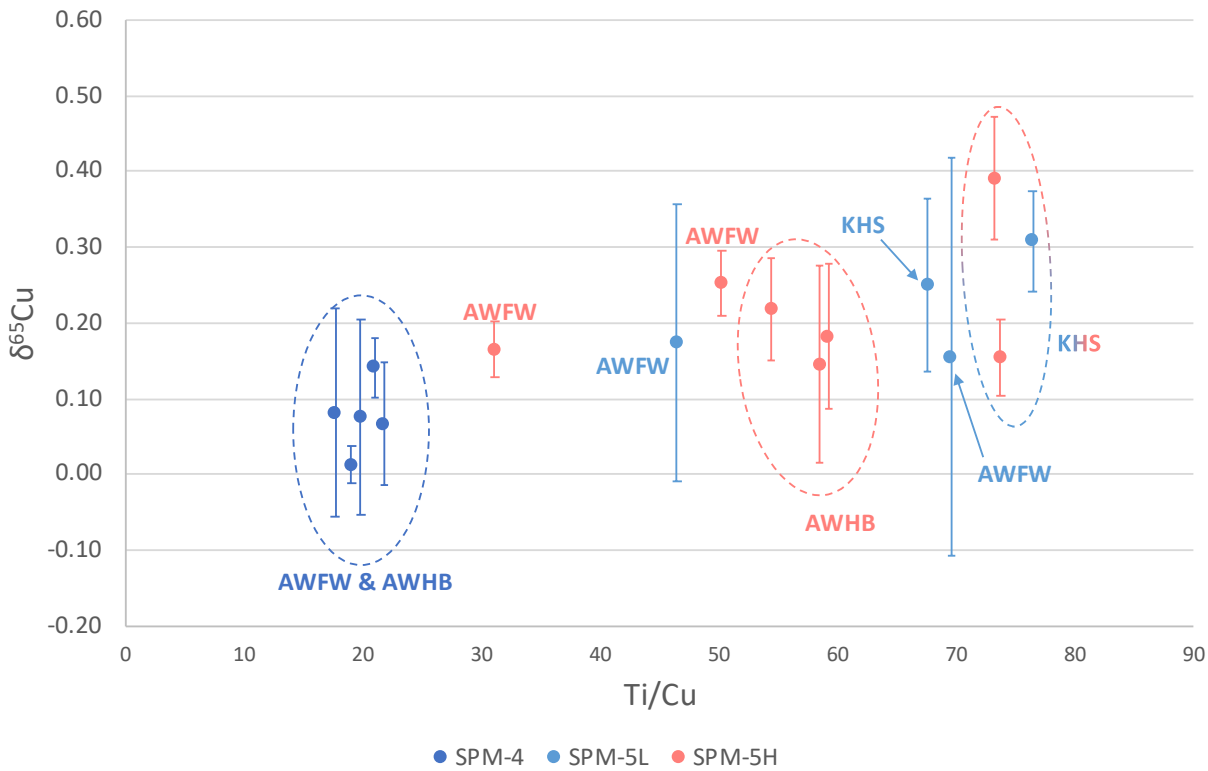

Figure 18. *Ti-normalized Cu concentrations and Cu isotopic composition of particulate UAW samples.*

8. <u>Dissolved Concentrations in SFA (Storm Flow Archive) Samples</u>

Concentrations of trace and major elements in the dissolved fraction are highly variable over the different storm events, and between KHS and MWK stations, in some cases by an order of magnitude. Most trace element concentrations, however, are lower or within in the range of SFA samples for MWK_{LFM} and KHS_{UAW}, with the exception of Mn, which is much more abundant in both modern low flow samples (**Table 13**).

Historical data (see De Carlo et al., 2004) based on the analysis of quarterly, low flow sampling trips between 1997-1999 (data not reported) were gathered to compare modern low flow conditions to those extant about 20 years prior, in order to ascertain whether LFM and UAW samples are representative of a longer-term average of low flow waters (indicated by

concentrations of major elements) and to determine if there are large differences in trace element concentrations between SFA samples, quarterly sample (QS) archives, and modern low flow concentrations.

A comparison of concentrations between QS, SFA and baseflow samples is shown in **Figure 19** for Cu, and in **Figure 20** for major elements. Data from sample MWK_{LFM} are within the range of the QS archive data or very close thereto for all major elements, while sample KHS_{UAW} exhibits lower Si, Ca, and Mg concentrations than the QS archives. Additionally, sample KHS_{UAW} is richer in K than the high end of the QS range. For all four major elements reported here (Mg, Ca, Si, K), sample KHS_{UAW}, despite its "low flow" status, is closer in composition to storm runoff samples than to the quarterly low flow conditions. Similar to K, the concentration of Cu_{DIS} in MWK_{LFM} is in the range of QS samples, while the Cu_{DIS} content of KHS_{UAW} is higher than in QS samples at the same station, and within the range defined by the KHS_{SFA} samples.

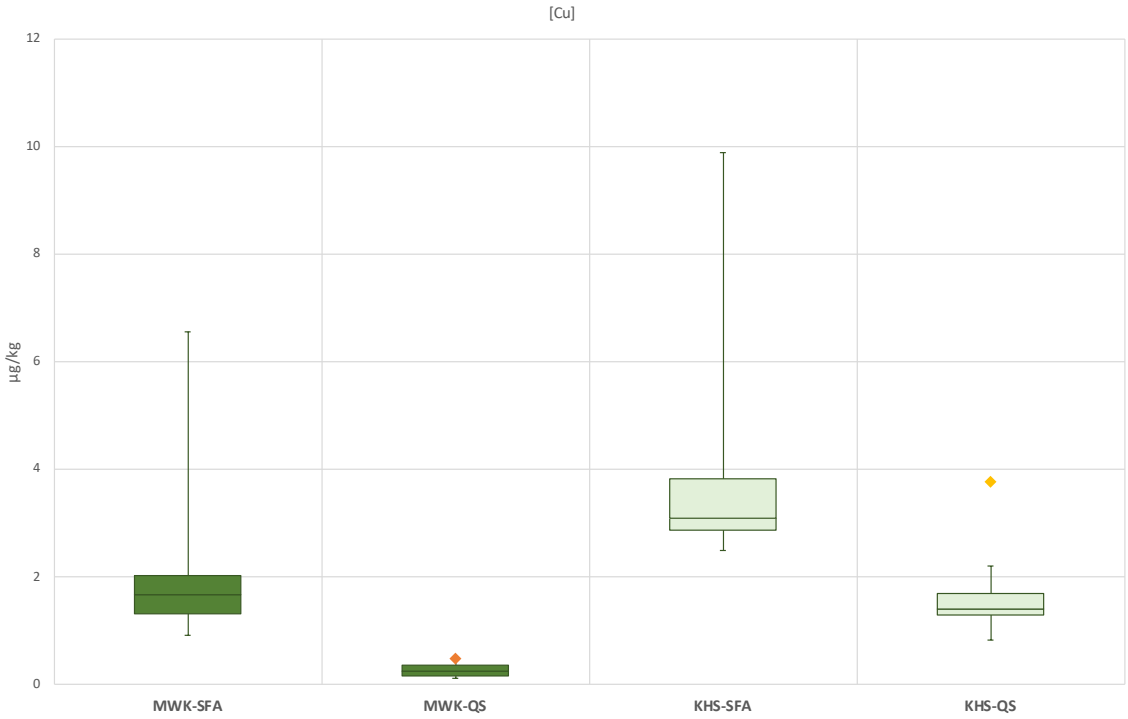

Figure 19. *Concentrations of dissolved Cu in SFA samples compared to LFM and UAW samples at the same stations, and quarterly low flow samples (QS) collected in the late 1990s (De Carlo et al., 2004).*
The box delineates the 1st and 3rd quartile values, the horizontal line represents the median, and the whiskers indicate minimum and maximum values.

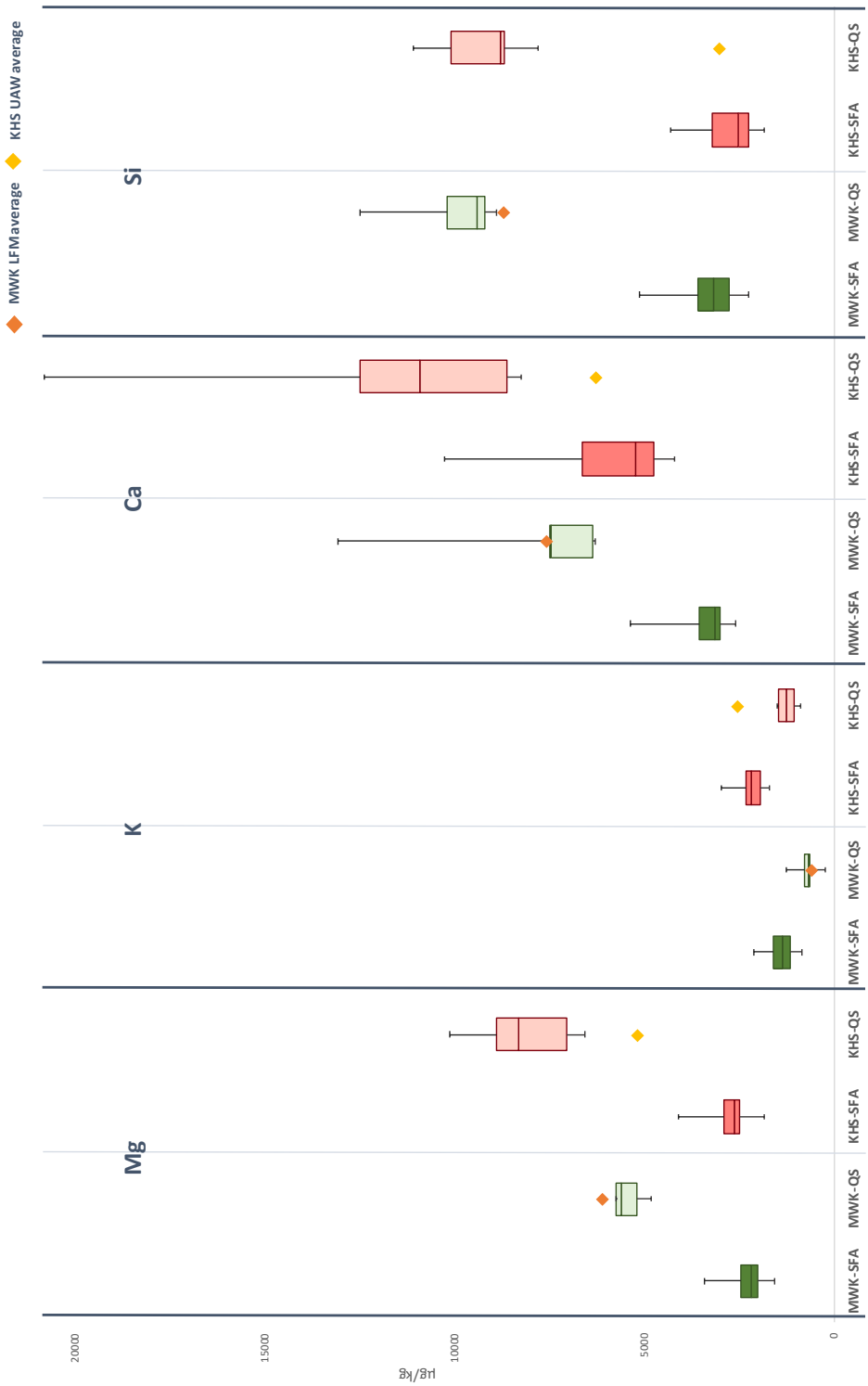

***Figure 20**. Dissolved concentrations of major elements in SFA samples compared to LFM and UAW samples collected at the same stations, and quarterly low flow sampling (QS) in the late 1990s (De Carlo et al., 2004). The box delineates the 1st and 3rd quartile values, the horizontal line represents the median, and the whiskers indicate minimum and maximum values.*

9. Isotopic Composition of Copper and Iron in Dissolved Storm Flow Archive Samples

Statistics of Cu isotopic ratios in SFA samples are reported in **Table 16**. The δ^{65}Cu of modern KHS_{UAW} samples is within the range defined by the KHS_{SFA} storm samples. The MWK_{SFA} samples are, on average, isotopically lighter than both the KHS_{SFA} storm samples, and the LFM samples.

SFA δ^{65}Cu	***Mean***	***Min***	***Max***	***SD***
Kaimuki High (KHS)	0.48	-0.17	0.54	0.25
Waiakeakua (MWK)	0.36	-0.67	0.40	0.24

Table 16. *Statistics of δ^{65}Cu for SFA samples.*

There is large variability in Cu isotopic composition of SFA samples at both locations. An obvious candidate for control of concentrations and isotopic ratios is the stream discharge, shown in **Figure 21** for a selected storm at MWK. There does not seem to be any relationship between discharge and the amount of runoff during storms and the $\delta^{65}Cu_{DIS}$ in SFA samples at either MWK or KHS. De Carlo et al., (2004) observed a first flush effect, which is confirmed by the current study in the form of high Cu concentrations during initial high discharge (**Figure 21**). This first flush, however, is not accompanied by any specific isotopic signature. Within each storm, the $\delta^{65}Cu_{DIS}$ is mostly constant with some excursions to much lighter (i.e. negative) $\delta^{65}Cu_{DIS}$. The latter do not seem to be coupled with changes in discharge or Cu_{DIS} concentrations. All SFA samples with negative $\delta^{65}Cu_{DIS}$ values are statistical outliers. Other potential reasons for differences between SFA samples and baseflow $\delta^{65}Cu_{DIS}$, as well as variability at each SFA station are discussed in the Synthesis section.

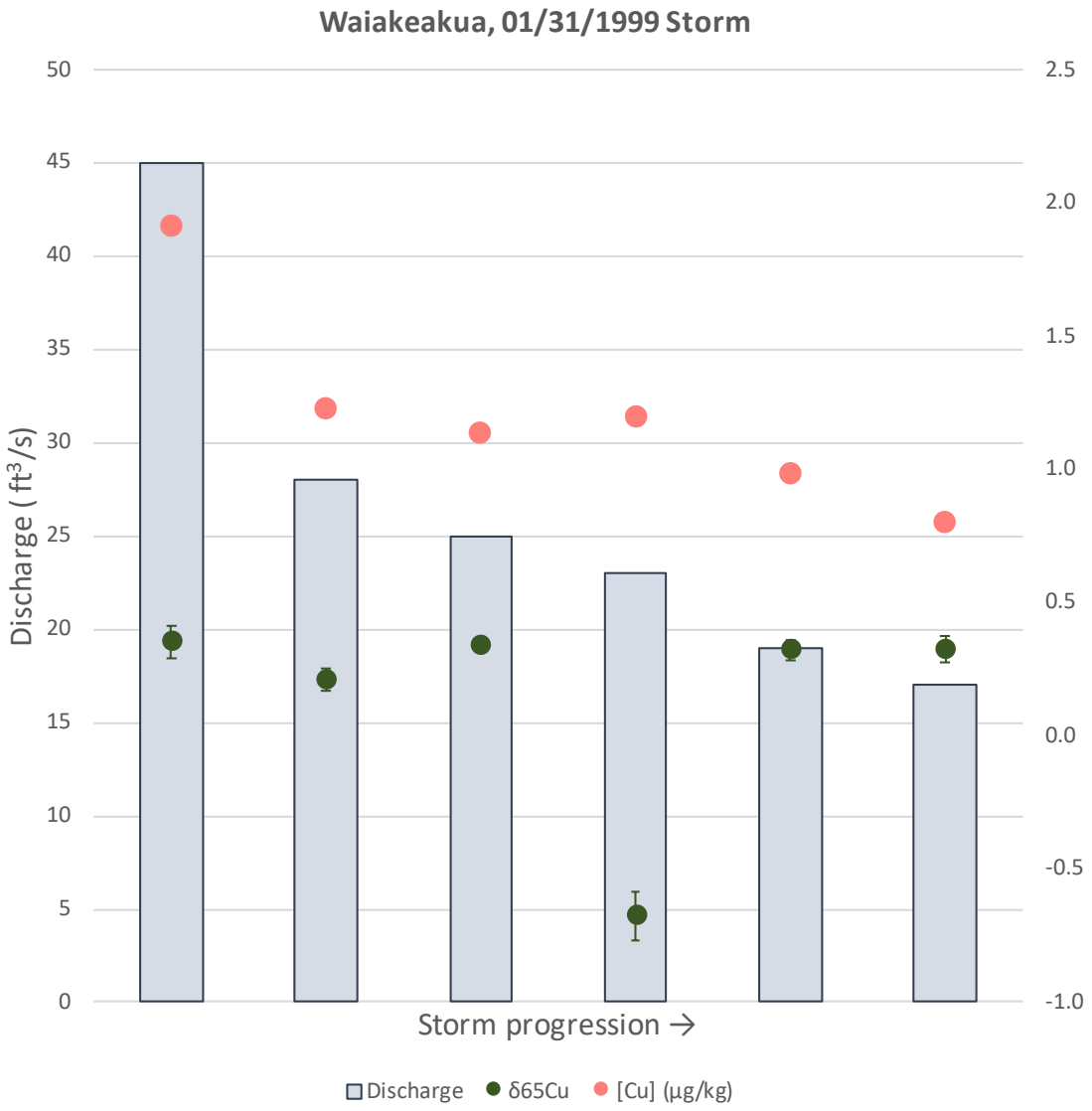

Figure 21. *Discharge (ft^3/s), $\delta^{65}Cu_{DIS}$ (‰) and Cu concentrations (µg/kg) at MWK during the 01/31/1999 storm (sampling interval: 30min).*

Synthesis

After the detailed description of the geochemistry of the individual study sites in the Results and Discussion sections, the synthesis section below focuses on the processes at play and that are influencing Cu and Fe in the Ala Wai watershed. The dominant processes are inferred from variations in concentrations and isotopic ratios, taking a step back and examining the watershed-scale drivers and how these may be relevant for a wide range of geochemical scenarios globally.

1. Redox Cycling and Soil Processes

The redox regimes of most low-temperature natural environments are not extreme enough to promote reduction of Cu(II) to Cu(I) (Moynier et al., 2017). However, more redox-sensitive chemical phases, such as the hydroxyl-oxides of Fe and Mn, can adsorb Cu, and the redox transformation of these two carrier phases are associated with Cu isotopic fractionation. An example of this is the reductive dissolution of Fe-oxides in soils (e.g. Vance et al., 2016). Two stations in the upper Ala Wai watershed exhibit features that suggest the presence of reduced Fe sources, likely associated with the degradation of organic matter in soils and within the groundwater at MRC and MWH, respectively. There is evidence for redox cycling in δ^{56}Fe signatures, but δ^{65}Cu is not impacted, suggesting that copper isotopic fractionation is not controlled by Fe-oxyhydroxides.

At station MWH, concentrations of dissolved Mn and particulate Fe (especially the Fe/Al) are elevated, while the dissolved concentration of V is low compared to what is observed at other stations. Manganese and Fe are both mobilized (soluble) under reducing conditions, whereas reduced V is immobile and oxidized V is soluble. Reducing conditions are common in groundwater, and groundwater is usually enriched in both dissolved Mn and Fe due to reductive dissolution of their oxides, while concentrations of V are low due to reductive precipitation (Wehrli and Stumm, 1989; Barnhart, 1997; Bonatti et al., 1971). As the groundwater comes in contact with the oxygenated stream water, both Fe(II) and Mn(II) are oxidized to Fe(III) and Mn(IV), albeit at vastly different rates. These elements will then precipitate out of solution, with precipitation of Fe(oxy-hydroxides) occurring very close to the groundwater/oxic interface. The high abundance of Mn in the dissolved phase and that of Fe in the particulate phase at MWH are consistent with faster kinetics of oxidation and precipitation for Fe than Mn (Stumm & Morgan, 2012). Further support for a reducing groundwater source of these elements comes from a previous study on rare earth elements (Knor et al., 2017), which found a negative Ce anomaly at MWH. Cerium has been shown to be a common indicator for redox cycling (e.g., Goldberg et al., 1963; Koeppenkastrop & De Carlo, 1992; Bau, 1999). At station MRC, concentrations of dissolved Fe are the highest among the upper watershed stations, while particulate concentrations are the lowest. Hence, Fe is likely associated with oxidized colloidal material, or with the truly dissolved reduced form. The evidence for a reducing groundwater source which supplies soluble Fe is corroborated by the high concentrations of dissolved Mn. The area around station MRC is

characterized by increasing soil development, thus the source of reducing conditions here could be organic matter decomposition in soils, the signature of which is carried by groundwater seeps.

Isotopic signatures of water samples from sites associated with reduced sources point to differences between the two locations. Redox cycling of Fe is known to lead to its isotopic fractionation (e.g. Dauphas & Rouxel, 2006; and references therein). Precipitation of oxidized Fe(III) is expected to enrich the precipitate in heavy ^{56}Fe, leaving the residual Fe(II) in solution enriched in light ^{54}Fe (Dauphas & Rouxel, 2006). However, in samples from station MWH, such a negative δ^{56}Fe signature for dissolved Fe is absent, despite the clear evidence of redox cycling (see **Figure 17**). This suggests that quantitative oxidation of the reduced Fe occurs in the stream water, leading to isotopic ratios that are indistinguishable from the rock source of the reduced groundwater (**Figure 22**). In samples from station MRC, on the other hand, both particulate and dissolved iron show very negative (i.e. light) δ^{56}Fe, a signature that is also propagated to the next (downstream) station. This observation suggests that Rayleigh-type fractionation occurs at this station due to incomplete precipitation of the dissolved Fe that is being oxidized. Both dissolved (likely mostly colloidal), and particulate Fe in water from MRC and the subsequent station (MKW) bear the light isotopic signature of Fe derived from the precipitation of Fe supplied by reduced waters, either groundwater or soil water.

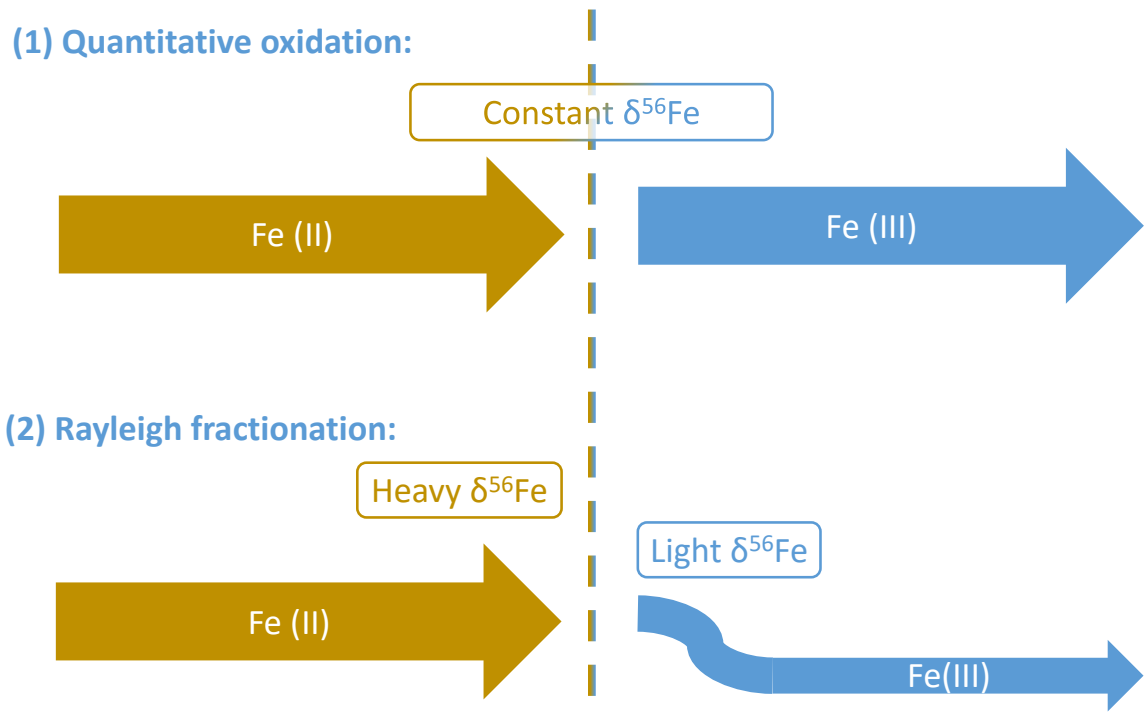

Figure 22. *Schematic of Fe oxidation at the interface of reduced ground- and soil waters and oxic stream water, with (1) Quantitative oxidation as observed at MWH, and (2) Rayleigh fractionation as observed at MRC.*

The $\delta^{65}Cu_{DIS}$ is practically uniform in the water samples from all the upper watershed stations. Thus, precipitation of Fe-oxides along with potential scavenging of Cu_{DIS} does not appear to impact the isotopic signatures of dissolved Cu. The $\delta^{65}Cu_{SUS}$ is 0.85‰ lighter in water from

MRC than observed at MWH. Because Fe in water samples from MRC is predominantly in the <0.22µm fraction, and because adsorption onto Fe-oxyhydroxides enriches particles in heavy Cu, the light particulate Cu signature observed here cannot be associated with oxidative precipitation, but could reflect fractionation during soil processes.

A multitude of processes can impact the isotopic ratios of Cu in soils, which then translate to the δ^{65}Cu in stream water (e.g. Bigalke et al., 2011; Vance et al., 2016). Oxic weathering is associated with Cu loss from soils, during which the heavy isotope is enriched in the weathering solution, and the light Cu isotope in the residue (Vance et al., 2016). Multiple cycles of this process could eventually result in particulate Cu that is substantially lighter than the original bedrock composition, such as the -0.91‰ $\delta^{65}Cu_{SUS}$ measured at MRC, the most negative value observed in this study (see **Figure 16**). Additionally, soil organic matter and plant litter are both expected to be enriched in the light isotope due to the preferential uptake of ^{63}Cu by organisms (e.g. Navarrette et al., 2011; Weinstein et al., 2011). The relative importance of Cu derived from organic-rich particles and Cu adsorbed onto inorganic, residual oxides, however, could only be assessed with additional data on particulate organic carbon, and the examination of soil profiles. The light $\delta^{65}Cu_{SUS}$ signature observed at MRC is not propagated downstream, indicating that it may be a local snapshot of a process, rather than a watershed-scale driver of δ^{65}Cu.

In the upper watershed, weathering and redox cycling during low flow conditions are the dominant controls on the isotopic ratios of Cu and Fe. Storm runoff also accesses more pools of metals whose isotopic compositions have been shaped by soil processes, which is discussed in the section on storm runoff.

2. <u>Interactions Between Particulate and Dissolved Loads</u>

Partitioning and exchange between Cu species adsorbed to inorganic or organic particles and colloids, and the organic ligands in the dissolved phase have been invoked as an important control of riverine δ^{65}Cu by a number of studies (e.g. Vance et al., 2008; El Azzi et al., 2013; Guinoiseau et al., 2017; Petit et al., 2013). In the dataset presented here, Cu isotopic ratios in water samples collected at the estuarine stations partly support the notion that exchange between dissolved and particulate fractions controls Cu isotopic composition, while data derived from samples collected in the upper watershed are better explained by other processes.

The δ^{65}Cu of the dissolved fraction in low-flow samples is relatively similar throughout the whole watershed (0.62 to 1.06‰), and consistently heavier than the particulate fraction, as well as the bedrock (0.04-0.14‰; Liu et al., 2015). The upstream (LFM) particulate fractions, however, span a much larger range of isotopic ratios between -0.91 and +0.34‰, and the $\Delta^{65}Cu_{DIS\text{-}SPM}$ varies greatly between stations. These observations suggest that under low flow conditions (i.e., large groundwater contribution), a relatively homogenous isotopic signature of dissolved Cu, likely complexed by organic matter, is acquired before entering the streambed, and is then maintained throughout the stream and well into the high-salinity region of the Ala Wai Canal. Particulate Cu in water samples from the upper watershed, on the other hand, can be characterized as a

snapshot at each station of a combination of various inputs (e.g. soil materials, stream sediment resuspension, anthropogenic, plant litter) that have heterogeneous isotopic compositions. Because the total distance between the most upstream- and the most downstream LFM stations is only a little more than 5 km, it is likely that there is not enough transport time in the river water for significant isotopic exchange between particulate and dissolved fractions.

At the estuarine stations, Cu concentrations are enriched ten- to twenty-fold in both the particles and the dissolved phase relative to water from the upper watershed. This is partly due to an increase in the concentration of SPM downstream: Although absolute particulate Cu concentrations increase tremendously, especially between the lowest LFM station (MKW) and the first UAW station (KHS), Cu/Ti ratios of particles only increase two- to five-fold (**Table 17**). The largest increase is observed between KHS and AWFW, the first high salinity station, and the highest values occur in the UAW-4 samples. The corresponding increase in the concentration of Cu_{DIS} is likely derived from solubilization of the increased particulate Cu which is then complexed with organic ligands.

LFM		***UAW***	
Station	Cu/Ti_{SPM}	Station	Cu/Ti_{SPM}
MWK	0.01	**KHS-4**	0.03
		KHS-5L	0.01
MWH	0.02	**KHS-5H**	0.01
MRC	0.02	**AWFW-4**	0.06
		AWFW-5L	0.02
MKW	0.02	**AWFW-5H**	0.03
		AWHB-4	0.05
		AWHB-5H	0.02

Table 17*. Ti-normalized Cu concentrations (g/g) of particles at LFM and UAW stations.*

The large increase in SPM, and consequently the changes in concentrations of Cu_{DIS} and Cu_{SPM} as a function of distance downstream (**Figure 23**) also reflect a shift in sources from the more natural, upstream (high watershed) rock and soil sources, to the addition of urban, anthropogenic components in the lower portions of the watershed, which are discussed in the subsequent section on anthropogenic sources. Throughout the estuary, there is a constant offset about 0.6‰ between dissolved- and particulate $\delta^{65}Cu$. This offset is smaller than the 0.8-1.6‰ reported by Vance et al. (2008). Vance et al. (2008) observed homogeneity in $\delta^{65}Cu$ along the salinity gradient of two British estuaries. Following their arguments, thermodynamic partitioning between a dominant organically complexed dissolved pool and a particulate fraction is a possible interpretation that explains why large changes in Cu concentrations, suspended particles, flow regime, salinity and biological activity throughout the Ala Wai Canal do not translate into shifts

in the offset between particulate and dissolved $\delta^{65}Cu$. It is possible that, due to the longer water residence times in the Ala Wai Canal (Freeman, 1993) compared to upper reach of the watershed, Cu adsorbed onto particulate matter, and organically complexed dissolved Cu achieve more complete isotopic exchange. However, the offset could also be an artifact of two different pools dominating $\delta^{65}Cu_{DIS}$ and $\delta^{65}Cu_{SPM}$, respectively: (1) Continuing organic complexation of the dissolved fraction that keeps $\delta^{65}Cu_{DIS}$ constant from upstream sites, and (2) a mixture of lithogenic and anthropogenic particulate sources that combines to form a particulate Cu pool that is about 0.6‰ lighter.

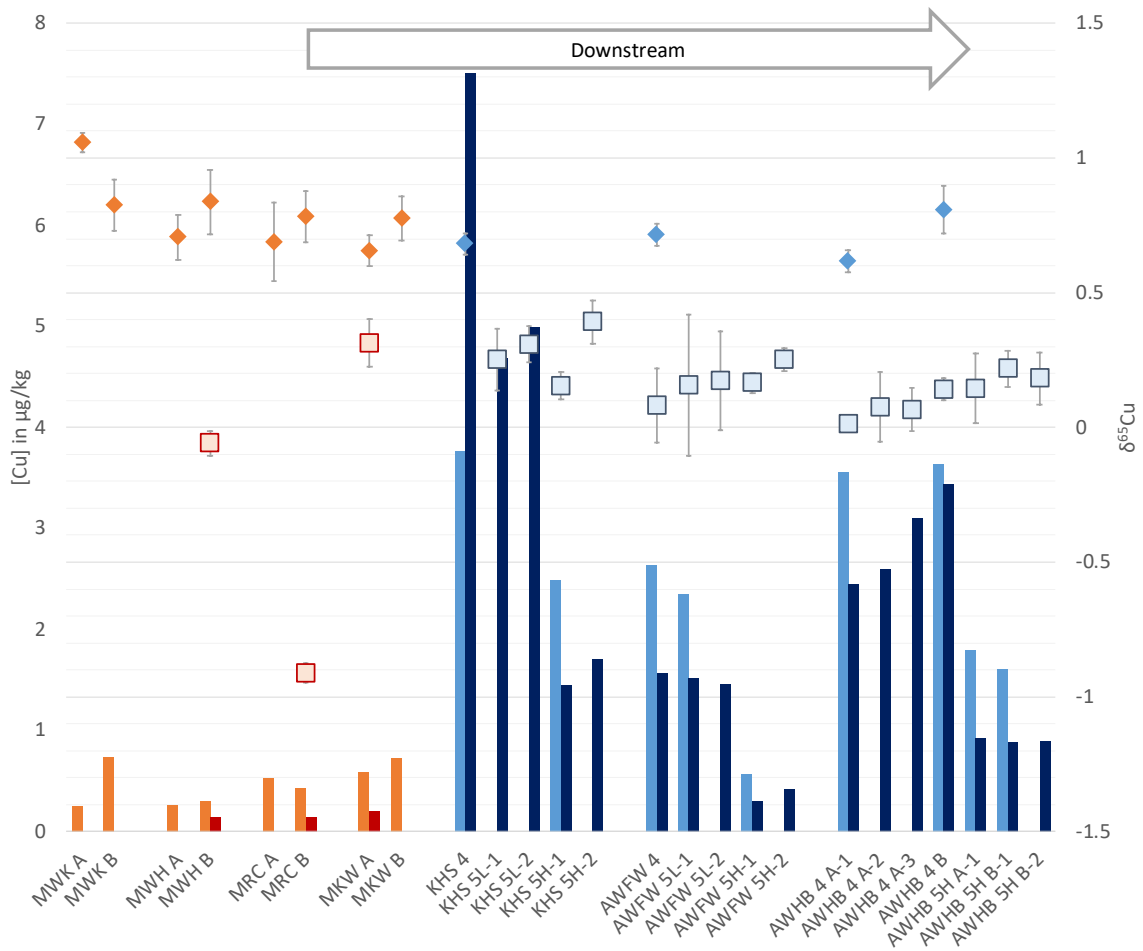

Figure 23. *$\delta^{65}Cu$ of dissolved (rhombus) and particulate (square) fractions along the Ala Wai watershed (± 2SD) and Cu concentrations of dissolved (orange bars, light blue bars) and particulate (red bars, dark blue bars) of LFM (MWK to MKW)) and UAW (KHS to AWHB) samples.*

In contrast to the relatively homogenous isotopic composition of particles and dissolved fractions in samples from the estuarine stations, the suspended particles collected in the upper watershed are much less uniform. The dissolved Cu fraction, however, shows a practically constant isotopic composition throughout low flow Manoa and urban Ala Wai sample sets. It therefore seems likely that the $\delta^{65}Cu_{DIS}$ in baseflow waters throughout is controlled by processes that preferentially release heavy Cu, which then forms organic complexes within the soil

horizons, prior to entering the streams. This will be explored in the following sections. Processes which enrich heavy Cu in solution include the dissolution of bedrock, especially leaching from sulfide phases (Mathur et al., 2012), oxic weathering of soils (Vance et al., 2016), or plant uptake of light Cu (Weinstein et al., 2011).

An offset of the Fe isotopic ratios of the particulate and dissolved fractions is also observed in the upper watershed, with lighter $\delta^{56}Fe$ in solution than in suspended particles. Similar to the $\Delta^{65}Cu_{DIS\text{-}SPM}$, the $\Delta^{56}Fe_{DIS\text{-}SPM}$ also changes throughout the upper watershed. The offset is within the analytical error for samples from the two most upstream stations, but increases for the two lower locations, consistent with an incomplete isotopic exchange between particulate and dissolved pools throughout the stream. Additionally, unlike dissolved Cu, the dissolved Fe pool is not entirely made up of dissolved Fe complexed by organic ligands, but likely a combination of various different species, including colloidal Fe-(hydr)oxide, as well as dissolved organic complexes (e.g. Gledhill & Buck, 2012, and references therein). Consequently, variations in the $\delta^{56}Fe$ are better explained by the processes described in the previous and following sections, as opposed to a simple exchange interaction between the SPM and the dissolved fractions.

3. Rock Weathering and Groundwater

So far, only a few studies have focused on the isotopic fractionation of Cu during weathering of primary minerals (see recent review by Moynier et al., 2017). In one experimental- and one observational study on the incongruous dissolution of minerals bearing copper-sulfide phases, Fernandez & Borrock (2009) and Mathur et al. (2012) observed preferential release of heavy Cu into solution. This is consistent with the $\delta^{65}Cu_{DIS}$ signature found in the current study that is, in all cases, heavier than bedrock $\delta^{65}Cu$ (average 0.09‰; Liu et al., 2015). The geochemical composition and hydrological environment of LFM samples indicate that they are dominated by groundwater and rock-water interactions. During base flow conditions, the majority of river water is commonly groundwater that seeps through the streambed after a prolonged contact with bedrock, as opposed to the rapid surface runoff that characterizes storm conditions (Stumm & Morgan, 2012). This notion is supported by the major element ratios and concentrations of the LFM samples from the current study.

The vast majority of dissolved Si in freshwater bodies, which is elevated in concentration in Hawaiian stream- and especially groundwaters, is derived from rock weathering, with a lesser influence from biological cycling (e.g. Mortlock & Frohlich, 1987). Calcium (Ca^{2+}) and Mg^{2+} to a larger extent, and K^{+} to a lesser extent, also have large bedrock sources, because they are easily solubilized during chemical weathering. However, these species also tend to become more enriched with increasing contributions from other sources, such as runoff and aerosols containing sea salt, as well as concrete and cement (mostly for Ca). Sulfur (as SO_4^{2-}) does not have significant rock sources, but can be seen as a proxy for sea salt (from saltwater intrusions, aerosols or urban runoff) in this watershed (Visher & Mink, 1964). Non-rock sources are all expected to increase in importance at more urban, anthropogenically impacted stations with increasing distance from the high mountainous source waters. Despite these additional sources, major element ratios are similar in all LFM samples, and close to ratios observed for groundwater-

and bedrock. When normalized to the concentration of Si, i.e. correcting for dilution with surface runoff (**Table 18**), only S and K show a downstream change in concentration, with the Si/K and Si/S decreasing by around 30% and 50%, respectively, from the most upstream to the most downstream stations, while the Si/Ca and Si/Mg ratios stay constant. This observation supports a dominant rock weathering signature for the elemental composition of LFM samples at all locations, with minor contributions from other sources downstream. These downstream additions likely occur mostly in the form of inputs of sea salt aerosols, and are more obvious in the Si/K and Si/S ratios of water samples, due to the smaller rock sources for these elements (**Table 18**).

	Si/Ca	Si/Mg	Si/K	Si/S	Si/Cu ($x10^5$)
MWK A	1.2	1.4	15.7	9.1	2.8
MWK B	1.2	1.4	15.3	11.3	8.4
MWH A	0.9	1.0	10.6	6.9	3.4
MWH B	0.9	1.0	11.0	6.9	4.2
MRC A	1.0	1.1	13.2	6.3	6.0
MRC B	1.0	1.2	13.6	6.5	5.0
MKW A	0.9	1.1	9.1	5.2	6.8
MKW B	0.8	1.0	9.0	5.0	8.5
Basalt average[1]	3.9	3.7	202	703	

Table 18.1 *Ratios of dissolved major elements and Cu/Si in LFM samples.* [1]*Clague & Frey, 1982; Frey et al., 1994; Norman et al., 2004; Patino, 2003; Roden et al., 1984; Sutherland, 1999; Sutherland & Tolosa, 1999*

	Mg/Ca	S/Mg	S/Ca	K/Mg	K/S	K/Ca
LFM	**0.84**	**0.17**	**0.14**	**0.10**	**0.58**	**0.08**
Groundwater[1]	0.50	0.25	0.16	0.30	1.20	0.19
Basalt average[2]	1.04	<0.02	<0.02	0.02	3.48	0.02
Ko'olau Series average[2]	0.98	<0.02	<0.02	0.04	7.99	0.04
Honolulu Volcanic Series average[2]	1.21	<0.02	<0.02	<0.02	1.41	0.01
Seawater[3]	3.14	0.70	2.20	0.31	0.44	0.97

Table 18.2 *Dissolved major element ratios of LFM samples, and groundwater and bedrock endmembers reported in the literature.*
[1]Visher & Mink, 1964
[2]Clague & Frey, 1982; Frey et al., 1994; Norman et al., 2004; Patino, 2003; Roden et al., 1984; Sutherland, 1999; Sutherland & Tolosa, 1999
[3] Stumm & Morgan, 2012

Dissolved and particulate concentrations of Cu normalized to bedrock-derived elements are also relatively uniform throughout the weathering-dominated (LFM) samples. The Si/Cu_{DIS} varies by a factor of about 2.5, but both the minimum and the maximum values are observed at the most upstream station, and the Cu/Ti_{SPM} shows the same magnitude of variability (**Table 17**).

Yet, even the water samples that are expected to be influenced almost exclusively by water-rock interactions are fractionated in their Cu_{DIS} isotopic composition relative to bedrock by around 0.6 to 1‰.

Based on the above observations, it is proposed that chemical weathering of basalt in subsurface aquifers is the main source of dissolved Cu in the upper Manoa watershed, and that this process preferentially releases the heavier Cu isotope into solution. Experiments with basalt leaching would be necessary to determine whether this heavier $\delta^{65}Cu_{DIS}$ signature is a direct result of chemical weathering, or if it is mostly a result of the preferential complexation of ^{65}Cu by organic ligands in solution (**Figure 24**). A study of Cu isotope composition of seafloor altered basalts has shown that low temperature water-rock interactions produce limited variability in Cu isotope ratios (Huang et al., 2016). Results from that study, however, do not exclude the possibility that dissolved Cu, which represent a small pool of Cu leached from the rock, may be

isotopically fractionated as a result of incongruent dissolution and Cu adsorption onto secondary clay minerals and Fe-oxyhydroxides (Balistrieri et al., 2008; Pokrovsky et al., 2008).

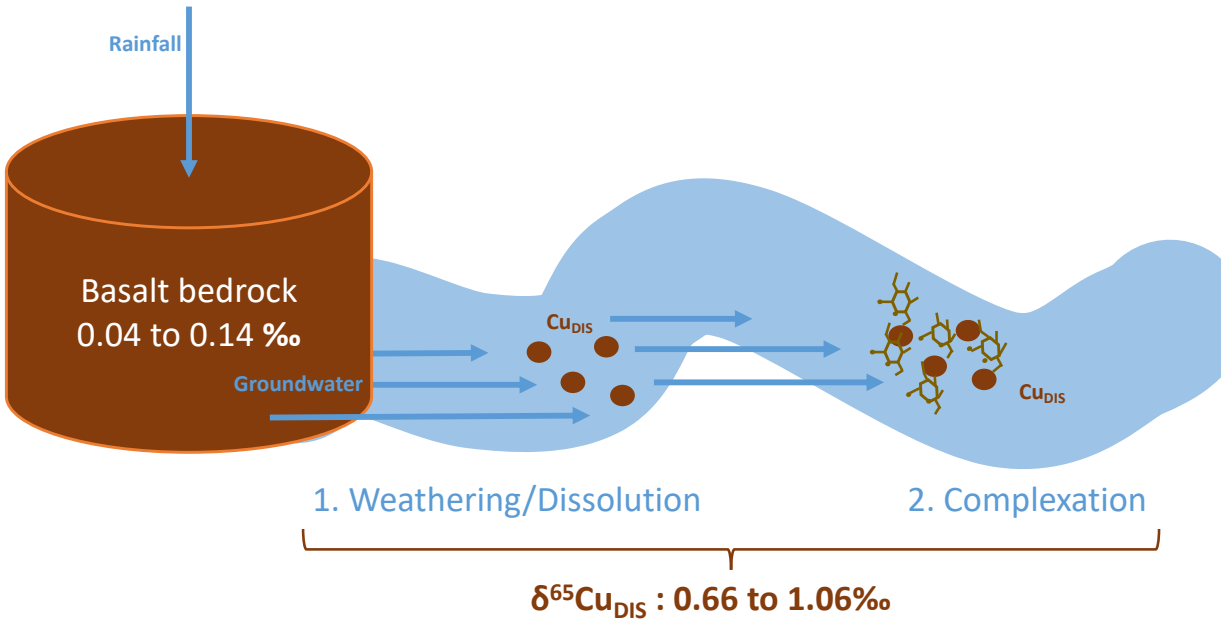

Figure 24. *Schematic of the reactions (chemical weathering- and solution complexation) that control the dissolved Cu isotopic composition of baseflow, upper watershed samples.*

The δ^{56}Fe of both the particulate and dissolved phases are close to bedrock composition in the two uppermost watershed samples. This suggests that, whereas Cu isotopes are fractionated by chemical weathering of basalt to a significant extent, the isotopes of Fe are not. This probably is probably due to the occurrence of colloids within the dissolved Fe fraction that formed during physical weathering (i.e. release of fine lithogenic material) and/or chemical alteration under oxidizing conditions leading to quantitative oxidation of reduced Fe from igneous minerals and organic-replete conditions, preventing organic matter binding to Fe, which has been widely shown to fractionate Fe isotope in streams and rivers (Ilina et al., 2013a).

4. <u>Anthropogenic Copper</u>

Anthropogenic sources of Cu such as brake pads, anti-fouling paints and fungicides, vary in isotopic composition (Dong et al. 2017). Source tracking for anthropogenic Cu in past studies has mostly focused on acid mine drainage (e.g. Song et al., 2016) and vineyard soils treated with fungicides (e.g. Babscanyi, 2015; Babscanyi et al., 2016). In both cases, there were point sources of Cu pollution that overwhelmed natural contributions, which is not the case in this study area. However, the large increase in the concentrations of Cu both downstream- and during storm events reflects a mix of various natural and anthropogenic sources, the latter likely including street runoff and inputs from locally applied fertilizers. Compared to major rivers worldwide

(**Figure 25**), upper watershed dissolved concentrations of Cu are at only 30% of the world average, but concentrations observed here in the estuarine samples are on a par with those of the polluted Seine river in Paris, France, despite the dilution with rainwater during storms. The waters of the Ala Wai watershed span a large range of dissolved Cu concentrations that are consistent with a transition from natural sources (upper watershed, low flow) to anthropogenic (lower watershed, storm flow) inputs.

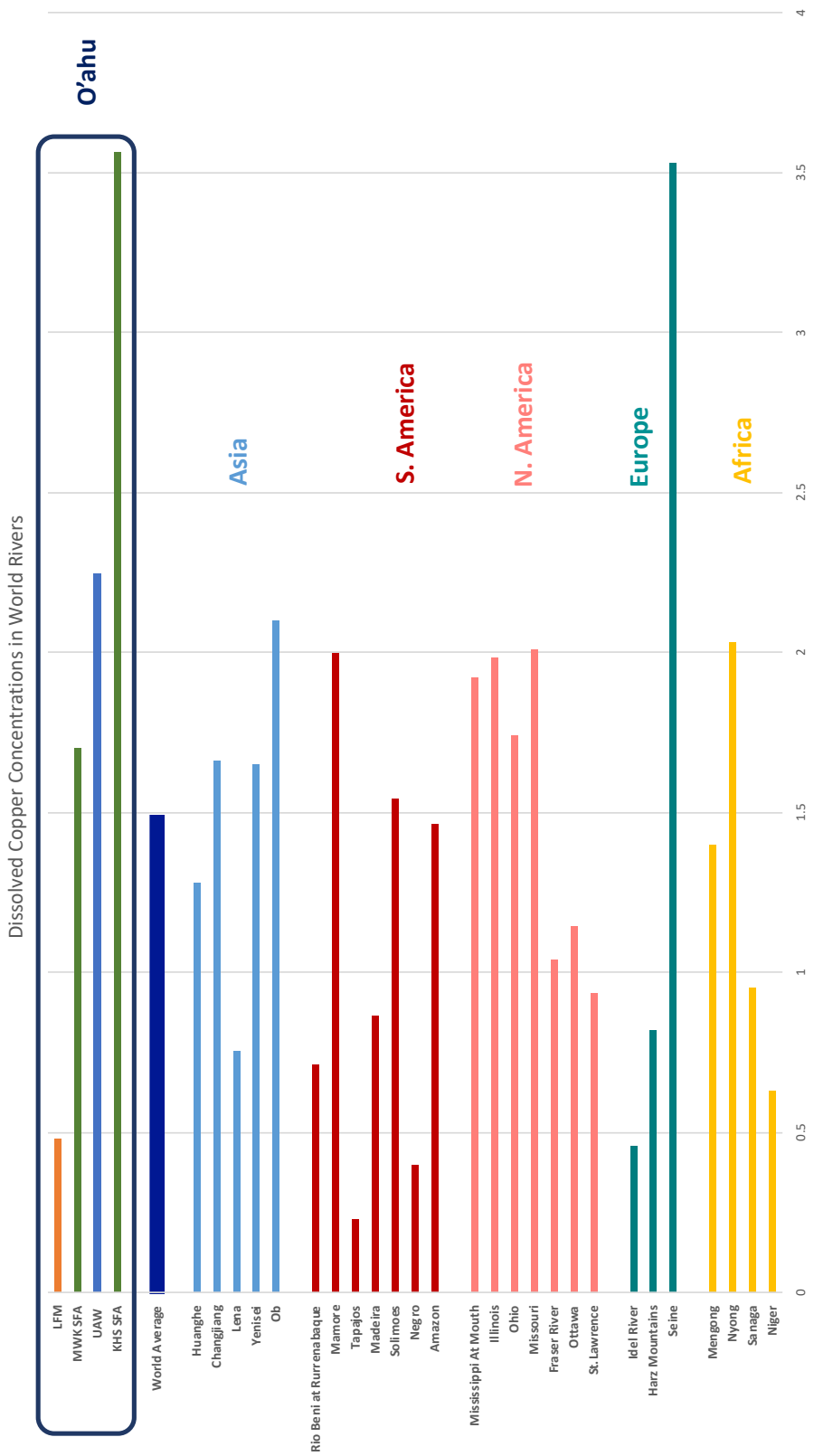

Figure 25. *Dissolved concentrations of Cu (µg/kg) of major world rivers, and the current dataset. World river data compiled by Gaillardet (2014).*

In the SPM, Cu enrichment, as indicated by the Cu/Ti_{SPM} ratios, is most pronounced in the estuarine region during the UAW-4 sampling trip (**Figure 26**). Interestingly, the variability in the Cu/Ti_{SPM} is larger temporally than spatially, stressing the importance of sampling at high temporal resolution to characterize small tropical watersheds (see e.g. Tomlinson & De Carlo, 2003). The Cu/Ti_{SPM} at AWFW and AWHB, for example, varies about three-fold between sampling trips, while the same ratio in most upper watershed samples fall between the minima and maxima for the earlier two stations. Furthermore, this only describes the low flow variability, without taking storm runoff into consideration. Overall, the isotopic composition of Cu varies little between different Cu/Ti_{SPM}, suggesting that either (1) urban Cu input is only varying in magnitude, and coming from a relatively isotopically homogeneous source, or (2) processes within the estuary, such as the isotopic exchange between dissolved and particulate fractions discussed earlier, largely overprint $\delta^{65}Cu$ of inputs.

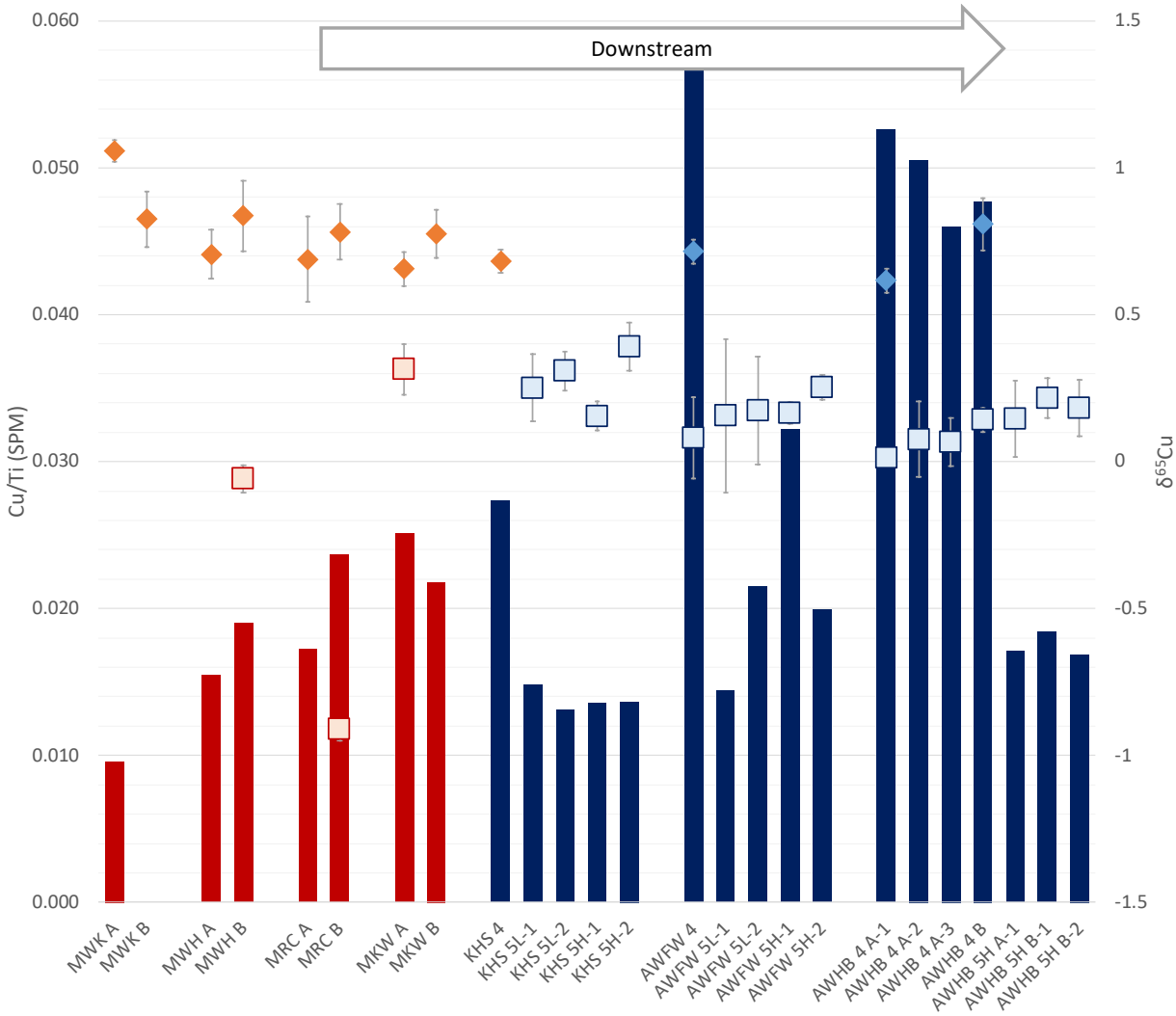

Figure 26. *$\delta^{65}Cu$ of dissolved (diamonds) and particulate (square) fractions along the Ala Wai watershed (± 2SD), and Ti-normalized particulate Cu concentrations of LFM (red bars) and UAW (dark blue bars) samples.*

The particulate Cu isotopic composition of estuarine samples, although homogeneous over a range of Cu/Ti, indicates anthropogenic inputs that are consistent with the δ^{65}Cu values reported by Dong et al., 2017. **Figure 27** shows that typical soil, and basalt δ^{65}Cu are too light to explain δ^{65}Cu of UAW particulates. However, the SPM samples are well within the range of various road-derived sources measured by Dong et al. (2017), such as brake pads, road dust, road paint, and car tires. This indicates that the particulate $\delta^{65}Cu_{SPM}$ reflects road-derived pollution in the estuarine stations.

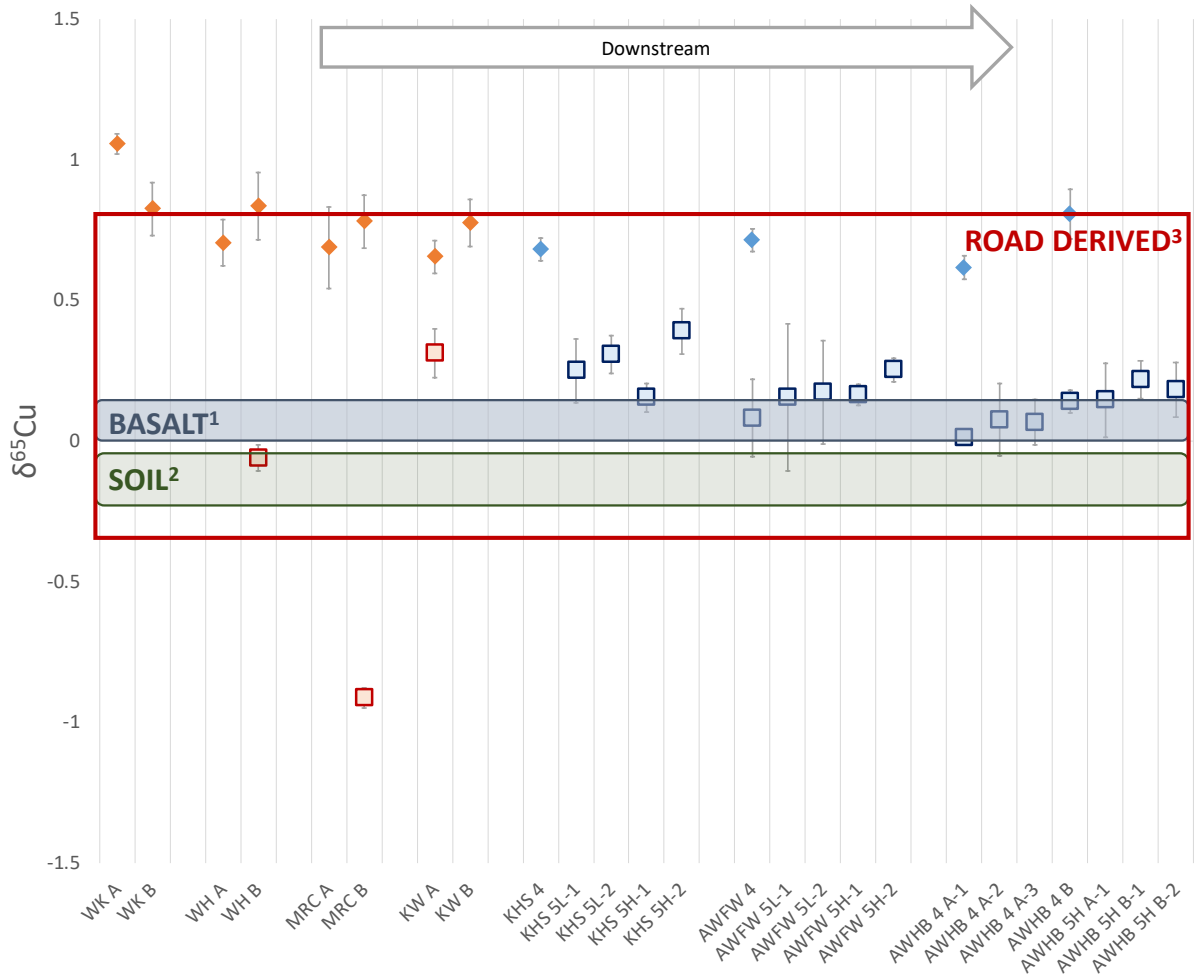

Figure 27. *Isotopic ratios of LFM and UAW samples, and composition of possible sources of particulate Cu. Boxes represent ranges of reported δ^{65}Cu values.*
[1]Liu et al., 2015
[2]Vance et al., 2016
[3]Dong et al., 2017

5. Storm Runoff

There are differences in the concentrations and isotopic compositions between storm runoff and baseflow samples. This is consistent with the idea that, contrary to groundwater-dominated base flow conditions, the majority of stream water during storm flow is derived from surface runoff and shallower subsurface waters (**Figure 28**; Stumm & Morgan, 2012).

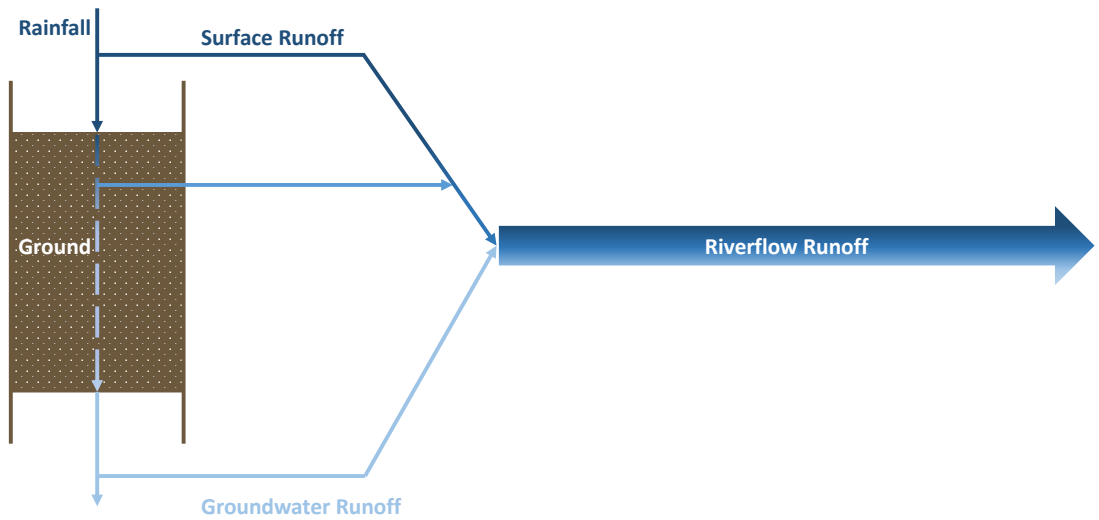

Figure 28. *Schematic of water source contributions to stream flow, with "Surface Runoff" dominating during storm events, and "Groundwater Runoff" dominating during baseflow. Modified from Stumm & Morgan, 2012.*

The composition of storm runoff differs from that of water under low flow conditions and reflects differences in source waters. Runoff-dominated waters display a considerably different chemistry than the rock-derived baseflow. The main differences become evident when comparing the major element concentrations and ratios at the same stations during low and storm flow, respectively (**Table 19**). They reveal what appears to be an anthropogenic input of K and Ca during storm runoff, with excess Ca likely being supplied by concrete structures, and at least one source of K that is closely linked with Cu inputs.

	Mg	Si	S	K	Ca
LFM	7344	8429	1258	717	8799
MWK_{SFA}	2245	3297	765	1402	3363
KHS_{UAW}	5159	3004	3013	2531	6268
KHS_{SFA}	2760	2799	1509	2185	5998

Table 19. *Average dissolved major element concentrations (µg/kg) during low- and storm flow in water from the upper and lower watershed stations.*

All measured major elements except for K in storm water from the upper watershed (LFM; MWK SFA), are diluted 30 to 50 % with rainwater (**Table 19**). The concentration of K, on the other hand, increases two-fold during storms (see also: **Figure 21**). At station KHS, the uppermost estuarine station in an urban channel, only Mg and S are diluted considerably during storms, while K, Ca, and Si occur at similar levels during both flow regimes. From the upper watershed to its lower reaches, concentrations of Mg, Si, and Ca all decrease downstream (LFM to KHS_{UAW}) during low flow, while S and K increase. The concentrations observed here indicate that rocks are a major source of Mg, Si, and Ca during low flow, while K and S have more significant inputs downstream that are different from bedrock. There should only be small differences in the weathering rates of Mg, Ca, and K from basalt as a function of flow regime: All three major ions come from silicates that are, on average, lost entirely from basalt bedrock during chemical weathering (Mackenzie, & Garrels, 1971). To gain a better understanding of the sources controlling major elements, it is again advisable to examine and compare elemental ratios in potential source components and in water (**Table 20**). Two other sources besides rock weathering that are expected to influence major element concentrations in stream water are sea salt aerosols and concrete/cement. If the two endmembers of major element ratios were a fluid at equilibrium with respect to rock-water interactions and seawater, the actual composition of the sampled fluids could be used to calculate the proportions of these two processes leading to the observed chemistry. Using this approach, samples collected upstream and during low flow (LFM) are considered to reflect rock-derived ratios, while both storm-water and low flow samples collected downstream should tend towards seawater-like ratios. For S/Mg, this trend is observed: Both elements show a transition to seawater dominance downstream-and during stormflow (**Table 20**). Downstream, the S/Ca and Mg/Ca ratios observed during low flow approach seawater values, as expected, but also drop back towards and below bedrock values in KHS_{SFA} samples. This indicates that there is a likely third source of excess Ca in downstream storm samples, which is overprinting both the basaltic bedrock and the seawater signatures. It seems likely that this source is originating from the concrete and cement urban structures, as these materials are very rich in Ca (Thomas & Jennings, N.D.). In addition to this anthropogenic concrete derived Ca, variations in the K/S ratio in the same water samples from those of anticipated sources indicate an excess in K during storm flow. Cement, unfortunately, has ratios of the other major elements that are too similar to those of seawater that it cannot be distinguished from sea salt as a source of S, Mg, and K. Based on these observations, sea salt aerosols from rain and street runoff cannot be the only source of K during storms.

	S/Mg	S/K	S/Ca	Mg/Ca
LFM	0.2	1.7	0.1	0.8
MWK SFA	*0.3*	*0.6*	*0.2*	*0.7*
KHS UAW	0.6	1.4	0.8	1.16
KHS SFA	*0.6*	*0.7*	*0.3*	*0.5*
Seawater[1]	0.7	2.3	2.2	3.1
Cement[2]	0.7	2.8	<0.03	<0.03

Table 20. *Average ratios of dissolved major element in LFM samples (this work), and in seawater and cement endmembers (Stumm & Morgan, 2012; Thomas & Jennings, N.D.).*

Concentrations of dissolved K and Cu were significantly positively correlated (Pearson correlation coefficient R=0.853, p<0.0001) in all low-salinity samples across sample sets (**Figure 29**). Concentrations of both constituents increase downstream, and from low flow samples to storm samples, suggesting at least one source for both of these elements that is associated with storm runoff, and that also increases with urbanization, and that this source is concentrated enough to overprint dilution with rainwater during storms. Street runoff containing sea salt (K) and vehicle-derived Cu cannot be the only source for these two elements, based on the observed dilution of major sea salt ions, except for K, discussed above. Street runoff is therefore only one of several sources of Cu. the isotopic composition of road-derived Cu is expected to be quite variable, and centered around 0.23‰ (Dong et al., 2017). There are several additional potential sources for K and Cu including soils and plant litter, fertilizers, and pesticides, which will be discussed in detail below. Cu isotopic composition of storm samples is shown in **Figure 30**, and displays a mixture of at least three different Cu sources, that result in an average of storm samples that is lighter than that of baseflow samples. The $\delta^{65}Cu_{DIS}$ ratios show that storm runoff is associated with an upstream light source of Cu that is depleted in both K and Cu compared to downstream storm runoff, but enriched compared to baseflow (see **Figure 30**). Additionally, there is a downstream source of heavier Cu (closer to bedrock $\delta^{65}Cu$) that is enriched in K and Cu compared to both upstream samples and low flow conditions. Soil organic matter and clay minerals can be invoked as a source for the low concentration and light $\delta^{65}Cu_{DIS}$ pool in MWK_{SFA} samples, whereas fertilizers, pesticides and road sources could be responsible for the greater concentration and heavy $\delta^{65}Cu_{DIS}$ pool in KHS_{SFA} samples.

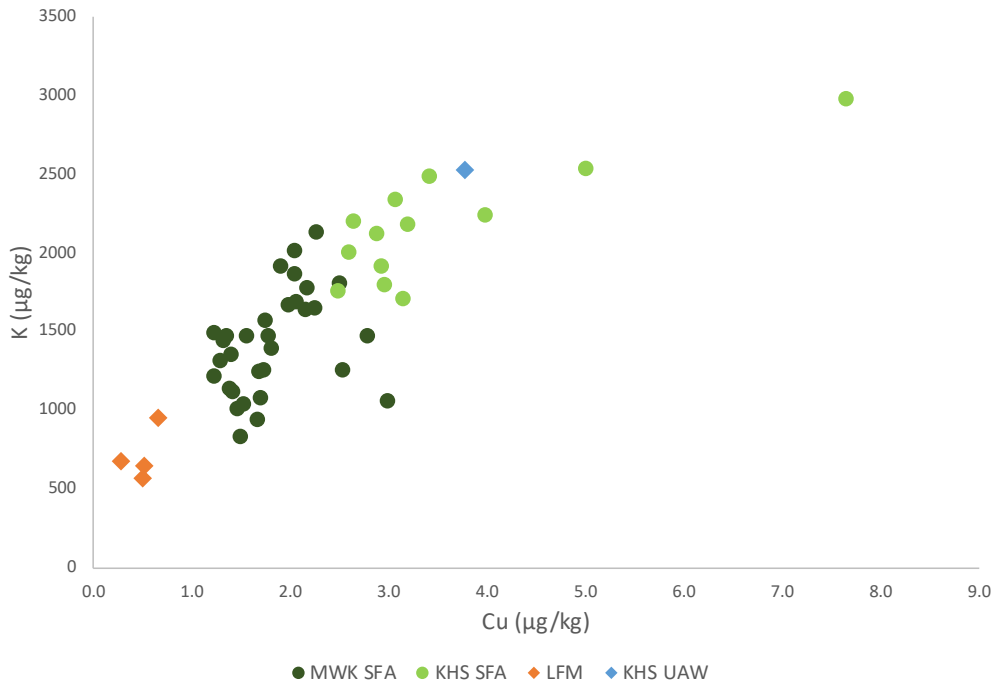

Figure 29. *Concentrations (µg/kg) of dissolved K against Cu (R=0.853) in LFM and SFA water samples, and at* KHS_{UAW}*.*

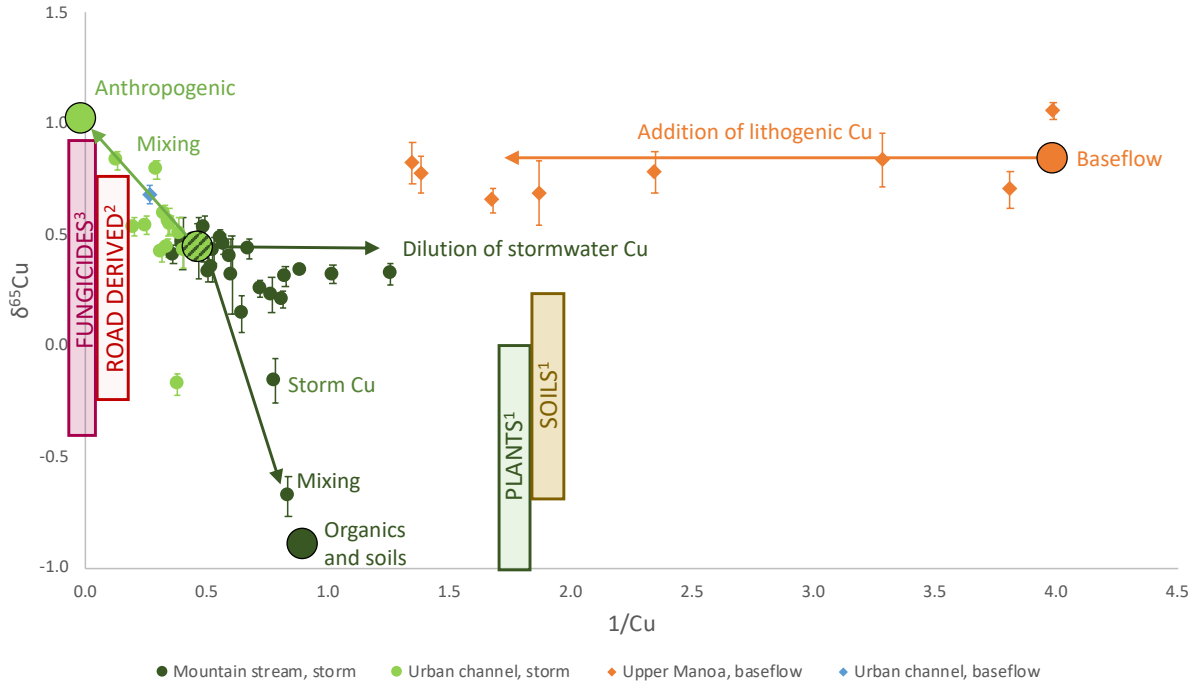

Figure 30. *Cu isotopic composition vs. inverse Cu concentration of low flow and storm samples, with potential sources of stormwater Cu.*
[1]Vance et al., 2016
[2]Dong et al., 2017
[3]Babscanyi, 2015; Blotevogel et al., 2017

Because the composition of storm samples is expected to be dominated by the principle constituents of surface runoff, soils are likely a more important source of dissolved and suspended elements in streams during storm conditions. Soils in the Hawaiian Islands are rich in organic matter, especially in regions that experience abundant rainfall, where soil organic matter constitutes up to 30% of the total soil colloidal material (Hough et al., 1941). This colloidal organic matter pool is thought to retain major cations, such as K^+, that were solubilized during bedrock weathering, with K bound more efficiently in colloids of highly weathered soils in high rainfall, such as those in Manoa valley, compared to less weathered, low-rainfall environments (Albrecht, 1943; Hough et al., 1941). Because K is an essential and major nutrient for plants, plant litter contains considerable amounts of K that is released to soils during decomposition and leaching by surface water. Copper in soils has a strong affinity for organic matter, which could result in a casual rather than causal correlation between K and Cu (Schnitzer & Skinner, 1965, 1966). Soil organic matter is often stabilized by interactions with clay minerals in tropical soils (Wattel-Koekkoek et al., 2001). Clay minerals that are common in Hawai'i soils, such as smectite and kaolinite, contain exchangeable K^+ between layers, and fixed K^+ within the crystalline structures (Johnsson et al., 1993). Kaolinite and montmorillonite (a type of smectite) are also known to adsorb heavy metal cations, with kaolinite having a particularly high affinity for Cu(II) (Yavuz et al., 2003; Bhattacharyya et al., 2008). The adsorption reaction is accompanied by isotopic fractionation, with an offset of $\Delta^{65}Cu_{kaolinite\text{-}solution} \approx -0.2‰$ due to preferential adsorption of light Cu (Li et al., 2015). Thus, Cu associated with soil organic matter or plant material is also expected to be enriched in the light Cu isotope (e.g. Weinstein et al., 2011). It is therefore suggested that a pool of Cu and K and in storm runoff in pristine mountain streams derived from erosion and flushing of soils, especially soil organic matter and clay minerals, by rainwater, would be enriched in the light Cu isotope.

The downstream increase in the concentrations of Cu and K during storms, however, is unlikely to be due to a soil organic matter source of these elements, since this pool is not expected to increase with urbanization.

One anthropogenic source of K that decouples it from other major cations (e.g., Ca, Mg) is potash-rich fertilizer, which contains around 15% K_2O (Barker, 1999). There is relatively little commercial agriculture in the Ala Wai watershed, but most runoff in urban areas comes either from sealed concrete surfaces or residential yards, where application of fertilizers to lawns, gardens, and parks is likely to be considerable. Phosphorous is another main component of many fertilizers, and a correlation of P with K is observed throughout the data from the current study (**Figure 31**, Pearson correlation coefficient $R=0.705$, $p<0.0001$), substantiating the idea of fertilizers as a source whose importance increases as a function of the abundance of surface runoff, and with increased urbanization.

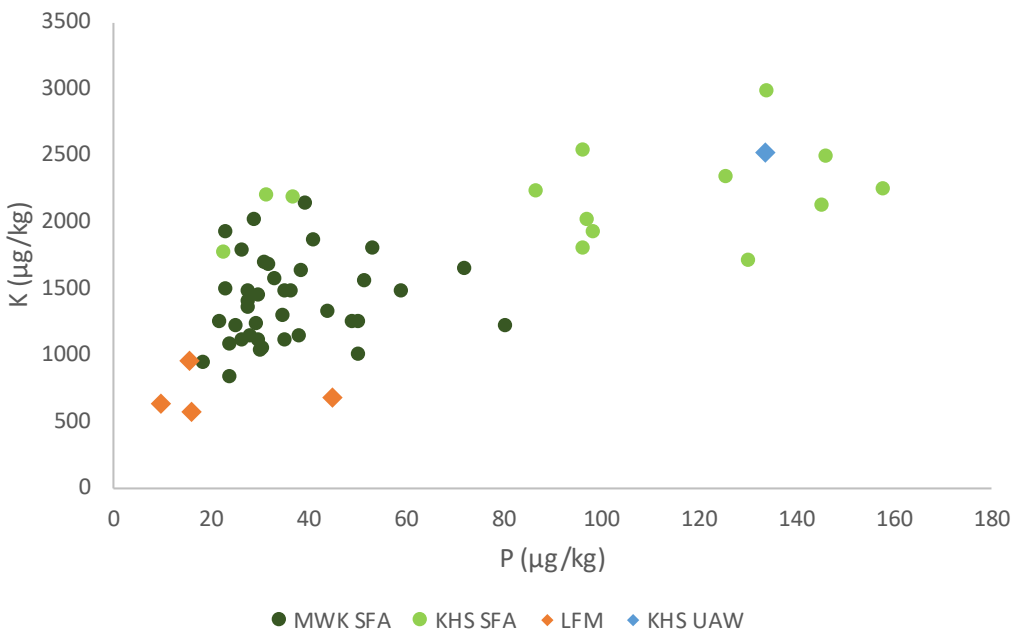

Figure 31. *Concentrations (µg/kg) of dissolved P against K (R=0.705) in LFM and SFA water samples, and at* KHS_{UAW}.

Copper, however, is likely not derived from fertilizers but rather from other chemicals used in gardening and yard work, e.g., Cu-based fungicides and pesticides. The Cu derived from fungicides tends to accumulate in the surface horizons of soils due to its high affinity for both particles and organic matter (e.g. Merry et al., 1983). The Cu isotopic composition of fungicides spans a wide range from $\delta^{65}Cu$ of -0.49 to 0.91‰ (Babscanyi, 2015; Blotevogel et al., 2017). Consequently, $\delta^{65}Cu$ cannot be used to distinguish fungicide as a specific source of Cu, although it could well be responsible for the heavier $\delta^{65}Cu_{DIS}$ of (downstream) KHS_{SFA} compared to (upstream) MWK_{SFA} samples (**Figure 30**).

Overall, storm runoff can mobilize Cu, K, and P from urban cultivated soils, which would lead to the observed downstream increase in the concentrations of these elements in stream water. Fertilizers and fungicides could be important sources of Cu, K and P to urban storm runoff. However, to quantify the relative contributions from street runoff, natural soils, and fertilizers and fungicides to increasing Cu concentrations during storms, it would be necessary to quantify both the concentrations and isotopic compositions of Cu in a broad range of natural and cultivated watershed soils, as well as available pesticides. This is clearly beyond the scope of the current work.

The isotopic composition of Fe in streams during storm runoff was measured only at the upper watershed station (MWK_{SFA}) in samples from four different storm events. The storm runoff is enriched in Fe, and the trend observed for isotopic ratios of Fe is somewhat opposite to that of Cu at the same station: $\delta^{56}Fe_{DIS}$ of storm flow samples is heavier than the $\delta^{56}Fe_{DIS}$ of low flow samples (**Tables 9, 13**). Interestingly, the higher the Fe concentrations are, the lighter the $\delta^{56}Fe_{DIS}$ becomes, with the Fe in the highest concentration samples approaching isotopic values

measured in the low flow samples. Consequently, although a pool of heavier Fe isotopes is mobilized during storms, as the concentration of Fe increases, the isotopic signature tends back towards the lighter bedrock composition. A potential source of heavy Fe that is also consistent with the explanation previously provided for Cu in this section, is a soil reservoir of heavy Fe, that is initially eroded and carried by surface runoff during storms, but not present in groundwater contributions that are more important during low flow conditions. As described in the introductory section, oxic weathering of basalt-derived soils preferentially mobilizes heavy Cu and light Fe (Vance et al., 2016). A soil pool of residual light Cu and heavy Fe that is more important in storm runoff than in base flow, can account for the storm flow isotopic signature observed in the current work at the uppermost watershed station. It also documents a shift from deeper- to more shallow source waters during storm runoff.

6. Estuarine Mixing

Few studies have focused on the isotopic geochemistry of Cu within estuaries. Vance et al. (2008) observed basically constant δ^{65}Cu of particles and dissolved fractions throughout the salinity gradient in the Itchen estuary in the UK, which they attribute to the previously mentioned equilibration between particulate and dissolved pools of Cu. Petit et al. (2008) evaluated particulates and sediments from Scheldt estuary (Belgium/Netherlands) with δ^{65}Cu values of -0.38 to 0.23‰, and concluded that there was mixing of a high concentration, light δ^{65}Cu freshwater pool with a low concentration, heavy δ^{65}Cu oceanic pool. In a later study, Petit et al. (2013) attributed much of the Cu isotopic fractionation in the Garonne estuary, in France, to biological activity, with uptake of light Cu by plankton producing low-δ^{65}Cu organic particles, and the degradation of organic matter releasing heavy Cu into the dissolved phase

Because biological productivity is extremely high in the Ala Wai Canal (Laws et al., 1993), it is likely that Cu is also actively cycled by plankton. All $\delta^{65}Cu_{SPM}$ in the Ala Wai are heavier than the expected bedrock isotopic composition, but SPM is nonetheless enriched in the light isotope compared to the dissolved Cu fraction (**Figure 26**). Particulate organic carbon measurements would be necessary to identify the actual composition of SPM, and to evaluate the relative importance of organic particles and rock- and soil-derived particles. Concentrations of Cu or their isotopic ratios do not change consistently along the salinity gradient within each sampling trip, thus the flocculation and settling of Fe-oxides, which commonly scavenge heavy metals such as Cu, does not seem to be a major control of Cu behavior in this estuary. However, the high tide samples at all three stations show lower concentrations of Cu, and potentially also a slightly heavier isotopic signature in $\delta^{65}Cu_{SPM}$, which could be derived from a greater influence during high tide of an isotopically heavier, lower concentration oceanic signature similar to that observed by Petit et al. (2008).

Conclusions

This study has shown that the Ala Wai watershed is a completely different system during storm flow compared to baseflow. In this small tropical stream system, basalt weathering controls Cu concentrations and results in an isotopically heavy dissolved Cu composition during baseflow in the upper watershed, while anthropogenic sources in the urban canal enhance concentrations and cause a shift towards isotopically heavier particulate Cu. During storms, surface Cu pools from roads and soils contribute to enhanced concentrations and variable isotopic signatures. Overall, ratios of particles are more sensitive to changes in Cu sources than the dissolved fraction.

The following conclusions are reached based on the hypotheses set for this research project.

Regarding Hypothesis 1, that ***basalt weathering controls δ^{65}Cu in Manoa stream****: Isotopic exchange between dissolved and particulate Cu species creates an offset from basaltic parent material:*

1. **Dissolved δ^{65}Cu** of baseflow in the upper watershed is **consistently heavier than parent material,** controlled by **mineral dissolution** and **organic complexation.**
2. **Particulate δ^{65}Cu is lighter** than the dissolved fraction, and highly variable, providing a **snapshot of local conditions** at each site.
3. **Isotopic exchange** between dissolved and particulate Cu plays a **minor role.**

Regarding Hypothesis 2, that ***anthropogenic Cu input increases downstream:*** *Urban areas supply additional Cu that can be traced with Cu isotopic ratios. Increasing ionic strength and changes in the flow regime through the Ala Wai Canal estuary control the transfer of Cu into coastal waters, and δ^{65}Cu can reveal processes during estuarine mixing:*

1. **Dissolved** Cu concentrations are **higher** in the estuarine stations, without any change in the δ^{65}Cu signature, suggesting **continuing control by organic complexation.**
2. Significant **anthropogenic input** is suggested by the δ^{65}Cu of **particles**, which are isotopically **heavier than natural sources,** but **within the range of road-derived materials.**
3. **Particulate** Cu is extremely **variable in concentrations,** but has a **constant -0.5 ‰ offset** from dissolved isotopic ratios.
4. **Temporal variability** of Cu in the lower reaches of the Ala Wai watershed is greater than spatial changes.

Regarding Hypothesis 3, that ***storm events enhance runoff of heavy metals, and mobilize different Cu pools from baseflow conditions****: δ^{65}Cu allows tracing of temporal and spatial changes in inputs:*

1. Storm runoff is **enriched in dissolved Cu** concentrations at pristine and urban stations **relative to baseflow.**
2. **Upstream**, storm runoff mobilizes **light Cu** that is not evident during baseflow. **Natural and cultivated soils** are likely sources.
3. **Downstream,** higher concentrations of Cu during storms are likely from **anthropogenic sources,** including **road derived pollution and Cu fungicides**, that are **close to lithogenic δ^{65}Cu.**

Future Research

More data collected at high spatial and temporal resolution are needed to uncover the statistical significance of the trends described above, and to quantify contributions of processes like tidal mixing, discharge, or anthropogenic inputs in explaining changes in Cu concentrations and isotopic composition. Additionally, to explore anthropogenic signatures, it is crucial to quantify Cu concentrations and especially isotopic compositions of potential contaminants, such as road dust or Cu fungicides available in Hawai'i.

To be able to fully characterize the Ala Wai watershed system with respect to Cu sources and transport, two major investigations are necessary. Firstly, more information is needed on the geochemical makeup of the Cu pools within the stream system, specifically the speciation of both dissolved and particulate phases, and the isotopic signatures associated with these chemical species. This could be uncovered using ultrafiltration, in addition to DOC and POC analysis, as well as mineralogy of particulates. Secondly, a comprehensive survey of the Cu geochemistry of additional watershed component, namely soils, sediments, and bedrock, is needed to characterize the influence of land use changes on Cu transfer.

Acknowledgements

I want to thank Sea Grant, Ifremer and the University of Hawai'i for funding for a research assistantship, materials and analyses. Thank you to my advisor and committee, Olivier Rouxel, Eric De Carlo and Chris Measures for their support, advice and insight. Also, thank you to Ken Rubin at the Department of Geology and Geophysics for some good tips. I'm grateful for support from Van Tranh and Kristin Momohara, and the Oceanography cohort at UH. Of course, I also thank my friends and family and Wesley, for being who you are and making everything easy. Special thanks to my mother, Anette, for helping with sampling and risking her life by falling on the banks of the Ala Wai Canal.

References

Aiuppa, A., Allard, P., D'Alessandro, W., Michel, A., Parello, F., Treuil, M., & Valenza, M. (2000). Mobility and fluxes of major, minor and trace metals during basalt weathering and groundwater transport at Mt. Etna volcano (Sicily). *Geochimica et Cosmochimica Acta, 64*(11), 1827–1841. doi:10.1016/s0016-7037(00)00345-8

Albrecht, W. A. (1943). Potassium in the soil colloid complex and plant nutrition. *Soil Science, 55*(1), 13–22. doi:10.1097/00010694-194301000-0000

An, W. C., & Li, X. M. (2008). Phosphate adsorption characteristics at the sediment-water interface and phosphorus fractions in Nansi Lake, China, and its main inflow rivers. *Environmental Monitoring and Assessment, 148*(1-4), 173–184. doi:10.1007/s10661-007-0149-6

Anbar, A.D., Rouxel, O., 2007. Metal stable isotopes in paleoceanography. *Ann. Rev. Earth Planet. Sci., 35,* 717-746.

Andrews, S., & Sutherland, R., (2003). Cu, Pb, and Zn contamination in Nuuanu watershed, Oahu, Hawaii. *Science of the Total Environment, 324,* 173-182.

Anthony, S., Hunt, C., Brasher, A., Miller, L., & Tomlinson, M. (2004). *Water Quality on the Island of Oahu, Hawaii, 1999-2001 (Circular 1239).* Reston, Virginia: U.S. Geological Survey.

Babscányi, I., (2015). *Copper transport and isotope fractionation in an agrosystem* (Dissertation). Université de Strasbourg, France.

Babscsányi, I., Imfeld, G., Granet, M., & Chabaux, F. (2014). Copper stable isotopes to trace copper behavior in wetland systems. *Environmental Science and Technology, 48,* 5520-5529.

Baconnais, I., Rouxel, O., Dulaquais, G. & Boye, M. (in press). Determination of the copper isotope composition of seawater revisited: A case study from the Mediterranean Sea. *Chemical Geology*. doi: 10.1016/j.chemgeo.2018.09.009

Baken, S., Salaets, P., Desmet, N., Seuntjens, P., Vanlierde, E., & Smolders, E. (2015). Oxidation of iron causes removal of phosphorus and arsenic from streamwater in groundwater-fed lowland catchments. *Environmental Science & Technology*, *49*(5), 2886-2894.

Balistrieri, L., Borrok, D., Wanty, R., & Ridley, W. (2007). Fractionation of Cu and Zn

isotopes during adsorption onto amorphous Fe(III) oxyhydroxide: Experimental mixing of acid rock drainage and ambient river water. *Geochimica et Cosmochimica Acta, 72,* 311-328.

Barnhart, J. (1997). Chromium chemistry and implications for environmental fate and toxicity. *Journal of Soil Contamination, 6*(6), 561-568. doi: 10.1080/15320389709383589.

Barker, A.V. (1999, April). *Organic Farming and Gardening – Chapter 7: Fertilizers.* University of Massachusetts Amherst. Retrieved Nov. 28, 2018 from people.umass.edu/psoil120/guide/chapter7.htm

Bau, M. (1999). Scavenging of dissolved yttrium and rare earths by precipitating iron oxyhydroxide: experimental evidence for Ce oxidation, Y-Ho fractionation, and lanthanide tetrad effect. *Geochimica et Cosmochimica Acta*, *63*(1), 67-77.

Beard, B.L., Johnson, C.M., von Damm, K.L., & Poulson, R.L. (2003). Iron isotope constraints on Fe cycling and mass balance in oxygenated Earth oceans. *Geology, 31,* 629-632.

Beltran, V. L., & De Carlo, E. H. (2005). Storm-Driven Variability of Particulate Metal Concentrations in Streams of a Subtropical Watershed. In *Environmental Chemistry* (153-175). Springer, Berlin, Heidelberg.

Bergquist, B.A., Boyle, E.A., 2006. Iron isotopes in the Amazon River system: Weathering and transport signatures. *Earth. Planet. Sci. Lett., 248*(1-2): 54-68.

Bhattacharyya, K. G., & Gupta, S. S. (2008). Adsorption of a few heavy metals on natural and modified kaolinite and montmorillonite: A review*. Advances in Colloid and Interface Science, 140*(2), 114–131. doi:10.1016/j.cis.2007.12.008

Bigalke, M., Weyer, S., & Wilcke, W. (2010a). Stable copper isotopes: a novel tool to trace copper behaviour in hydromorphic soils. *Soil Science American Journal, 74,* 60-73.

Bigalke, M., Weyer, S., Kobza, J., & Wilcke, W. (2010b). Stable Cu and Zn isotope ratios as tracers of sources and transport of Cu and Zn in contaminated soil. *Geochimica et Cosmochimica Acta, 74*, 6801-6813.

Bigalke, M., Weyer, S., & Wilcke, W. (2010c). Copper isotope fractionation during complexation with insolubilized humic acid. *Environmental Science and Technology, 44*(14), 5496-5502.

Bigalke, M., Weyer, S., & Wilcke, W. (2011). Stable Cu isotope fractionation in soils during oxic weathering and podsolization. *Geochimica et Cosmochimica Acta, 75,* 3119-3134.

Biggs, R.R., & Cronin, L.E. (1981. Special characteristics of estuaries. In Neilson, J., & Cronin, L.E. (eds.), *Estuaries and nutrients*. Humana Press, Clifton, New Jersey.

Blotevogel, S., Oliva, P., Sobanska, S., Viers, J., Vezin, H., Audry, S., Prunier, J., Darrozes, J, Orgogozo, L., Courjault-Radé, P., & Schreck, E. (2018). The fate of Cu pesticides in vineyard soils: A case study using δ^{65}Cu isotope ratios and EPR analysis. *Chemical Geology, 477,* 35–46. doi:10.1016/j.chemgeo.2017.11.032

Borrok, D., Nimick, D., Wanty, R., & Ridley, W. (2007). Isotopic variations of dissolved copper and zinc in stream waters affected by historical mining. *Geochimica et Cosmochimica Acta, 72,* 329-344.

Bonatti, E., Fisher, D.E., Joensuu, O., & Rydell, H.S. (1971). Postdepositional mobility of some transition elements, phosphorus, uranium and thorium in deep sea sediments. *Geochimica et Cosmochimica Acta*, *35*(2), 189-201. doi:10.1016/0016-7037(71)90057-3

Boyle, E.A., Edmond, J.M., Sholkovitz, E.R. (1977). The mechanism of iron removal in estuaries. *Geochimica et Cosmochimica Acta*, *41*(9), 1313-1324.

Boyle, E., John, S., Abouchami, W., Adkins, J., Echegoyen-Sanz, Y., Ellwood, M., Flegal, A., Fornace, K., Gallon, C., Galer, S., Gault-Ringold, M., Lacan, F., Radic, A., Rehkämper, M., Rouxel, O., Sohrin, Y., Stirling, C., Thompson, C., Vance, D., Xue, Z., Zhao, Y. (2012). GEOTRACES IC1 (BATS) contamination-prone trace element isotopes Cd, Fe, Pb, Zn, Cu, and Mo intercalibration. *Limnology and Oceanography Methods, 10,* 653-665.

Brand, L. E., Sunda, W. G., & Guillard, R. R. (1986). Reduction of marine phytoplankton reproduction rates by copper and cadmium. *Journal of Experimental Marine Biology and Ecology*, *96*(3), 225-250.

Brantley, S.L., Liebermann, L., Bullen, T.D. (2001). Fractionation of Fe isotopes by soil microbes and organic acids. *Geology, 29,* 535-538.

City and County of Honolulu Department of Environmental Services (June 2015). Implementation and Monitoring Plan for Ala Wai Canal Wasteload Allocation for the City and County of Honolulu Municipal Separate Storm Sewer System, NPDES Permit No. HI S000002. Retrieved Nov. 27, 2018 from www.honolulu.gov/rep/site/dfmswq/dfmswq_docs/swq_swmpp_I4.pdf

Chen, J.B., Busigny, V., Gaillardet, J., Louvat, P., Wang, Y.N., 2014. Iron isotopes in the Seine River (France): Natural versus anthropogenic sources. *Geochim. Cosmochim. Acta, 128*: 128-143.

Chever, F., Rouxel, O., Croot, P.L., Ponzevera, E., Wuttig, K., Auro, M. (2015). Total dissolvable and dissolved iron isotopes in the water column of the Peru upwelling regime. . *Geochim. Cosmochim. Acta*, *162,* 66–82.

Clague, D. A., & Frey, F. A. (1982). Petrology and trace element geochemistry of the Honolulu Volcanics, Oahu: implications for the oceanic mantle below Hawaii. *Journal of Petrology*, *23*(3), 447-504.

Clague, D., Frey, F., Garcia, M., Huang, S., McWilliams, M., & Beeson, M. (2016). Compositional heterogeneity of the Sugarloaf melilite nephelinite flow, Honolulu Volcanics, Hawai'i. *Geochimica et Cosmochimica Acta, 185,* 251-277.

Clayton, R.E., Hudsonedwards, K.A., Houghton, S.L. (2005). Isotopic effects during Cu sorption onto goethite. *Geochimica et Cosmochimica Acta*, 69, A216.

Cole, R. H., Frederick, R. E., Healy, R. P., & Rolan, R. G. (1984). Preliminary findings of the priority pollutant monitoring project of the nationwide urban runoff program. *Journal (Water Pollution Control Federation)*, 898-908.

Conway, T.M., John, S.G., 2014. Quantification of dissolved iron sources to the North Atlantic Ocean*. Nature, 511*(7508), 212-216.

Crosby, H.A., Johnson, C.M., Roden, E.E., & Beard, B.L. (2005). Coupled Fe(II)-Fe(III) electron and atom exchange as a mechanism for Fe isotope fractionation during dissimilatory iron oxide reduction. *Environmental Science and Technology, 39,* 6698-6704.

Dai, M. H., & Martin, J. M. (1995). First data on trace metal level and behaviour in two major Arctic river-estuarine systems (Ob and Yenisey) and in the adjacent Kara Sea, Russia. *Earth and Planetary Science Letters*, *131*(3-4), 127-141.

Dauphas, N., John, S., Rouxel, O., 2017. Iron isotope systematics. *Reviews in Mineralogy & Geochemistry, 82*, 415-510.

Dauphas, N., & Rouxel, O. (2006). Mass spectrometry and natural variations of iron isotopes. *Mass Spectrometry Reviews*, *25*(4), 515-550.

Davis, A. P., Shokouhian, M., & Ni, S. (2001). Loading estimates of lead, copper, cadmium, and zinc in urban runoff from specific sources. *Chemosphere*, *44*(5), 997-1009.

Davis, J.A. (1984). Complexation of trace metals by adsorbed natural organic matter. *Geochimica et Cosmochimica Acta*, *48*(4), 679-691.

De Carlo, E., & Anthony, S., (2002). Spatial and temporal variability of trace element

concentrations in an urban subtropical watershed, Honolulu, Hawaii. *Applied Geochemistry, 17,* 475-492.

De Carlo, E., Beltran, V., & Tomlinson, M. (2004). Composition of water and suspended sediment in streams of urbanized subtropical watersheds in Hawaii. *Applied Geochemistry, 19,* 1011-1037.

De Carlo, E. H., & Spencer, K. J. (1995). Records of lead and other heavy metal inputs to sediments of the Ala Wai Canal, O'ahu, Hawai'i. *Pacific Science*, *49*(4), 471-491.

De Carlo, E., Tomlinson, M., & Anthony, S. (2005). Trace elements in streambed sediments of small subtropical streams on O'ahu, Hawai'i: Results from the USGS NAWQA program. *Applied Geochemistry, 20,* 2157-2188.

Dong, S., Ochoa Gonzalez, R., Harrison, R., Green, D., North, R., Fowler, G. & Weiss, D. (2017). Isotopic signatures suggest important contributions from recycled gasoline, road dust, and non-exhaust traffic sources from copper, zinc, and lead in PM_{10} in London, United Kingdom. *Atmospheric Environment, 165,* 88-98.

El Azzi, D., Viers, J., Guiresse, M., Probst, A., Aubert, D., Caparros, J., Charles, F., Guizien, K. & Probst, J.L. (2013). Origin and fate of copper in a small Mediterranean vineyard catchment: New insights from combined chemical extraction and delta Cu-65 isotopic composition. *Sci. Total Environ., 463*, 91-101.

Escoube, R., Rouxel, O. J., Sholkovitz, E., & Donard, O. F. X. (2009). Iron isotope systematics in estuaries: The case of North River, Massachusetts (USA). *Geochimica et Cosmochimica Acta, 73*(14), 4045–4059. doi:10.1016/j.gca.2009.04.026

Escoube, R., Rouxel, O., Pokrovsky, O.S., Schroth, A.W., Holmes, R.M., Donard, O.F.X. (2015). Iron isotope systematics in Arctic rivers. *C. R. Geoscience, 347*, 377-385.

Fantle, M.S., DePaolo, D.J. (2004). Iron isotopic fractionation during continental weathering. *Earth and Planetary Science Letters, 228,* 547-562.

Fekiacova, Z., Cornu, S., & Pichat, S., (2015). Tracing contamination sources in soils with Cu and Zn isotopic ratios. *Science of the Total Environment, 517,* 96-105.

Fernandez, A., & Borrok, D. M. (2009). Fractionation of Cu, Fe, and Zn isotopes during the oxidative weathering of sulfide-rich rocks. *Chemical Geology*, *264*(1-4), 1-12.

Fitzsimmons, J.N., Conway, T.M., Lee, J.M., Kayser, R., Thyng, K.M., John, S.G., Boyle, E.A. (2016). Dissolved iron and iron isotopes in the southeastern Pacific Ocean. *Global Biogeochem. Cycles, 30*(10): 1372-1395.

Fletcher, C. (2010). *Hawai'i's Changing Climate*. Honolulu, Hawai'i: University of Hawai'i Sea Grant College Program Center for Island Climate Adaption and Policy.

Förstner, U., & Wittmann, G. T. (2012). *Metal pollution in the aquatic environment*. Springer Science & Business Media.

Freeman, William, (1993, November). *Revised total maximum daily load estimates for six water quality limited segments, island of Oahu, Hawaii*. Pacific Environmental Research.

Frey, F. A., Garcia, M. O., & Roden, M. F. (1994). Geochemical characteristics of Koolau Volcano: Implications of intershield geochemical differences among Hawaiian volcanoes. *Geochimica et Cosmochimica Acta*, *58*(5), 1441-1462.

Fuji, T., Moynier, F., Abe, M., Nemoto, K., & Albarède, F., (2013). Copper isotope fractionation between aqueous compounds relevant to low temperature geochemistry and biology. Geochimica et Cosmochimica Acta, *110,* 29-44.

Fuji, T., Moynier, F., Blichert-Toft, J., & Albarède, F., (2014). Density functional theory estimation of isotope fractionation of Fe, Ni, Cu and Zn among species relevant to geochemical and biological environments. Geochimica et Cosmochimica Acta, *140,* 553-576.

Gaillardet, J., Viers, J., & Dupré, B. (2014). Trace elements in river waters. *Treatise on Geochemistry (2nd ed.)*, 605.

Garnier, J., Garnier, J.M., Vieira, C.L., Akerman, A., Chmeleff, J., Ruiz, R.I., Poitrasson, F., 2017. Iron isotope fingerprints of redox and biogeochemical cycling in the soil-water-rice plant system of a paddy field. *Sci. Total Environ., 574,* 1622-1632.

Giambelluca, T. W., Chen, Q., Frazier, A. G., Price, J. P., Chen, Y. L., Chu, P. S., Eischeid, J.K., & Delparte, D. M. (2013). Online rainfall atlas of Hawai'i. *Bulletin of the American Meteorological Society*, *94*(3), 313-316.

Gledhill, M., & Buck, K. N. (2012). The organic complexation of iron in the marine environment: a review. *Frontiers in microbiology*, *3*, 69.

Glenn, C., Rajan, S., McMurtry, G., & Benaman, J. (1995). Geochemistry, mineralogy, and stable isotopic results from Ala Wai estuarine sediments: Records of hypereutrophication and abiotic whitings. *Pacific Science, 49*(4), 367-399.

Goldberg, E. D., Koide, M., Schmitt, R. A., & Smith, R. H. (1963). Rare-earth distributions in the marine environment. *Journal of Geophysical Research*, *68*(14), 4209-4217.

Gonzalez, F. I. (1971). *Descriptive study of the physical oceanography of the Ala Wai Canal.* Hawai'i Institute of Marine Biology, University of Hawai'i. Report No.: 26.

Guinoiseau, D., Gélabert, A., Allard, T., Louvat, P., Moreira-Turcq, P., & Benedetti, M. F. (2017). Zinc and copper behaviour at the soil-river interface: New insights by Zn and Cu isotopes in the organic-rich Rio Negro basin. *Geochimica et Cosmochimica Acta*, *213*, 178-197.

Hassani, S., Karbassi, A.R., & Ardestani, M. (2017). Role of estuarine natural flocculation process in removal of Cu, Mn, Ni, Pb and Zn. *Global Journal of Environmental Science and Management, 3*(2), 187-196. doi: 10.22034/gjesm.2017.03.02.007

Hoover, D. (2002). Fluvial Nutrient Fluxes to Oahu Coastal Waters: Land Use, Storm Runoff and Impacts on Coastal Ecosystems.Dissertation, Dep.Oceanography , Univer. Hawaii Manoa, Honolulu.

Hough, G. J., Foster, Z. C., & Gile, P. L. (1941). *Rock weathering and soil profile development in the Hawaiian Islands* (Vol. 751). US Dept. of Agriculture.

Huang, J., Liu, S.A., Gao, Y.J., Xiao, Y.L., Chen, S., 2016. Copper and zinc isotope systematics of altered oceanic crust at IODP Site 1256 in the eastern equatorial Pacific. J. Geophys. Res.-Solid Earth, 121(10): 7086-7100.

Hunter, K. A. (1983). On the estuarine mixing of dissolved substances in relation to colloid stability and surface properties. *Geochimica et Cosmochimica Acta, 47*(3), 467–473. doi:10.1016/0016-7037(83)90269-7

Icopini, G.A. Anbar, A.D., Ruebush, S.S., Tien, M., & Brantley, S.L. (2004). Iron isotope fractionation during microbial reduction of iron: The importance of adsorption. *Geology, 32,* 205-208.

Ilina, S.M., Poitrasson, F., Lapitskiy, S.A., Alekhin, Y.V., Viers, J., Pokrovsky, O.S. (2013)a. Extreme iron isotope fractionation between colloids and particles of boreal and temperate organic-rich waters. Geochim. Cosmochim. Acta, 101: 96-111.

Ilina, S.M., Viers, J., Lapitsky, S., Mialle, S., Mavromatis, V., Chmeleff, J., Brunet, P., Alekhin, Y., Isnard, H., & Pokrovsky, O. (2013)b. Stable (Cu, Mg) and radiogenic (Sr, Nd) isotopic fractionation in colloids of boreal organic-rich waters. Chemical Geology, *342,* 63-75.

Ingri, J., Malinovsky, D., Rodushkin, I., Baxter, D. C., Widerlund, A., Andersson, P., Gustafsson,

Ö., Forsling, W., & Öhlander, B. (2006). Iron isotope fractionation in river colloidal matter. *Earth and Planetary Science Letters, 245*(3-4), 792–798. doi:10.1016/j.epsl.2006.03.031

Jaworski, N. A. (1981). Sources of nutrients and the scale of eutrophication problems in estuaries. In *Estuaries and nutrients* (pp. 83-110). Humana Press.

Johnson, C.M., Beard, B.L., Albarède, F., 2004. *Geochemistry of Non-Traditional Stable Isotopes.* Reviews in Mineralogy and Geochemistry, 55. Mineralogical Society of America, 454 pp.

Johnsson, M. J., Ellen, S. D., & McKittrick, M. A. (1993). Intensity and duration of chemical weathering: An example from soil clays of the southeastern Koolau Mountains, Oahu, Hawaii. Geological Society of America Special Papers, 147–170. doi:10.1130/spe284-p147

Karbassi, A., Bidhendi, G.N., Saeedi, M., & Rastegari, A. (2010). Metals removal during estuarine mixing of Arvand River water with the Persian Gulf water. *Open Geosciences, 2*(4), 531-536.

Knor, L. A., Bau, M., Rouxel, O., Tepe, N., De Carlo, E. H. (2017, February). Basalt weathering and its contribution to trace metal composition of stream water in O'ahu, Hawai'i. Poster presented at the ASLO Ocean Sciences Meeting, Honolulu, Hawai'i.

Koeppenkastrop, D., & Eric, H. (1992). Sorption of rare-earth elements from seawater onto synthetic mineral particles: An experimental approach. *Chemical Geology*, *95*(3-4), 251-263.

Kusonwiriyawong, C., Bigalke, M., Abgottspon, F., Lazarov, M., Schuth, S., Weyer, S., & Wilcke, W., (2017). Isotopic variation of dissolved and colloidal iron and copper in a carbonatic floodplain soil after experimental flooding. Chemical Geology, *459,* 13-23.

Laws, E.A., Doliente, D., Hiayama, J., Hokama, M.L., Kim, K., Li, D., Minami, S. and Morales, C., (1993). Hypereutrophication of the Ala Wai Canal, Oahu, Hawaii: prospects for cleanup. *Pacific Science, 47*(1), 59-75.

Lead, J., & Wilkinson, K. (2006). Aquatic colloids and nanoparticles: Current knowledge and future trends. *Environmental Chemistry, 3,*159-171.

Li, Y. H. (1988). Denudation rates of the Hawaiian Islands by rivers and groundwaters. *Pacific Science*, *42*(3-4).

Li, D., Liu, S. A., & Li, S. (2015). Copper isotope fractionation during adsorption onto kaolinite:

Experimental approach and applications. *Chemical Geology*, *396*, 74-82.

Li, S., Zhu, X., Wu, L., & Luo, Y., (2016)a. Cu isotopic compositions in Elsholtzia splendens: Influence of soil condition and growth period on Cu isotopic fractionation in plant tissue. Chemical Geology, *444*, 49-58.

Li, Y., Zhu, J., & Li, S., (2016)b. Copper and zinc isotope fractionation during deposition and weathering of highly metalliferous black shales in central China. Chemical Geology, *445*, 24-35.

Little, S., Vance, D., Walker-Brown, C., & Landing, W., (2014). The oceanic mass balance of copper and zinc isotopes, investigated by analysis of their inputs, and outputs to ferromanganese oxide sediments. Geochimica et Cosmochimica Acta, *125*, 673-693.

Liu, S., Huang, J., Liu, J., Wörner, G., Yang, W., Tang, Y., Chen, Y., Tang, L., Zheng, J., & Li, S., (2015). Copper isotopic composition of the silicate earth. Earth and Planetary Science Letters, *427*, 95-103.

Liu, S., Teng, F., Li, S., Wie, G., Ma, J., & Li, D., (2014). Copper and iron isotope fractionation during weathering and pedogenesis: Insights from saprolite profiles. Geochimica et Cosmochimica Acta, *146*, 59-75.

Macdonald, G. A., Abbott, A. T., & Peterson, F. L. (1983). *Volcanoes in the sea: the geology of Hawaii*. University of Hawaii Press.

Mackenzie, F. T., & Garrels, R. M. (1971). *Evolution of sedimentary rocks*. New York: Norton.

Mair, A., & Fares, A. (2010). Influence of groundwater pumping and rainfall spatio-temporal variation on streamflow. *Journal of Hydrology, 393*(3-4), 287-308. doi:10.1016/j.jhydrol.2010.08.026

Maréchal, C., & Albarède, F. (2002). Ion-exchange fractionation of copper and zinc isotopes. *Geochimica et Cosmochimica Acta*, *66*(9), 1499-1509.

Maréchal, C., Télouk, P., Albarède, F., 1999. Precise analysis of copper and zinc isotopic compositions by plasma-source mass spectrometry. Chemical Geology, *156,* 251-273.

Markl, G., Lahaye, Y., & Schwinn, G., (2006). Copper isotopes as monitors of redox processes in hydrothermal mineralization. Geochimica et Cosmochimica Acta, *70*, 4215-4228.

Mathur, R., Jin, L., Prush, V., Paul, J., Ebersole, C., Fornadel, A., Williams, J., &

Brantley, S., (2012). Cu isotopes and concentrations during weathering of black shale of the Marcellus Formation, Huntingdon County, Pennsylvania (USA). Chemical Geology, *304-305*, 175-184.

McBride, M., Tiller, K., & Merry, R. (1981). Copper in soils and plants. *Forms and distribution of copper in solid and solution phases of soil*, 25-45.

McKenzie, R. (1989). Manganese oxide and hydroxides. In: *Minerals in soil environments* (eds., J. B. Dixon and S. B. Weed) Soil science society of America n.1. Madison, Wisconsin, USA.

McMurtry, G.M., Snidvongs, A., & Glenn, C.R. (1995). Modeling sediment accumulation and soil erosion with 137Cs and 210Pb in the Ala Wai Canal and central Honolulu watershed. *Hawai'i Pacific Science, 49,* 412-451.

Merry, R.H., Tiller, K.G., Alston, A.M., 1983. Accumulation of copper, lead and arsenic in some Australian orchard soils. *Australian Journal of Soil Resources, 21,* 549-561.

Milliman, J. D., & Syvitski, J. P. (1992). Geomorphic/tectonic control of sediment discharge to the ocean: the importance of small mountainous rivers. *The Journal of Geology*, *100*(5), 525-544.

Mills, G.L., Hanson, A.K., Quinn, J.G., Lammela, W.R., Chasteen, N.D., 1982. Chemical studies of copper-organic complexes isolated from estuarine waters using C18 reverse-phase liquid chromatography. Mar. Chem., *11(*4*)*, 355-377.

Morgan, J.L.L., Wasylenki, L.E., Nuester, J., Anbar, A.D. (2010). Fe Isotope Fractionation during Equilibration of Fe-Organic Complexes. *Environ. Sci. Technol., 44*(16), 6095-6101.

Mortlock, R. A., & Frohlich, P. N. (1987). Continental weathering of germanium: in the global river discharge. *Geochimica et Cosmochimica Acta, 51*(8), 2075–2082. doi:10.1016/0016-7037(87)90257-2

Moynier, F., Vance, D., Fuji, T., Savage, P. (2017) The isotope geochemistry of zinc and copper. *Reviews in Mineralogy and Geochemistry, 82, 543-600.*

Muller, F.L.L., Gulin, S.B., Kalvoy, A. (2001). Chemical speciation of copper and zinc in surface waters of the western Black Sea. *Marine Chemistry, 76,* 233-251.

Muller, F.L.L., Larsen, A., Stedmon, C.A., Sondergaard, M. (2005). Interactions between algal-bacterial populations and trace metals in fjord surface waters during a nutrient-stimulated summer bloom. *Limnology and Oceanography, 50*, 1855-1871.

Mulholland, D.S., Poitrasson, F., Boaventura, G.R., Allard, T., Vieira, L.C., Santos, R.V., Mancini,

L. & Seyler, P. (2015). Insights into iron sources and pathways in the Amazon River provided by isotopic and spectroscopic studies. *Geochim. Cosmochim. Acta, 150*, 142-159.

Murphy, B.P., Johnson, J.P.L., Gasparini, N.M., Sklar, L.S., 2016. Chemical weathering as a mechanism for the climatic control of bedrock river incision. Nature, *532*(7598), 223 - 227.

Navarrete, J., Borrok, D., Viveros, M., & Ellzey, J., (2011). Copper isotope fractionation during surface adsorption and intracellular incorporation by bacteria. Geochimica et Cosmochimica Acta, *75,* 784-799.

Nixon, S. W. (1981). Remineralization and nutrient cycling in coastal marine ecosystems. In *Estuaries and nutrients* (pp. 111-138). Humana Press.

Norman, M. D., Garcia, M. O., & Bennett, V. C. (2004). Rhenium and chalcophile elements in basaltic glasses from Ko'olau and Moloka'i volcanoes: Magmatic outgassing and composition of the Hawaiian plume. *Geochimica et Cosmochimica Acta*, *68*(18), 3761-3777.

Novak, M., Sipkova, A., Chrastny, V., Stepanova, M., Voldrichova, P., Veselovsky, F., Prechova, E., Blaha, V., Curik, J., Farkas, J., Erbanova, L., Bohdalkova, L., Pasava, J., Mikova, J., Komarek, A., & Krachler, M., (2016). Environmental Pollution, *218,* 1135-1146.

Patino, L. C., Velbel, M. A., Price, J. R., & Wade, J. A. (2003). Trace element mobility during spheroidal weathering of basalts and andesites in Hawaii and Guatemala. *Chemical Geology*, *202*(3-4), 343-364.

Peacock, C.L., Sherman, D.M. (2004). Copper(II) sorption onto goethite, hematite and lepidocrocite: a surface complexation model based on ab initio molecular geometries and EXAFS spectroscopy. *Geochimica et Cosmochimica Acta*, *68*, 2623-2637.

Petit, J. C. J., de Jong, J., Chou, L., & Mattielli, N. (2008). Development of Cu and Zn Isotope MC-ICP-MS Measurements: Application to Suspended Particulate Matter and Sediments from the Scheldt Estuary. Geostandards and Geoanalytical Research, 32(2), 149–166. doi:10.1111/j.1751-908x.2008.00867.x

Petit, J. C., Schäfer, J., Coynel, A., Blanc, G., Deycard, V. N., Derriennic, H., Lanceleur, L., Dutruch, L., Bossy, C., & Mattielli, N. (2013). Anthropogenic sources and biogeochemical reactivity of particulate and dissolved Cu isotopes in the turbidity gradient of the Garonne River (France). *Chemical Geology*, *359*, 125-135.

Poitrasson, F., Freydier, R., 2005. Heavy iron isotope composition of granites determined by high resolution MC-ICP-MS. *Chem. Geol., 222*, 132-147.

Pokrovsky, O., Viers, J., Emnova, E., Kompantseva, E., & Freydier, R., (2008). Copper isotopic fractionation during its interaction with soil and aquatic microorganisms and metal oxy(hyr)oxides: Possible structural control. Geochimica et Cosmochimica Acta, *72*, 1742-1757.

Radic, A., Lacan, F., Murray, J.W., 2011. Iron isotopes in the seawater of the equatorial Pacific Ocean: New constraints for the oceanic iron cycle. *Earth. Planet. Sci. Lett., 306*(1-2), 1-10.

Rauch, J., & Pacyna, J., (2009). Earth's global Ag, Al, Cr, Cu, Fe, Ni, Pb, and Zn cycles. *Global Biogeochemical Cycles, 23,* GB2001.

Roden, M. F., Frey, F. A., & Clague, D. A. (1984). Geochemistry of tholeiitic and alkalic lavas from the Koolau Range, Oahu, Hawaii: implications for Hawaiian volcanism. *Earth and Planetary Science Letters*, *69*(1), 141-158.

Rouxel, O.J., Auro, M., 2010. Iron isotope variations in coastal seawater determined by multicollector ICP-MS. *Geostandards and Geoanalytical Research, 34*(2), 135-144.

Rouxel, O.J., Bekker, A., Edwards, K.J., 2005. Iron isotope constraints on the Archean and Paleoproterozoic ocean redox state. *Science, 307*(5712), 1088-1091.

Rowland, S., & Garcia, M. (2005). Southeast O'ahu Geology field Trip Guide. Retrieved May 12, 2015, from www.soest.hawaii.edu/SOEST_News/SEoahufieldtrip4.pdf

Ryan, B., Kirby, J., Degryse, F., Scheiderich, K., & McLaughlin, M., (2014). Environmental Science and Technology, *48*, 8620-8626.

Schopka, H.H., Derry, L.A. (2012). Chemical weathering fluxes from volcanic islands and the importance of groundwater: The Hawaiian example. *Earth and Planetary Science Letters, 339-340,* 67-78.

Schmitt, C., & Brumbaugh, W., (1990). National Contaminant Biomonitoring Program: Concentrations of arsenic, cadmium, copper, lead, mercury, selenium, and zinc in U.S. freshwater fish, 1976-1984. *Archives of Environmental Contamination and Toxicology, 19,* 731-747.

Schnitzer, M., & Skinner, S. I. M. (1965). Organo-metallic interactions in soils: 4. Carboxyl and hydroxyl groups in organic matter and metal retention. *Soil Science, 99,* 278-284.

Schnitzer, M., & Skinner, S. I. M. (1966). Organo-metallic interactions in soils: 5. Stability

constants of Cu^{++}, Fe^{++}, and Zn^{++} fulvic acid complexes. *Soil Science, 102*(6), 361–365. doi:10.1097/00010694-196612000-00002

Schuth, S., Mansfeldt, T., 2016. Iron isotope composition of aqueous phases of a lowland environment. *Environmental Chemistry, 13*(1), 89-101.

Shank, C.G., Skrabal, S.A., Whitehead, R.F., Kieber, R.J. (2004)a. Strong copper complexation in an organic-rich estuary: the importance of allochthonous dissolved organic matter. *Marine Chemistry, 88*, 21-39.

Shank, C.G., Skrabal, S.A., Whitehead, R.F., Avery, J.B., Kieber, R.J. (2004)b. River discharge of strong Cu-complexing ligands to South Atlantic Bight waters. *Marine Chemistry, 88,* 41-51.

Sherrod, D., Sinton, J., & Brunt, K. (2007). Geological Map of the State of Hawaii, Sheet 3 – Island of O'ahu. Retrieved May 12, 2015, from pubs.usgs.gov/of/2007/1089/Oahu_2007.pdf

Shiller, A.M., 1997. Dissolved trace elements in the Mississippi River: Seasonal, interannual, and decadal variability. *Geochimica et Cosmochimica Acta, 61*, 4321-4330.

Sholkovitz, E.R., Boyle, E.A., & Price, N.B. (1978). The removal of dissolved humic acids and iron during estuarine mixing. *Earth and Planetary Science Letters, 40*(1), 130-136.

Sholkovitz, E. R., & Copland, D. (1982). The chemistry of suspended matter in Esthwaite Water, a biologically productive lake with seasonally anoxic hypolimnion. *Geochimica et Cosmochimica Acta*, *46*(3), 393-410.

Skrabal, S.A., Donat, J.R., Burdige, D.J. (1997). Fluxes of copper-complexing ligands from estuarine sediments. *Limnology and Oceanography*, *42*, 992-996.

Skulan, J.L., Beard, B.L., & Johnson, C.M. (2002). Kinetic and equilibrium Fe isotope fractionation between aqueous Fe(III) and hematite. *Geochimica et Cosmochimica Acta, 66,* 2995-3015.

Spencer, K.J., De Carlo, E. H., McMurtry, G. M. (1995). Isotopic clues to sources of natural and anthropogenic lead in sediments and soils from O'ahu, Hawai'i. *Oceanographic Literature Review*, *8*(43), 833.

Song, S., Mathur, R., Ruiz, J., Chen, D., Allin, N., Guo, K., & Kang, W., (2016). Fingerprinting two metal contaminants in streams with Cu isotopes near the Dexing Mine, China. *Science of the Total Envrionment, 544,* 677-685.

Stumm, W., & Morgan, J. J. (2012). *Aquatic chemistry: chemical equilibria and rates in natural waters* (Vol. 126). John Wiley & Sons.

Sutherland, R. (2000). Bed sediment associated trace metals in an urban stream, Oahu, Hawaii. *Environmental Geology, 39,* 611-627.

Sutherland, R., & Tolosa, C., (2000). Multi-element analysis of road-deposited sediment in an urban drainage basin, Honolulu, Hawaii. *Environmental Pollution, 110,* 483-495.

Tang, D., Warnken, K.W., Santschi, P.H. (2002). Distribution and partitioning of trace metals (Cd, Cu, Ni, Pb, Zn) in Galveston Bay waters. *Marine Chemistry, 78,* 29-45.

Takano, S., Tanimizu, M., Hirata, T., & Sohrin, Y. (2013). Determination of isotopic composition of dissolved copper in seawater by multi-collector inductively coupled plasma mass spectrometry after pre-concentration using an ehylenediaminetriacetic acid chelating resin. *Analytica Chimica Acta, 784.*

Takano, S., Tanimizu, M., Hirata, T., & Sohrin, Y. (2014). Isotopic constraints on biogeochemical cycling of copper in the ocean. *Nature Communications, 5*, 5663.

Tardy, Y., (1997). *Petrology of Laterites and Tropical soils*. Rotterdam, Netherlands: A.A. Balkema.

Teng, F.-Z., Dauphas, N., Huang, S., & Marty, B. (2013). Iron isotopic systematics of oceanic basalts*. Geochimica et Cosmochimica Acta, 107*, 12–26. doi:10.1016/j.gca.2012.12.027

Tessier, A., Fortin, D., Belzile, N., DeVitre, R.R., Leppard, G.G. (1996). Metal sorption to diagenetic iron and manganese oxyhydroxides and associated organic matter: narrowing the gap between field and laboratory measurements. *Geochimica et Cosmochimica Acta, 60,* 387-404.

Thomas, J., & Jennings, H. (N.D.). Mineral and oxide composition of Portland cement. Retrieved from: iti.northwestern.edu/cement/monograph/Monograph3_6.html (Nov. 6, 2018).

Thompson, A., Ruiz, J., Chadwick, O. A., Titus, M., & Chorover, J. (2007). Rayleigh fractionation of iron isotopes during pedogenesis along a climate sequence of Hawaiian basalt. *Chemical Geology*, *238*(1-2), 72-83.

Tomlinson, M., & De Carlo, E. (2003). The need for high resolution time series data to characterize Hawaiian streams. *Journal of the American Water Resources Association, 39,* 113-123.

US Army Corps of Engineers (March 3, 2013). Review Plan: Ala Wai Canal (a.k.a. Ala Wai

Watershed) Project, Island of Oahu, Hawaii, Feasibility Report. Retrieved Nov. 27, 2018 from www.poh.usace.army.mil/portals/10/docs/projectreviewplans/alawaireviewplanapproved.pdf

Van der Grift, B., Rozemeijer, J. C.; Griffioen, J., van der Velde, Y. (2014). Iron oxidation kinetics and phosphate immobilization along the flow-path from groundwater into surface water. *Hydrol. Earth Syst. Sci., 18,* 4687–4702.

Vance, D., Archer, C., Bermin, J., Perkins, J., Statham, P., Lohan, M., Ellwood, M., & Mills, R., (2008). The copper isotope geochemistry of rivers and the oceans. *Earth and Planetary Science Letters, 274,* 204-213.

Vance, D., Matthews, A., Keech, A., Archer, C., Hudson, G., Pett-Ridge, J., & Chadwick, O., (2016). The behaviour of Cu and Zn isotopes during soil development: Controls on the dissolved load of rivers. Chemical Geology, *445*, 36-53.

Visher, F. N., & Mink, J. F. (1964). *Ground-water resources in southern Oahu, Hawaii*. U.S. Government Publishing Office.

Vitousek, P.M., Chadwick, O., Crews, T.E., Fownes, J., Hendricks, D.M. & Herbert, D. (1997). Soil and ecosystem development across the Hawaiian Islands. *GSA Today, 7,* X1-8.

Wattel-Koekkoek, E. J., van Genuchten, P. P., Buurman, P., & van Lagen, B. (2001). Amount and composition of clay-associated soil organic matter in a range of kaolinitic and smectitic soils. *Geoderma, 99*(1-2), 27–49. doi:10.1016/s0016-7061(00)00062-8

Wehrli, B., & Stumm, W. (1989). Vanadyl in natural waters: adsorption and hydrolysis promote oxygenation. *Geochimica et Cosmochimica Acta*, *53*(1), 69-77.

Weinstein, C., Moynier, F., Wang, K., Paniello, R., Foriel, J., Catalano, J., & Pichat, S., (2011). Isotopic fractionation of Cu in plants. Chemical Geology, *286*, 266-271.

Wells, M.L., Kozelka, P.B., Bruland, K.W. (1998). The complexation of "dissolved" Cu, Zn, Cd and Pb by soluble and colloidal organic matter in Narragansett Bay, RI. *Marine Chemistry, 62*, 203-217

Wilson, M., Wilson, D., & Mathur, R., (2016). Tracing the source of native copper mineral specimens with copper isotope values. Rocks and Minerals, *91*(4), 352-356.

Wiederhold, J., (2015). Metal stable isotope signatures as tracers in environmental geochemistry. *Environmental Science and Technology, 49,* 2606-2624.

Yavuz, Ö., Altunkaynak, Y., & Güzel, F. (2003). Removal of copper, nickel, cobalt and manganese from aqueous solution by kaolinite. *Water Research, 37*(4), 948–952.

Zhu, X.K., Guo, Y., Williams, R.J.P., O'Nions, R.K., Matthews, A., Belshaw, N.S. Canters, G.W., deWaal, E.C., Weser, U., Burgess, B.K., Salvato, B. (2002). Mass fractionation processes of transition metal isotopes. *Earth Planet. Sci. Lett.*, *200,* 47-62.